



UiT The Arctic University of Norway

Department of Pharmacy (Institutt for farmasi – IFA)

Mass Spectrometry Based Metabolomic and Lipidomic Analyses of Algal Biomass

A comparison between two different extraction methods for metabolomic and lipidomic analyses, and use of high-resolution mass spectrometry to identify possible bioactive metabolites

Magnus Andersland Antonsen

Master's thesis in Pharmacy (FAR-3911) May 2023

Acknowledgement

The work presented in this thesis was performed at Marbio and at the Department of Pharmacy (IFA) at UiT - the Arctic University of Norway from August 2022 to May 2023, with the support of local industry collaborators whose contributions cannot be acknowledged due to confidentiality.

First of all, I would like to thank my main supervisor and Associate Professor Terje Vasskog for the guidance during this period, but most of all for all knowledge shared about analytical chemistry through my pharmaceutical education at UiT. You are an exceptional lecturer with exceptional pedagogic skills, making it a joy to learn about analytical chemistry.

I would like to give a special thanks to my co-supervisor and Associate Professor Kine Østnes Hansen for the consistent and invaluable guidance through all work done at Marbio. You have always been available for advice and constructive feedback from the start to the end of the thesis. Another special thanks go to my co-supervisor and Professor Espen Holst Hansen, who taught me how to use metabolomic-oriented platforms and guided me during the work.

I have benefited a lot from cooperation with two PhD students. I would therefore like to thank Kim van Wezel and Marit Huizer for all the help and discussion around analyses of the microalgal biomass. In addition, I would like to thank Head Engineer Kirsti Helland for teaching me how to conduct a selection of bioassays. To all other researchers and employees at Marbio, thank you for all your support and guidance through my time at the research group. I have learned a lot about your work and wish you all the best in the future.

I would also like to thank all my fellow pharmacy students, who have contributed to a great learning environment and for cooperation in overlapping projects. A special thanks go to my co-student and dear friend Rasmus Pedersen and to my girlfriend Trine Marie Henriksen, who has been great company and active in discussions throughout the entire pharmaceutical education.

Tromsø, May 2023

Magnus Andersland Antonsen

Abstract

Background: In a project at UiT - the Arctic University of Norway, the lipid profile of the microalgal biomass from the specie *Porosira glacialis* is mapped using HRMS lipidomic analyses to evaluate the potential for the biomass to be used as fish feed. At the same time, it is desired to screen the same biomass for bioactivities using bioassays in combination with HRMS metabolomic analyses. The two processes use two different extraction methods. To evaluate the differences between the extraction methods, a comparison between one of each extract was done in this thesis. Fractions from extracts are also tested for bioactivity and analysed on HRMS to initiate the mapping of bioactivity.

Method: Microalgal biomass of *P. glacialis* was extracted using two different extraction methods, yielding an aqueous, an organic and a lipid extract. The metabolic and lipidomic profile of the organic and the lipid extract was compared using HRMS metabolomic and lipidomic analyses. The aqueous and the organic extracts were fractionated using flash chromatography, before being tested for various bioactivities and analysed using HRMS. Observed activity was investigated and a potential bioactive compound was isolated and tested for anti-cancer activity.

Results: There were no obvious differences in the metabolomic and lipidomic profiles between the organic and the lipid extracts, but some trends could be observed. The lipidomic analyses showed low lipid detection not consistent with previous research, which needs further investigation. In fractions obtained from the microalgal biomass from *P. glacialis*, anticancer activity against human melanoma A2058 cancer cells and growth inhibition against the bacteria *Streptococcus agalactiae* were observed, as well as anti-inflammatory activity in an ELISA immunoassay. An isolated potential bioactive compound showed no activity against human melanoma A2058 cancer cells at five different test concentrations.

Conclusion: None of the extraction methods can be considered favourable over the other based on the comparison in this thesis. Various bioactivities were observed for fractions derived from the microalgal biomass of *P. glacialis*, but more investigation must be done to identify the compounds responsible for the activity.

Table of Contents

Acknowledgement.....	II
Abstract	III
Graphical Overview of the Thesis.....	IX
Abbreviations	X
1 Introduction	1
1.1 Background	1
1.2 Bioprospecting.....	2
1.2.1 Marine Bioprospecting in Northern Climate	3
1.3 Marine Microalgae	4
1.3.1 Diatoms	4
1.3.2 <i>Porosira Glacialis</i>	5
1.4 Metabolomics and Lipidomics	5
1.5 Sample Preparation.....	6
1.5.1 Solid-Liquid Extraction	7
1.5.2 Lipid Extraction (Folch Extraction)	7
1.6 Chromatography and Mass Spectrometry	8
1.6.1 Liquid Chromatography	8
1.6.2 Flash Chromatography	9
1.6.3 Preparative HPLC.....	10
1.6.4 Mass Spectrometry	10
1.7 Identification of Compounds.....	14
1.7.1 Retention time	14
1.7.2 Isotope Pattern and Accurate Mass	14
1.7.3 Fragmentation.....	15
1.7.4 Identification of Metabolites	16
1.7.5 Identification of Lipids	16
1.8 Data Acquisition and Interpretation	18
1.8.1 Unifi, Progenesis QI and EZInfo.....	18
1.8.2 AcquireX and LipidSearch.....	18
1.9 Bioassays	19
1.9.1 Biofilm Formation Assay	19
1.9.2 Cancer Cell Viability Assay	20
1.9.3 Anti-Bacterial Growth Assay	21
1.9.4 Immunoassay and ELISA.....	21
2 Aim of the Thesis	23
3 Materials and Methods	24
3.1 Extraction Method for Metabolomics	24
3.1.1 Aqueous Extraction	24
3.1.2 Organic Extraction	25
3.2 Flash Chromatographic Method	25
3.2.1 Column and Extract Preparation	25
3.2.2 Chromatography	26
3.2.3 Drying the Fractions.....	27
3.2.4 Dissolution of Fractions to Known Concentrations	27
3.3 Lipid Extraction Method for Lipidomics	27
3.3.1 Extraction	27
3.4 UHPLC-HRMS Methods	28
3.4.1 Preparation of Samples.....	28
3.4.2 Metabolomic Analysis (UHPLC-IMS-qToF).....	28
3.4.3 Lipidomic Analysis (UHPLC-Orbitrap MS).....	29
3.5 Bioassays	32

3.5.1	Bioassays Preparation.....	33
3.5.2	Inhibition of Biofilm Formation Assay	33
3.5.3	Anti-bacterial Growth Assay	35
3.5.4	Viability Assay	36
3.5.5	Immunoassay	38
3.6	Dereplication Method for Metabolomic Analyses	41
3.7	Isolation and Bioactivity Testing of Top Candidate.....	42
3.7.1	Isolation Preparation of the Aqueous Extract.....	42
3.7.2	Isolation Method.....	42
3.7.3	Bioactivity Testing of the Isolate	43
4	Results and Discussion	44
4.1	Recovery of Extracts and Fractions.....	44
4.1.1	Recovery of Extracts	44
4.1.2	Recovery of Fractions	44
4.2	Comparing the Extraction Methods.....	45
4.2.1	Metabolomic Comparison	45
4.2.2	Lipidomic Comparison.....	52
4.2.3	Summary of the Extraction Method Comparison.....	56
4.3	Bioassay Results.....	56
4.3.1	Biofilm Formation.....	57
4.3.2	Anti-bacterial Growth Assay	57
4.3.3	Viability.....	58
4.3.4	Immunoassay (ELISA).....	59
4.3.5	Summary of Bioassay Results	60
4.4	Dereplication of Bioactivity	61
4.4.1	Bioactivity in Aqueous Fraction 5.....	61
4.4.2	Bioactivity in Organic Fraction 7	63
4.5	Isolation and Bioactivity Testing of Isolate.....	64
4.6	Limitations	66
4.7	Conclusion and Future Perspectives.....	67
	Works Cited.....	68
	Appendix	71

List of Tables

Table 1: How the scores from the formation of biofilm assay correspond to each category; active (A), questionable (Q) and inactive (I).....	20
Table 2: How the scores from the viability assay correspond to each category; active (A), questionable (Q) and inactive (I).....	21
Table 3: How the measured absorbance from the anti-bacterial growth assay correspond to each category; active (A), questionable (Q) and inactive (I).....	21
Table 4: How the scores from the immunoassay correspond to each category; active (A), questionable (Q) and Inactive (I).....	22
Table 5: Equipment and chemicals used for extraction, flash chromatography and LC-MS analyses.	24
Table 6: Parameters associated with the IMS-qToF MS method.....	29
Table 7: The exact setup for the mobile phase gradient over time used in lipidomic analyses.....	30
Table 8: Parameters used in the MS full scan orbitrap method.....	30
Table 9: Equipment and chemicals used in bioassays.....	32
Table 10: Pathogens and cell-lines used in bioassays.....	33
Table 11: An overview of the microtiter plate in the inhibition of biofilm assay. Column 1-6 are test columns where samples are added. 1-1 indicates the first fraction of the aqueous extract, while 2-1 indicates the first fraction of the organic extract. Column 7-10 are positive controls and column 11 is a negative control, while column 12 is a blank.....	34
Table 12: An overview of the microtiter plates in the anti-bacterial growth assay. Column 2-11 are test columns, column 1 is a medium blank and column 12 is a negative control. 1-1 indicates the first fraction tested against the first bacterial strain, while 2-1 indicates the first fraction tested against the second bacterial strain. Separate microtiter plates were prepared for each extract.....	36
Table 13: An overview of the microtiter plate in a viability assay. Column 2-9 are test columns, while column 10-12 are control columns. The samples are added as triplets. 1-1 represents the first fraction in the aqueous extract, while 2-1 indicates the first fraction in the organic extract.....	38
Table 14: An overview of the microtiter plate in an immunoassay. Column 2-9 are test columns, while column 10-12 are control columns. The samples are added as triplets. 1-1 indicates the first fraction in the aqueous extract, while 2-1 indicates the first fraction in the organic extract.....	39
Table 15: An overview of the microtiter plate when conducting ELISA. Column 1-8 are test columns, column 9-10 are control columns and column 11-12 are used for the TNF- α dilution series.....	40
Table 16: The most vital search parameters for dereplication in UNIFI®.....	41
Table 17: An overview of the microtiter plate set up for testing the anti-cancer activity against melanoma A2058 cancer cells for the isolated compound. Five different concentrations were tested in triplicates (50, 25, 12.5, 6.25 and 3.125 $\mu\text{g/mL}$) in column 8-10. Column 11 is a negative control, while column 12 is a positive control.....	43
Table 18: An overview of the different stock concentrations, the amount of recovered sample material and the volume of solvent DMSO for each fraction.....	45
Table 19: Results of the inhibition of biofilm assay showing no active fractions.....	57
Table 20: Results of the antibacterial growth assay showing scores for each bacterial strain. Score values marked in red are considered active (absorbance < 0.05), while score values marked in orange have questionable activity (absorbance = 0.05 - 0.09).....	58
Table 21: Results of the viability assay showing activity against human melanoma cancer cell line A2058 for aqueous fraction 5 (aq5) marked in red and questionable activity for aqueous fraction 6 (aq6) marked in orange.....	58
Table 22: Results of immunoassay showing activity (A) in red and questionable activity (Q) in orange. The scoring system is different for immunostimulatory activity compared to anti-inflammatory activity.....	60

List of Figures

Figure 1: An illustration of how the project at UiT – the Arctic University of Norway in collaboration with local industry will contribute to a circular economy and reduced pollution (created in BioRender).	1
Figure 2: The principles of solid-liquid extraction (28).	7
Figure 3: Illustration of the flash chromatographic workflow (created in BioRender).	9
Figure 4: An illustration of the preparative-HPLC-MS used for compound isolation at Marbio (33).	10
Figure 5: Schematic view of how ions travel through a quadrupole (28).	11
Figure 6: Isotope patterns for chloride (Cl) and bromine (Br) in mass spectra (28).	15
Figure 7: An illustration of how the fragmentation pattern is used to identify phospholipids. In this example, the structure of 2-Oleoyl-1-palmitoyl-sn-glycero-3-phosphocholine is used (created in ChemDraw).	17
Figure 8: An illustration of how the fragmentation pattern is used to identify triglycerides. In this example, the structure of 1,2-Dilinoleoyl-3-palmitoyl-rac-glycerol is used (created in ChemDraw)...	17
Figure 9: The reduction of MTS tetrazolium to formazan (48).	20
Figure 10: Illustration of the steps in ELISA; antibody (1), antibody coupled with antigen (2), ELISA-sandwich (3), antibody-binding reagents coupled with ELISA-sandwich (4) and antibody-binding reagents coupled with ELISA-sandwich resulting in colour change (5).	22
Figure 11: Solvent composition used as mobile phase and an illustration of the different fractions in the flash chromatographic method.	26
Figure 12: An illustration of the mobile phase gradient over time. Mobile phase A consisted of a mixture of MQ-water and acetonitrile (1:1), while mobile phase B consisted of 2-propanol:acetonitrile (1:1).	30
Figure 13: The mass spectrometric method performed on the orbitrap. The illustration shows how the MS ⁿ method is setup to acquire information for lipid identification.	31
Figure 14: How pathogens were streaked on blood agar plates.	34
Figure 15: The structure composition of a fluorophenyl column.	42
Figure 16: The organic and the lipid positive ionization integrated base peak intensity (BPI) chromatogram from injection 2 compared in UNIFI. The BPI chromatogram with the green line shows the difference in response between the extracts).	46
Figure 17: PCA-plot showing the relative variation between the organic and the lipid extracts with three sequential injections. The x-axis represents the relative variation between the extracts, while the y-axis represents the relative variation between the injections of the extracts.	47
Figure 18: S-plot comparing the lipid to the organic extract. The points marked in red were selected for comparing the organic and the lipid extracts (created in EZInfo).	48
Figure 19: A possible identification of the compound (C ₃₉ H ₅₂ N ₂ O ₁₀ , i-FIT = 71.13 %) only observed in the organic extract with m/z = 355.1886, z = 2 (Created in ChemDraw).	48
Figure 20: Illustration of a plausible fragmentation of N-Octylnonanamide (Created in ChemDraw).	49
Figure 21: A bar chart of the 10 compounds with the highest observed signal intensity from the 64 selected showing the average signal intensity of the compounds for each extract. The legend presents the retention time and either the observed m/z or the neutral mass of the compounds, depending on if the software could identify the neutral mass or not.	50
Figure 22: A possible identification for the peak with the highest signal intensity (Rt = 11.33 minutes) in the analysis, pyropheophorbide a (structure retrieved from ChemSpider).	50
Figure 23: Lipidomic profile of 2.5 mg/mL microalgal biomass extracts from Porosira glacialis. The figure shows detection of lipid classes in a blank sample (S1), a mixed sample (S2), the organic extract (S3) and the lipid extract (S4).	52
Figure 24: Lipidomic profile of 2.5 mg/mL microalgal biomass extracts from Porosira glacialis when the lipid class TG is excluded. The figure shows detection of lipid classes in a blank sample (S1), a mixed sample (S2), the organic extract (S3) and the lipid extract (S4).	52
Figure 25: TIC of 2.5 mg/mL of the lipid (red) and the organic (black) extracts.	54

Figure 26: Lipidomic profile of 2.5 mg/mL microalgal biomass extracts from <i>Porosira glacialis</i> with identification grade A or B. The figure shows detection of lipid classes in a blank sample (S1), a mixed sample (S2), the organic extract (S3) and the lipid extract (S4).....	54
Figure 27: A possible structure composition of the identified triglyceride (Rt = 24.20 minutes) with the fatty acids 16:0, 16:1 and 20:5.	55
Figure 28: A semi-quantification plot of the abundance of the TG with elemental composition C ₅₅ H ₉₄ O ₆ in the blank sample (s1), the mixed sample (s2), the organic extract (s3) and the lipid extract (s4). The concentration of the organic and the lipid extracts were 2.5 mg/mL.	56
Figure 29: Visual result of viability assay. Column 2-9 are test columns, columns 10 and 11 are negative controls, and column 12 is a positive control. Dark colour indicates cell growth.....	59
Figure 30: The positive mode ionization BPI integrated chromatograms for aq4 and aq5 compared in Unifi, showing a distinct difference for Rt = 12.70 minutes.	61
Figure 31: The molecular structure of erucamide (C ₂₂ H ₄₃ NO, ChemDraw).	62
Figure 32: The negative mode ionization BPI integrated chromatograms for aq4 and aq5 compared in Unifi.	63
Figure 33: The structure composition of scortechinone K, C ₃₄ H ₄₀ O ₁₀ (retrieved from ChemSpider)..	64
Figure 34: BPI chromatogram from preparative-HPLC, showing isolation of the peak with Rt = 14.99 minutes and m/z = 338.5. The purple line indicates the collected area.	65
Figure 35: The mass spectrum for the isolated compound at Rt = 14.99 minutes with m/z = 338.49. 65	

List of Equations

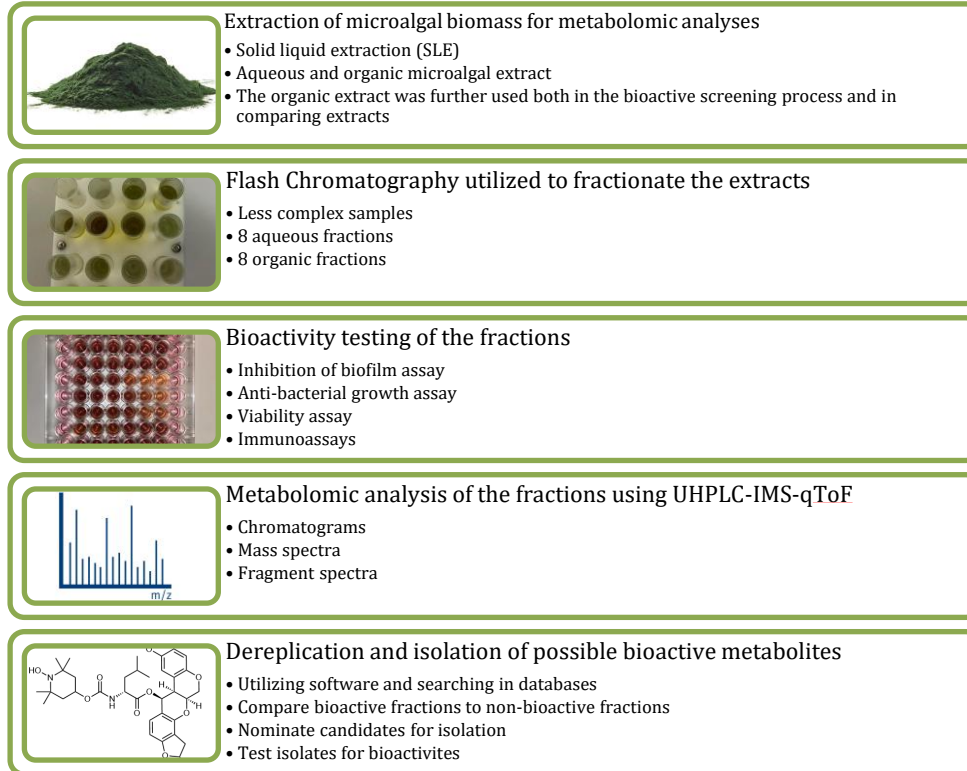
Equation 1: How to calculate resolution (Rs) using selectivity (α), number of theoretical plates (N) and retention factor (k').	8
Equation 2: Calculation of the number (n) of carbons using information from mass spectrometry....	14

List of Appendix

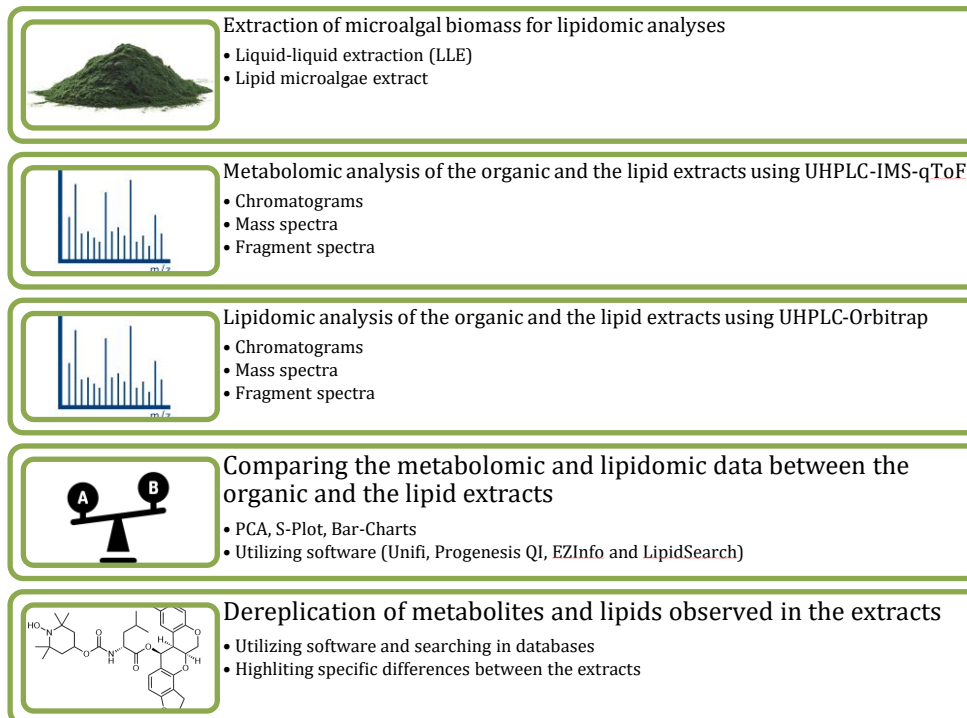
Appendix 1: Parameters used in the MS ⁿ method on the orbitrap.	71
Appendix 2: An overview of neutral loss of fatty acids and ammonia triggering MS ³ OT CID in lipidomic analyses.	72
Appendix 3: An overview of the lipid classes identified in LipidSearch.....	72
Appendix 4: An explanation of the grading system for identifications in LipidSearch.	73

Graphical Overview of the Thesis

Bioactivity Screening



Comparing Extracts



Abbreviations

Aq1 - 8	Aqueous fraction 1 - 8	MeCN	Acetonitrile
BPI	Base peak intensity	MeOH	Methanol
C₁₈	Octadecylsilane	MG	Monoglyceride
CID	Collision-induced dissociation	MGDG	Monogalactosyldiacylglycerol
CO₂	Carbon dioxide gas	MI	Molecular ion
DCM	Dichloromethane	MS	Mass spectrometry
DG	Diglyceride	N	Number of theoretical plates
DHA	Docosahexaenoic acid	NMR	Nuclear magnetic resonance
EI	Electron ionization	O₂	Oxygen gas
E_k	Kinetic energy	Org1 - 8	Organic fraction 1 - 8
ELISA	Enzyme-linked immunosorbent assay	P	Phosphorus
EPA	Eicosapentaenoic acid	PC	Phosphatidylcholine
ESI	Electrospray ionization	PCA	Principal component analysis
FA	Fatty acid	PCRC	Photosynthetic carbon reduction cycle
GC	Gas chromatography	PE	Phosphatidylethanolamine
GL	Galactolipid	PG	Phosphatidylglycerol
HCD	Higher-energy collision dissociation	PL	Phospholipid
HCE	High collision energy	Rs	Resolution
HPLC	High performance liquid chromatography	Rt	Retention time
HRMS	High resolution mass spectrometry	SLE	Solid-liquid extraction
IMS	Ion mobility spectrometry	TG	Triglyceride
k'	Retention factor	TMS	Tandem mass spectrometry
LC	Liquid chromatography	TNF-α	Tumour necrosis factor alpha
LCE	Low collision energy	ToF	Time-of-flight
LC-MS	Liquid chromatography mass spectrometry	UHPLC	Ultra-high performance liquid
LDL	Low-density lipoprotein	UiT	The Arctic University of Norway
LLE	Liquid-liquid extraction	v	Velocity
m	Mass	z	Charge
m/z	Mass to charge ratio	α	Selectivity
MarBank	Marine biobank		

1 Introduction

1.1 Background

As the world is facing global warming caused by escalating greenhouse gas emissions, and the growing issue of food deficiency due to overpopulation, innovative research remains crucial to confront these pressing challenges. In 2021, the European Union agreed to the European Climate Law, which aims to reduce emissions by 55 % by 2030 and reach carbon neutrality by 2050 (1). Incorporated in these goals EU defined numerous taxonomies. It is desirable to protect biodiversity, reduce pollution, have sustainable usage of water and marine resources, and focus on a circular economy (2). These taxonomies are exactly what the local industry in Northern Norway is focusing on, contributing to sustainable development, reduced pollution, and world health through a circular economy.

At UiT – the Arctic University of Norway (UiT), there is an ongoing project in collaboration with local industry aimed at the taxonomies defined by the EU. The strategy is to achieve a circular economy and reduced pollution by cultivating microalgae using carbon dioxide gas (CO₂) and other greenhouse gases to create a sustainable food chain for fish farming (**Figure 1**).

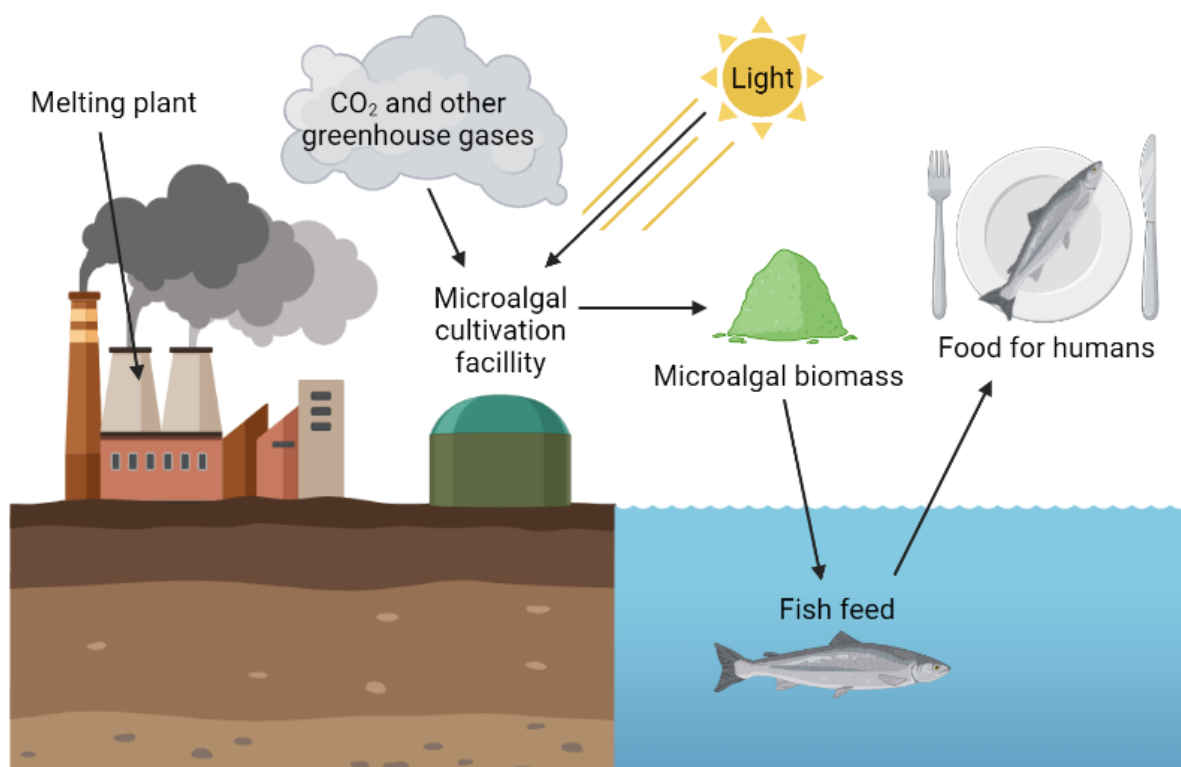


Figure 1: An illustration of how the project at UiT – the Arctic University of Norway in collaboration with local industry will contribute to a circular economy and reduced pollution (created in BioRender).

In this strategy the photosynthesis in microalgae is central, where expulsion of CO₂ and other greenhouse gases conveniently produces microalgal biomass. According to the Institute of Marine Research, the main ingredients in fish feed are proteins and lipids, which often come from vegetables (3). It is well known that microalgal biomass is affluent in lipids, but literature searches in scientific libraries suggest a research gap for using these lipids to replace the use of vegetables in fish feed. At UiT, it is therefore desired to investigate the lipid composition of the diatom microalgae *Porosira glacialis*, to evaluate the possibility of utilizing microalgal biomass from this specie in fish feed. In this project, a lipid extraction is conducted followed by mapping of the lipid composition using lipidomics on a Thermo IDX Tribrid Orbitrap MS.

In addition to highlighting the lipid profile of *P. glacialis*, it is desired to investigate if the microalgal biomass contains any bioactive metabolites compelling for further research. This part of the project is conducted at the research group Marbio at UiT, who wants to contribute to sustainable usage of marine resources and world health. Marbio specializes in bioactivity screening of marine microorganisms. In collaboration with the Norwegian national marine biobank MarBank, marine samples are collected, analysed, and tested for bioactivity. Marbio is screening marine algae, bacteria, fungi, and invertebrates, where *P. glacialis* is just one of many marine organisms in focus. In the screening process, the relevant biomass undergoes an aqueous extraction followed by an organic extraction before both extracts are fractionated and tested for bioactivity. A metabolomic analysis is then conducted on a UHPLC-IMS-qTOF to identify possible bioactive metabolites.

As part of the ongoing project around *P. glacialis*, it is desired to compare the two different extraction methods for lipidomic and metabolomic analyses which are currently used at UiT. The comparison will give insight into the possibilities of using one extraction method for both types of analyses. In addition, it is desired to screen the microalgal biomass for bioactivity in hope of discovering novel bioactive compounds. This thesis will therefore focus on lipidomic and metabolomic comparisons between extracts from *P. glacialis*, bioactivity testing and identification of possible bioactive metabolites.

1.2 Bioprospecting

Bioprospecting is defined as the search for products in nature that can be utilized by humans. This includes findings of actual products like genes, microorganisms, and molecules, but also inspiration for aerodynamic design, cultivation, or resource mapping. For the pharmaceutical industry, the aim of bioprospecting is most often to discover novel molecules with drug

development potential. These molecules can sometimes be utilized as drugs themselves but are often developed into drugs through medicinal chemistry optimizing activity and pharmacokinetic properties (4, 5).

Products associated with bioprospecting are a major contribution to drug discovery. Of all small-molecule discovered drugs between 1981 and 2019, 4.6 % were natural products, 18.9 % were derivatives of natural products, 18.4 % were biological macromolecules isolated from organisms and 25.7 % were drugs synthesized by mimicking natural products (6). In total, products associated with bioprospecting have contributed to the discovery of 67.6 % of small-molecule drugs between 1981 and 2019. These numbers explain the incentive behind the continuous efforts put into bioprospecting in the search for novel, bioactive compounds with the potential of being developed into drugs.

Historically, bioprospecting and exploration of nature date back at least 100 000 years, in the era when the development of the modern human occurred. It is known that civilizations in Mesopotamia, Egypt, Rome, and even the Neanderthals used herbs as natural medicine. Morphine is a well-known pain-relieving drug, which is said to be isolated from the opium plant for the first time by Sertüner in 1817 (4). However, elixir recipes containing the opium plant itself date back to the Roman Empire (7) but could have been used even before that time period. Acetylsalicylic acid is a commonly used drug to prevent cardiac complications as well as having a pain-relieving effect. Data extracted from the Norwegian Prescription Database at the Norwegian Institute of Public Health suggests that around 342 000 people in Norway were registered as users of this active ingredient in 2020 (8). This drug was for the first time synthesized from the natural compound salicylic acid in 1897 (9), which is a compound extracted from the willow tree (4). Both morphine and acetylsalicylic acid are products utilized by humans discovered from nature. These are early pharmaceutical examples of how humans have been doing bioprospecting for a long time.

1.2.1 Marine Bioprospecting in Northern Climate

Marine bioprospecting is the search for natural products in and around the sea. This is an exciting field of research for a country like Norway, which has the world's second longest coastline at around 100 000 km (10). The marine climate is dark, cold, and hostile, but still thrives of a broad diversity of flora and marine organisms. To survive in this kind of environment specialized abilities are required (11). Many of these abilities consist of chemical components, which are interesting from a bioprospecting perspective. At the research group

Marbio in Tromsø, secondary metabolites of marine organisms are investigated in collaboration with MarBank. Marine organisms are collected from the arctic sea and shipped as natural samples to the laboratory in Tromsø.

1.3 Marine Microalgae

Microalgae are small unicellular organisms (12) creating a large diverse group of microorganisms. Most microalgae are eukaryotic, but there are some prokaryotic algae species with great resemblance to many common bacteria. The chloroplast is considered one of the most essential structures of microalgae, making them capable of conducting photosynthesis. Protein-binding chlorophylls and carotenoids absorb photons and catalyse redox reactions to drive electrons from water into energy for the microalgae. The byproduct of this reaction is oxygen gas (O₂), which most life on Earth is depending on one way or the other. The energy produced is then used in the Photosynthetic Carbon Reduction Cycle (PCRC), where CO₂ is captured by the microalgae and converted into biomass (13). Using these mechanisms algae are consuming the atmospheric CO₂ while producing O₂ making humans able to survive. It is said that microalgae contribute to about half of the global photosynthetic activity (14), and are therefore a hot topic concerning global warming. In addition, microalgae are one of the most important primary producers (12) comprising plenty of biomass, functioning as feed for more than 70 % of the world's organisms (14).

1.3.1 Diatoms

Diatoms are small microalgae between 10 and 200 µm in diameter (15) often referred to as microalgae living in glass houses. This is because diatom microalgae differ from other microalgae by having silica-based walls protecting the contents of the cell (12). Because of the silica, diatoms are of great importance for the silica cycle (15), transporting silica across ecosystems. Despite silica being the seventh most abundant element on the planet, processes controlling the earth's silica level were initiated only in the late 20th century. Studies have shown that the silica cycle is strongly connected to the amount of CO₂ in the atmosphere (16), which could be explained by the diatom's compelling ability to convert CO₂ into biomass and O₂. Diatoms actually account for 20 - 25 % of the O₂ production in the world (15).

Diatoms' excellent ability to conduct photosynthesis is one reason why they are compelling candidates to convert CO₂ into fish feed. Another reason is their high growth rates. The reproduction of diatoms can occur both asexually and sexually. The most common is the asexual approach through binary fission, where synthesis of hypovalves occurs inside the parent

cell before exocytosis (17). For optimal reproductivity, diatoms however need sufficient amounts of silica, nutrition and trace metals including nitrogen, phosphorus, vitamins, iron, magnesium and cobalt (18). With optimal conditions, diatoms will rapidly reproduce resulting in effective production of biomass.

1.3.2 *Porosira Glacialis*

P. glacialis is a diatom microalgae specie, which is generally not very well known. The diameter of the microalgae is said to be 30 - 40 μm and it is best characterized by wavy stripes made up of areoles and delicate silicification (19). *P. glacialis* is considered an Antarctic microalgal specie and has been recorded to live in open ocean close to sea ice or in slushy conditions. Cultivation experiments have shown that *P. glacialis* also seem to survive in dark conditions for a long period of time (20). These characteristics suggest that the specie is well suited to survive along the Norwegian coastline, which explains why *P. glacialis* is actually one of the main planktonic components in Norwegian coast water in early spring when the sea ice is melting (19).

Since *P. glacialis* generally is not very well studied, it is an attractive object for research. Recent research supports *P. glacialis* as a potential specie for mass cultivation. An article written by Svenning, J. B et al. in 2019 concluded that the specie tolerates a broad temperature range, in addition to containing a lot of fatty acids (FAs) beneficial in fish feed (21). Another study revealed the specie's tolerability to increased CO₂-levels when exploiting algal photosynthesis for cultivation. At the same time, the study suggested that CO₂-conditioning increases the total lipid content in the specie (22). In total, *P. glacialis* is a robust microalgae specie, able to effectively use CO₂ to produce high lipid content biomass, at the same time as having great reproductive abilities as diatom microalgae. In a master thesis conducted by Kristine Haugland, the lipid class composition of *P. glacialis* was investigated. Haugland observed a high abundance of lipid classes like phosphatidylcholines (PCs), phosphatidylethanolamines (PEs), phosphatidylglycerols (PGs), diglycerides (DGs), monogalactosyldiacylglycerols (MGDGs) and triglycerides (TGs) (23).

1.4 Metabolomics and Lipidomics

Metabolomics is a type of study falling under the category of omics-studies. The omics term is meant to describe analyses aimed at understanding biological systems (24), from genotype to phenotype. In addition to metabolomics, the term includes genomics and transcriptomics, where

the DNA-sequence and transcription are in focus, as well as proteomics, the study of proteins and enzymatic reactions (25).

Metabolomics is defined as a comprehensive and quantitative analysis of all metabolites in a biological system, where the purpose is to map the entire metabolome. Metabolites are the smallest chemical molecules in a biological system part of a constant recirculating process. A biological system will therefore consist of vast amounts of different metabolites, making metabolomic studies comprehensive and time consuming. Under controlled conditions, the metabolome will be near constant for a biological system and could therefore be used as a metabolic fingerprint (25). When abnormalities in the metabolome occur, it often could mean a change in the biological systems conditions. This principle is used in modern medical diagnostics, where for example a high level of LDL-cholesterol indicates an increased risk of heart disease (26, 27).

Lipidomics could be considered a targeted metabolomic study. Targeted metabolomics is a quantitative analysis of a few or a group of metabolites. In a lipidomic target analysis the group of metabolites quantified are lipids or groups of lipids. Untargeted metabolomics is on the other hand a qualitative analysis where the metabolites studied are unknown. Here it is desired to identify the largest possible number of metabolites in a biological system (25). In this thesis, untargeted metabolomics is used to compare the metabolic profile between two extracts from microalgal biomass, while lipidomics is used to compare the lipidomic profile. Metabolomics is also used for identification of possible bioactive metabolites from the same biomass.

1.5 Sample Preparation

Sample preparation can be defined as everything done to a sample before analyses. There are many reasons to undergo sample preparation. The sample could be too complex, where a preparative fractionation step is needed to simplify the sample. The analyte concentration could be below the detection limit, which might induce the need to increase the concentration. The sample could also be contaminated or incompatible with the instrument (28). In untargeted analyses, it is desirable to identify as many compounds as possible from the specimen of interest. Therefore, it is important to use a sample preparation method which does not discriminate, degrade, or in any way lead to a loss of compounds. Simplicity, reproducibility, and time efficiency are also sought in sample preparation (29).

1.5.1 Solid-Liquid Extraction

Solid-liquid extraction (SLE, **Figure 2**) is a simple extraction method used mainly for extraction from solid samples. The solid sample is dried and powdered to increase the surface area before an aqueous or organic solvent is added. Increasing the surface area helps the analyte become more accessible to the solvent. Shaking is often done to speed up the extraction process. Over time the analyte will diffuse from the solid sample into the liquid solvent. The amount of diffused analyte depends on the analyte's chemical properties and the chosen solvent. Lipophilic analytes will have increased diffusion into a lipophilic solvent compared to into a hydrophilic solvent. The opposite applies to hydrophilic analytes. The main goal of the SLE is to capture a high concentration of analyte in the liquid phase after a specific amount of time. If the recovered concentration of the analyte is lower than desired, several repetitive extractions of the solid sample could be required.

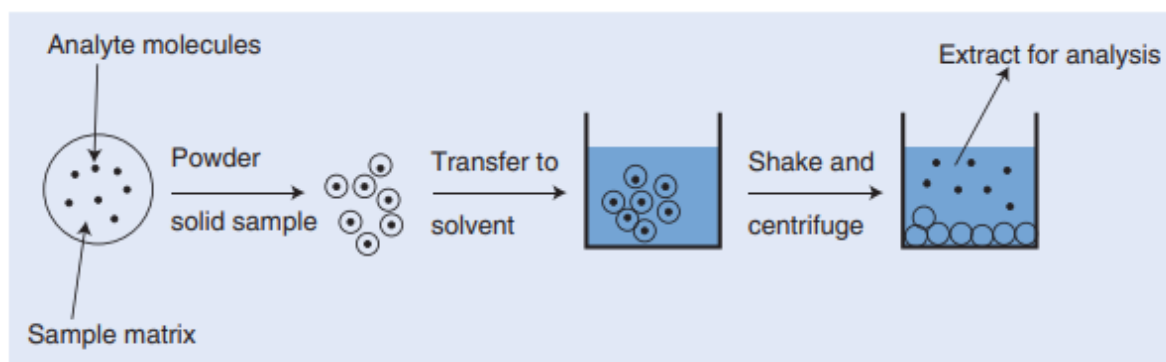


Figure 2: The principles of solid-liquid extraction (28).

After the extraction process is done, the remains of the solid sample are removed from the extract, while the liquid extract is used for analytical analyses. Removal of solid waste is often done by filtration or centrifugation (28). Filtration is as simple as letting the mixture flow through a filter, usually with the use of vacuum. Centrifugation uses centrifugal force to separate particles according to their density. Most often the solid particles will sediment as a precipitate, while the liquid phase will remain on top as a supernatant (30). After centrifugation, both the supernatant and the precipitate are easily collectable.

1.5.2 Lipid Extraction (Folch Extraction)

Folch extraction is considered the “gold standard” method for extracting lipids from microorganisms and hydrophobic biomass. In this method, a mixture of chloroform and methanol (MeOH) is used as an organic solvent to extract lipids from the biomass. Afterwards, an aqueous solvent is used to extract polar unwanted compounds back from the organic solvent

using the technique of liquid-liquid extraction (LLE). In LLE analytes are exposed to two non-miscible solvents, where hydrophilic analytes diffuse into the hydrophilic solvent, while lipophilic analytes diffuse into the lipophilic solvent. In lipid extraction, the lipophilic analytes are of interest, and therefore only the lipophilic extract is collected, while the hydrophilic extract goes to waste (31).

In this thesis, a lipid extraction method inspired by the Folch extraction is used, where chloroform is replaced with dichloromethane (DCM) because of reduced health risks. The lipid extract is then compared to an organic extract produced using an SLE extraction method meant for metabolomic analyses. Both the lipid and the metabolomic profiles of the extracts are compared.

1.6 Chromatography and Mass Spectrometry

1.6.1 Liquid Chromatography

Chromatography is a separation technique separating compounds based on differences in distribution between a mobile- and a stationary phase. In liquid chromatography (LC) the mobile phase consists of liquid solvents, while the stationary phase is a packed column of solid particles, typically silica-based particles. Samples are injected into the liquid mobile phase, where they are further carried into the column. In the column, the analytes experience retention based on chemical and physical properties. Analytes interacting more with the column will experience more retention than analytes interacting less with the column. This way, the analytes will be separated based on interactive properties with the column. The time a compound uses passing through a column is termed retention time (Rt), while Resolution (Rs) is the chromatographic system's ability to create narrow peaks and separate two closely eluting compounds. Resolution is decided by multiple parameters and can be calculated using **Equation 1** (28).

$$Rs = \frac{1}{4} \times (\alpha - 1) \times \sqrt{N \times \left(\frac{k'}{k' + 1} \right)}$$

Equation 1: How to calculate resolution (Rs) using selectivity (α), number of theoretical plates (N) and retention factor (k').

1.6.1.1 Reversed-Phase Chromatography

Reversed-phase chromatography is currently considered the most common separating method in analytical chemistry. The stationary phase consists of lipophilic particles, often octadecylsilane (C₁₈) attached to silica particles. The mobile phase in reversed-phase LC

consists of a mixture of water and a polar organic solvent miscible with water (often MeOH or acetonitrile). This layout ensures that the most polar compounds elute first, because of less interaction with the lipophilic column and more interactions with the polar mobile phase. More lipophilic compounds will however interact more with the lipophilic column, which results in higher retention time (28).

1.6.1.2 HPLC and UHPLC

High performance liquid chromatography (HPLC) is a chromatographic method where the mobile phase is forced through a column packed with small particles, creating a high pressure. Small and uniform particles enhance separation efficiency by increasing the number of theoretical plates (N), which leads to a further increase in resolution. Ultra-high performance liquid chromatography (UHPLC) is an even more advanced chromatographic system using even smaller column particles than HPLC-systems, creating an even higher pressure. If the goal is to analyse with high resolution and good separation, UHPLC is the state-of-the-art instrument to use (28).

1.6.2 Flash Chromatography

Flash chromatography (**Figure 3**) is based on the same principles as in ordinary chromatography, separation decided by differences in physicochemical properties.

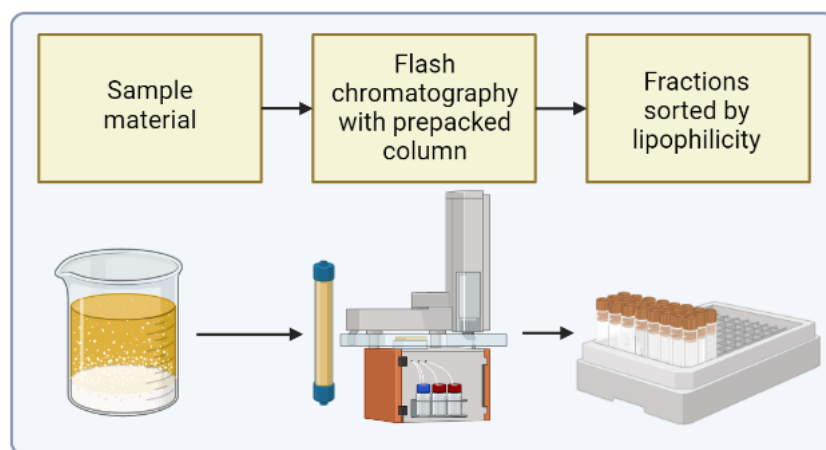


Figure 3: Illustration of the flash chromatographic workflow (created in BioRender).

Compared to HPLC and UHPLC, flash chromatography is a separation technique operating on a larger scale. Instead of small diameter columns consisting of very small particles, the columns are bigger in diameter with a bigger particle size (2.5 cm and 75-150 μm in this thesis). Because of the larger scale, flash chromatography offers less Rs, but in contrast to HPLC and UHPLC, the columns are loadable with a greater amount of sample material. The sample material is

moreover collected as fractions at the end of the chromatographic process, making the separation technique very utilizable as a preparative step before advanced analyses (32). In this thesis flash chromatography is used to fractionate organic and aqueous extracts from microalgal biomass, to simplify the extracts before bioactivity testing.

1.6.3 Preparative HPLC

Preparative HPLC (**Figure 4**) is based on the same separation principles as normal HPLC, where the purpose is to collect one or more target compounds after separation. Combining the high separation efficiency of the HPLC with the possibility of collecting separated compounds, unlocks the possibility of isolating products with high purity. The collection of a sample can be initiated in different ways, where it is for example possible to set a retention time window where collection is initiated. In this case, there is a risk of losing sample if a drift in retention time occurs during analyses. If the preparative HPLC is coupled with a mass spectrometer, it is instead possible to initiate sample collection when a specific m/z value is detected. This method can be considered more robust because the compound of interest will always be collected as long as the mass spectrometer detects the specific m/z value (33).

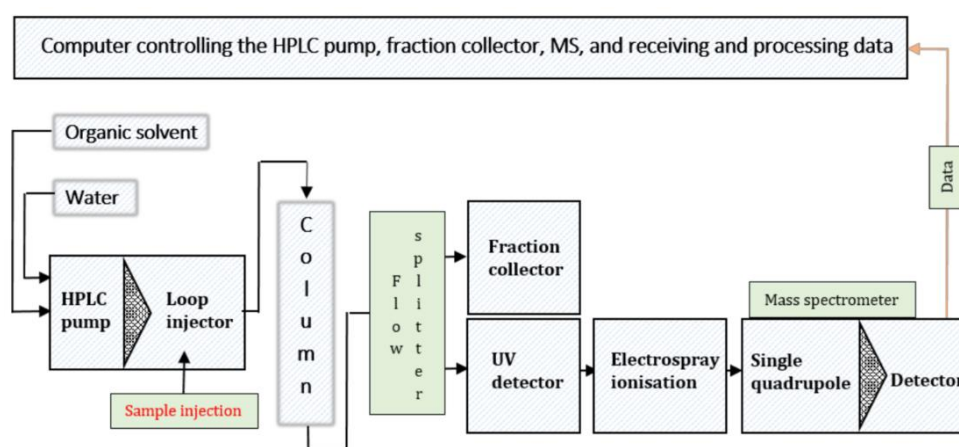


Figure 4: An illustration of the preparative-HPLC-MS used for compound isolation at Marbio (33).

1.6.4 Mass Spectrometry

A mass spectrometer is an instrument that separates ions based on their mass to charge ratio (m/z). Mass spectrometry (MS) is an analysis technique providing both qualitative and quantitative information. The main components of a MS-system are the ionization chamber, the mass filter with a mass analysing system and the detector. Coupled with a LC-instrument, it is possible to separate compounds from a sample and then collect information about the identity and the amount of each compound in the sample. The combined instrumentation of LC and MS

(LC-MS) is commonly used in pharmaceutical analyses, doping analyses, diagnostics and scientific research (28).

The first process in MS is the ionization of the analytes. Only ionized molecules will be detected by the mass spectrometer, while non-ionized molecules will go to waste. The analytes enter an ionization chamber, where an ion source is used for ionization. There are several types of ion sources. In gas chromatography (GC), electron ionization (EI) is most common where molecules are bombarded with electrons. This technique is only possible in GC because EI requires the analyte to be present in a gaseous state. In LC, the analytes are solved in a liquid mobile phase requiring a different ionization approach. The approach used in this thesis is electrospray ionization (ESI). In ESI, the sample gets exposed to an electric potential, making an aerosol of charged droplets. These droplets are further exposed to a vaporization process, where the droplets shrink in size. The consequence is a columbic explosion, due to charges getting too close to each other in the droplets. The final result of the process is ionized analytes in a vaporized state ready to enter the mass filter (28).

1.6.4.1 Mass Filter and Mass Analysing Systems

The mass filter has the objective of filtering out unwanted ions and that way facilitates analyses of selected ions. In most MS-instruments, the mass filter is a quadrupole, which consists of four parallel rods where voltage is applied to create an electric field. This electric field makes the analyte ions travel in complex trajectories depending on the ion's m/z value (**Figure 5**). Only ions with the m/z values chosen for the quadrupole will be able to travel further into the detector, while other ions will go to waste. With different settings, it is possible to choose which ions to further analyse to get optimal results (28).

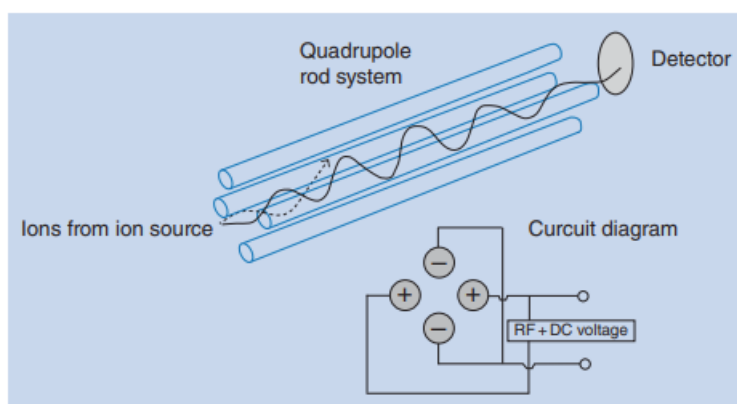


Figure 5: Schematic view of how ions travel through a quadrupole (28).

There are several advanced mass spectrometric analysing systems developed to measure and separate ions based on m/z values. The first example is Time-of-Flight (ToF) MS, which is a system where the m/z value is determined by the flight time of ions through a field-free tube with no electrostatic or magnetic disturbances (28). The theory is that ions with the same kinetic energy (E_k) but with different masses will fly through the tube with different velocities (34). Ions are collected on a back plate in the back of the ion source before they in pulses get accelerated with the same E_k . Since heavier ions desire more E_k than lighter ions to reach the same velocity ($E_k = 1/2 \times m \times v^2$) the lighter ions will fly faster through the tube than heavier ions. The flight time measured by a detector at the end of the tube can thereby be used to determine the m/z value. ToF MS gives high resolution data with a large mass range and is therefore especially beneficial in qualitative analyses (28).

An Ion trap is an example of a sensitive MS-system with the possibility of conducting multiple fragmentations. In an ion trap instrument, ions are collected in a chamber where a constant-frequency voltage is added causing the ions to travel around in stable trajectories. Changes in frequency will change the trajectory of the ions based on their m/z value. At some point ions with a specific m/z value will exit through an exit hole and hit a detector. The m/z value is thereby determined by the frequency used to cause ions to leave the ion trap. In an ion trap, there is a possibility to trap specific ions and collide them with an inert gas to produce fragments. This process can be repeated multiple times, which results in multiple fragmentation spectra that could be useful for identification of compounds (28). It exists both circular and linear ion traps, where circular ion traps are more frequently used as one mass analyser, while linear ion traps are often coupled with other mass analysers like for example an orbitrap. An ion trap coupled to an orbitrap can offer an increased linear dynamic range, resulting in more reliable quantitative analyses (34).

Orbitrap technology is used in instruments which currently offer the highest resolution. The orbitrap collects ions in a chamber, where electrostatic energy makes the ions travel in orbitals around an oval spindle (34). By applying an electric potential to the end caps of the spindle, the ions oscillate back and forth in line with the spindle. The oscillations are independent motions and do therefore not interfere with the orbital motions of the ions. Since the oscillations are only affected by the applied electric potential to the end caps, the frequency of the oscillations is measured and used to determine the m/z value of the ions (35). Orbitraps are currently considered the best technology for conducting qualitative analyses, but coupled with a linear ion trap quantitative analyses are also very feasible (34). The downside of orbitrap technology

is that it is very expensive, and the availability of the instrument is therefore limited. In addition, high resolution requires a longer scan time, which can lead to a reduced number of measurements over a chromatographic peak, and thereby unfavourable conditions for quantification.

1.6.4.2 Tandem Mass Spectrometry

Tandem mass spectrometry (TMS) is the coupling of two or multiple mass spectrometric systems to create more comprehensive analyses resulting in more information for identification of compounds. The simplest TMS technique is MS/MS where the first MS-system selects one or multiple ions to further analyse. These ions are then fragmented using a fragmentation technique and the fragments are analysed by the second MS-system. The result is a fragment spectrum providing valuable information for identification of compounds. In theory, it is possible to conduct this process multiple times (MS^n) to obtain more information. The downside of MS^n is the reduction of signal intensity when increasing the number (n) of fragmentations. It is therefore only feasible in practice to conduct three to four fragmentation processes before the signal is lost (36).

There are different mechanisms for fragmentation of ions, where the terms used for these mechanisms vary between suppliers. The first fragmentation mechanism to be explained is what Thermo terms collision-induced dissociation (CID). This is a fragmentation mechanism where the precursor ion only dissociates once before the fragments get detected. CID is therefore a soft fragmentation mechanism, resulting in higher m/z -valued fragments. In CID fragmentation, the weakest bonds of a precursor ion are most likely to break, which makes it easier to predict the fragmentation pattern of ions. Higher-energy collision dissociation (HCD) is a harder fragmentation mechanism in Thermo instruments, where the precursor ion might undergo multiple dissociations before detection. This results in lower m/z -valued fragments, because the higher m/z -valued fragments dissociate to lower m/z -valued fragments before detection (37). Combining different fragmentation mechanisms could provide comprehensive data for identification of compounds. In instruments from Waters, like the qToF used for metabolomics in this thesis, there is only one type of fragmentation mechanism. This mechanism is termed CID by Waters but has the same mechanism as what Thermo terms HCD. CID is therefore a hard fragmentation mechanism in Waters instruments. To clarify, the principle of soft and hard fragmentation is the same across instruments, while the CID/HCD terming is supplier specific.

1.7 Identification of Compounds

In general, there is no singular variable retrieved from LC-MS analyses that can be used to identify compounds. Instead, many variables must be put together to confidently present an identification of a compound. Sometimes, a complete identification cannot be acquired without using other analytical techniques like nuclear magnetic resonance (NMR) spectroscopy.

1.7.1 Retention time

Retention time (Rt) is a dynamic variable which varies between column, methods, and instruments, and therefore rarely give valuable identification information across laboratories. However, if the same column, the same method, and the same instrument are used, the Rt should remain almost constant every time the same compound is analysed. Rt is therefore useful if there is built in an in-house library of the compounds of interest. In addition, Rt could be used to confirm identification of compounds by analysing pure standards. If the pure standard has the same Rt as the suspected compound, as well as other variables, identification of the compound is confirmed (28). Use of Rt is frequently used in doping screening, where anti-doping labs possess big libraries of doping substances (38). There is even an approach where artificial neuron networks are used to predict Rt for doping substances based on the applied method (39). Rt alone is though not sufficient for identification of a doping substance.

1.7.2 Isotope Pattern and Accurate Mass

For the most common atoms in organic chemistry, the abundance of isotopes is very well known. The most abundant isotopes of for example carbon are ^{12}C with around 98.9 % abundance and ^{13}C with 1.1 % abundance. This knowledge is used in the early identification of compounds, by looking at the pattern and intensity of the signals retrieved in mass spectra. In a mass spectrum of an organic compound containing C-atoms, a high intensity m/z -value for the molecular ion (MI) is often observed, in addition to a lower intensity signal for the m/z -value corresponding to MI+1. The high intensity signal represents the ion containing only ^{12}C isotopes, while the lower intensity signal represents the same ion containing one ^{13}C isotope. The difference in intensity of the ^{12}C and ^{13}C signals is used to calculate the number (n) of carbons in a compound using **Equation 2** (28).

$$n = \frac{(\text{Intensity of } MI + 1)}{(\text{Intensity of } MI) \times 1.1 \%} * 100 \%$$

Equation 2: Calculation of the number (n) of carbons using information from mass spectrometry.

Chloride and bromide are examples of other atoms, which sometimes occur in organic compounds. Chloride has the isotopes ^{35}Cl with 76 % abundance and ^{37}Cl with 24 % abundance, while bromide has the isotopes ^{79}Br and ^{81}Br where the abundance is almost 50:50. Compounds containing atoms with these kinds of isotopes create characteristic isotope patterns in mass spectra (**Figure 6**), and it is therefore simple to either confirm or deny the presence of these atoms by looking at the signal intensity pattern in mass spectra (28).

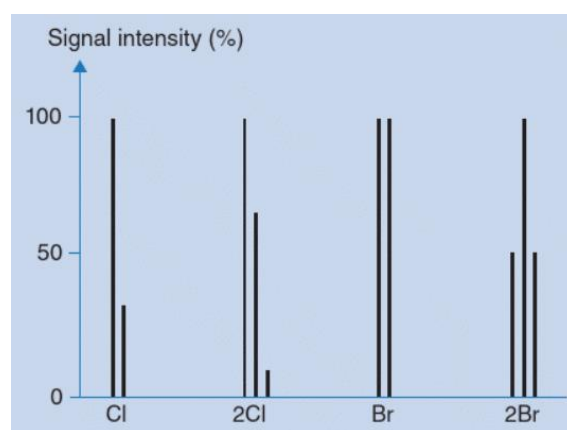


Figure 6: Isotope patterns for chloride (Cl) and bromine (Br) in mass spectra (28).

Using high resolution mass spectrometry (HRMS), accurate mass with 4 or 5 decimals could be provided. This makes it possible to calculate the exact elemental composition of ions and compare it with the literature (28). In practice, this is most often done by utilizing software created to make identification of compounds easier. First, the isotope pattern is investigated, and atoms are either included or excluded depending on what is observed in the mass spectrum. Then, the software calculates the elemental composition using the accurate mass and the chosen atoms, presenting a confidence value for the calculations. In the end, the elemental composition is used to search for known compounds in online databases (40).

1.7.3 Fragmentation

The fragmentation of ions creates fragmentation spectra, which is vital in identification process of a compound. The difference in the m/z -value of the fragment compared to the MI represent the m/z -value lost in the fragmentation process. This value is used to identify the part of the precursor ion lost in the fragmentation process. If the difference is observed to be for example $m/z = 16$ a cleavage of either oxygen (O) or an amine (NH_2) has most probably occurred. This is because the average molecular weight of O and NH_2 is 16 Da. With high resolution data, it will in this case be possible to differentiate the m/z between O and NH_2 . Some functional groups are more likely to dissociate from the MI and some bonds in the MI are more likely to undergo

cleavage, which in total provide valuable information. The fragmentation pattern can therefore be used as a puzzle to construct a structural composition of the MI, resulting in a possible identification of the compound (28).

In most cases constructing the structural composition is not straightforward, and software is therefore used to facilitate the process. By searching in online databases, the m/z -values of the fragments are matched with known fragments in the literature, where a higher number of matched fragments increases the confidence of a structural identification (40).

1.7.4 Identification of Metabolites

Metabolites are the smallest molecules present in an organism, as well as the group of molecules with the broadest variety in the organism. Unlike many lipid classes, there are no specific structural characteristics of metabolites, making identification more complicated. The strategy is therefore to first determine the elemental composition by using isotope pattern and accurate mass before using the fragment pattern to rank plausible structural compositions. Unfortunately, this information is not always sufficient to completely identify a metabolite, and other techniques like NMR spectroscopy may be required (40). In practice, software is utilized to search in databases for known compounds with matching elemental composition and fragments. A subjective evaluation of the identified matches is then conducted based on match scores given by the software.

1.7.5 Identification of Lipids

Lipids are classified as non-polar and polar lipids based on their hydrophobicity. The non-polar lipids consist of monoglycerides (MGs), DGs, TGs and steroids. The polar lipids are lipids containing a polar head group like phospholipids (PLs) and galactolipids (GLs). Both PLs and GLs are further classified into sub-groups based on the composition of the polar head group. Conveniently, lipids have characteristic fragmentation patterns based on the lipid group they belong to, which makes it possible to easily assign an unknown lipid to a lipid group (41).

The first step in identification of PLs is the cleavage of the head group. Using standard fragmentation technology, the head group fragments off, and the difference in m/z -value is used to identify the composition of the head group. For most PLs, the first fragmentation step also generates fragments corresponding to the FAs in the lipid. When both the head group and at least one of the FAs in the lipid are identified, sufficient information is retrieved to assign the lipid to a sub-group. For some PLs, like phosphatidylcholines (PC), a second fragmentation

step is needed to ensure identification of FA fragments, because the abundance of FA fragments in the first fragmentation step is too low (**Figure 7**). Fragmentation of GLs follows the same principles as fragmentation for PLs. Both fragments related to the hexose ring head group and to FAs are necessary for assignment to the lipid group. PLs and GLs are mostly ionized as proton- $[M+H]^+$ or sodium-adducts $[M+Na]^+$, which is important to note when navigating the m/z -values (41).

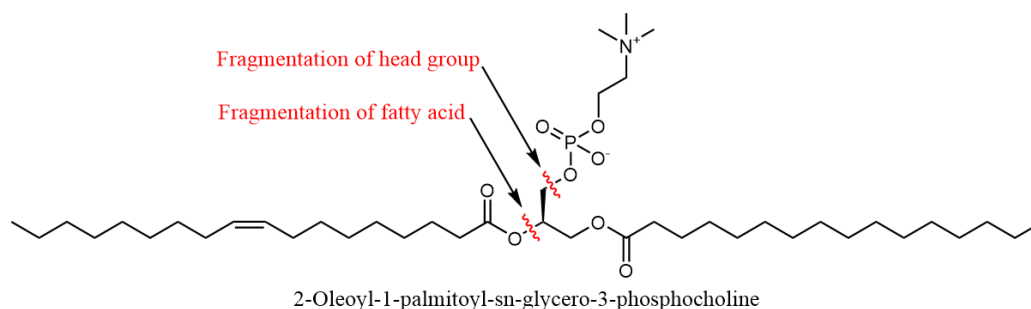


Figure 7: An illustration of how the fragmentation pattern is used to identify phospholipids. In this example, the structure of 2-Oleoyl-1-palmitoyl-sn-glycero-3-phosphocholine is used (created in ChemDraw).

Glycerol lipids (MG, DG, TG) only consist of a glycerol backbone and FAs, mostly ionized as ammonium- $[M+NH_4]^+$, sodium $[M+Na]^+$ and lithium $[M+Li]^+$ adducts in MS. To retrieve sufficient information to assign a lipid into one of these sub-groups, two fragmentation steps are needed (**Figure 8**). The first fragmentation will secure identification of one of the FAs, while the second fragmentation will secure identification of the next FA as well as the last FA connected to the glycerol backbone (41). To address the specific positioning of the FAs in lipids requires additional investigation. Earlier research found that the signal intensity ratios between the FAs were position specific in PCs. There might be a similar relationship for TGs, but that is yet to be explored. Identification of the number of double bonds in a FA is done by looking at the number of hydrogens compared to carbons, but addressing their specific positions is not possible without further analyses (42).

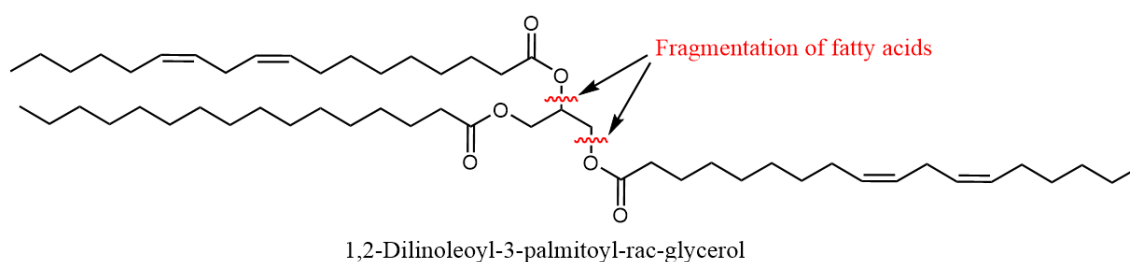


Figure 8: An illustration of how the fragmentation pattern is used to identify triglycerides. In this example, the structure of 1,2-Dilinoleoyl-3-palmitoyl-rac-glycerol is used (created in ChemDraw).

1.8 Data Acquisition and Interpretation

Data acquisition is about how the data from an analysis is retrieved. When conducting an analysis, it is desired that the data produced is relevant to the objective. There are therefore developed multiple techniques to prioritize which data is retrieved in analyses. Setting an intensity threshold for fragmentation is a simple example of data acquisition. By using this technique only m/z signals over a specified threshold are fragmented, resulting in a prioritization of the most abundant ions. There are multiple data acquisition software capable of conducting complex and a variety of data acquisition techniques.

When analysing complex samples like the ones in this thesis, a huge amount of data is generated. To manually interpret all the data takes a lot of time and is therefore not doable in practice. Different software are therefore developed to make data interpretation easier. These software makes it possible to review and investigate the data, search in databases, and make models to present the data. In untargeted analyses, especially where it is desired to discover novel compounds, dereplication is a major part of the data interpretation. Dereplication is to determine whether a compound is known or not (40). In this thesis, dereplication is conducted to identify possible bioactive compounds and compounds which differ between two different extracts.

1.8.1 Unifi, Progenesis QI and EZInfo

Unifi is a software from Waters used for setting up LC and MS methods as well as for the interpretation of data (43). This is the software operating the UHPLC-IMS-qToF placed at Marbio used in this thesis to conduct metabolomic analyses. It is also used for investigation and dereplication of the results. In Unifi it is possible to review chromatograms and mass spectra, and it is also possible to search in databases for matching results.

Progenesis QI and EZInfo are platforms developed to generate more information about the retrieved data. While progenesis QI is an analysis software created for metabolomics, EZInfo is a software for statistical analysis. These software are compatible with each other and are used in this thesis to compare the metabolic profile of extracts (44).

1.8.2 AcquireX and LipidSearch

AcquireX is a data acquisition software from Thermo Scientific to retrieve valuable data for small molecules, which in this thesis are lipids. The software makes it possible to acquire more fragmentation data for the ions in focus, resulting in more confident identifications (45).

Multiple fragmentation data is possible to acquire using an ID-sample, which is a pooled sample of all individual samples included in the analysis. Full scan analyses are performed for all individual samples, while MSⁿ analyses are performed for the ID-sample. Multiple injections of the ID-sample are performed to secure the fragmentation of a wide range of precursor ions. In the first injection, the set of precursor ions with the highest intensity is fragmented. These ions are then placed on an exclusion list to facilitate the fragmentation of the next set of precursor ions with high intensity. This setup prioritizes fragmentation of the precursor ions with the highest intensities as well as securing fragmentation of a high number of precursor ions. The number of injections of the ID-sample and the parameters for the exclusion list can be adjusted for the optimal acquisition for the specific analysis. When using AcquireX, full scan data supplied with a broad range of fragmentation data is acquired. In this thesis, AcquireX is used to acquire lipid fragment patterns for lipidomic analyses.

LipidSearch is a software from Thermo Scientific for processing LC-MS data for lipidomic analyses. The data is imported to the software and an alignment is conducted based on an algorithm. Utilizing the knowledge of fragmentation patterns for lipids, the markers are assigned to lipid classes. It is possible to generate bar plots and other charts over lipid classes, but it is also possible to identify specific lipids. With multiple functionalities, the software is made to more efficiently interpretate lipidomic data. In this thesis, the software is used to conduct a lipid profile comparison between two extracts and for identification of lipids.

1.9 Bioassays

Bioassays are testing of compounds to evaluate the compound's bioactivity. At Marbio, extracts, fractions and isolated compounds are tested using different *in vitro* bioassays, to screen for bioactive compounds in hope of discovering new potential pharmaceutical drugs (11). Results of all bioassays at Marbio are categorized as active (A), inactive (I) or questionable (Q). Which category a sample corresponds to is decided by measured absorbance or a scoring system. The score is calculated differently for each bioassay and the criteria for inclusion in each category varies between the assays.

1.9.1 Biofilm Formation Assay

A bacterial biofilm is an extracellular matrix providing structure and protection for bacterial colonies. Pathogens producing biofilm have shown increased resistance to a range of antibiotics and it is therefore desired to investigate strategies to lower the resistance level. One strategy is to target the biofilm in biofilm-producing pathogens in hope of increasing the pathogen's

sensitivity to antibiotics and the immune system. Biofilm formation assays are assays where the formation of biofilm is evaluated when exposed to samples. In these assays, a biofilm-producing bacteria is used for the production of biofilm, while a crystal violet chemical is used as a dying agent. Absorbance spectrometry is then performed to determine the amount of produced biofilm (46).

To evaluate the activity against biofilm formation at Marbio, the absorbance is used to calculate a score corresponding to an activity-level (**Table 1**).

Table 1: How the scores from the formation of biofilm assay correspond to each category; active (A), questionable (Q) and inactive (I).

Category	Score (%)
A	< 30
Q	30-40
I	> 40

1.9.2 Cancer Cell Viability Assay

Cancer cell viability assays are assays where the number of healthy cancer cells is evaluated after exposure to different samples (47). There are multiple methods for measuring cell viability, but in this thesis, the MTS-method is used. This is a method based on the reduction of MTS tetrazolium to formazan (**Figure 9**), causing a colour change in the medium. The reduction will only take place if there is mitochondrial activity in the cells, meaning that only healthy cells will contribute to the colour change (48). The absorbance measured at 490 nm is used to evaluate the degree of colour change and is directly proportional to the number of healthy cells.

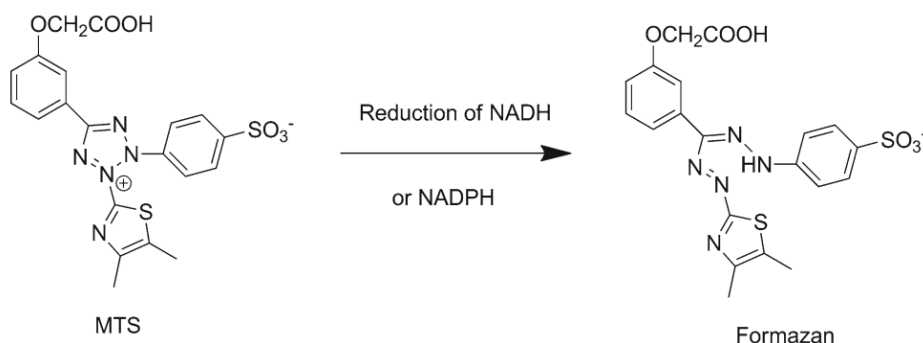


Figure 9: The reduction of MTS tetrazolium to formazan (48).

To evaluate the activity of samples at Marbio, the absorbance is used to calculate the percentage survival of healthy cells given as a score which corresponds to an activity-level (see **Table 2**).

Table 2: How the scores from the viability assay correspond to each category; active (A), questionable (Q) and inactive (I).

Category	Score (%)
A	< 50
Q	50-60
I	> 60

1.9.3 Anti-Bacterial Growth Assay

Antibiotic resistance is an increasing global problem and the need for new antibiotics is crucial (49). In research of new antibacterial agents, anti-bacterial growth assays are frequently used. Anti-bacterial growth assays are assays where bacterial cell proliferation is evaluated when exposed to samples. Cell proliferation of bacteria can be measured using absorbance spectrometry, where higher absorbance indicates a higher density of bacteria. If samples have anti-bacterial activity, the measured absorbance is low. The absorbance cut-off value for anti-bacterial activity at Marbio is given in **Table 3**.

Table 3: How the measured absorbance from the anti-bacterial growth assay correspond to each category; active (A), questionable (Q) and inactive (I).

Category	Score (abs)
A	< 0.05
Q	0.05-0.09
I	> 0.09

1.9.4 Immunoassay and ELISA

Immunoassays are assays where immune cells and antibodies are used to measure different biomarkers (50). In this thesis, inflammatory response will be measured utilizing the cytokine tumour necrosis factor alpha (TNF- α) as an inflammatory agent. The goal of the measurement is to either find compounds causing or inhibiting inflammatory response in cells. To evaluate the anti-inflammatory response, TNF- α secretion is induced in immune cells. If some of the samples inhibit TNF- α they will be considered as active. To evaluate the immunostimulatory response, TNF- α secretion is not induced. Here the samples will be considered active if the samples induce TNF- α secretion in the immune cells. The response is measured by conducting an assay called ELISA, where the amount of TNF- α after exposure to the samples is evaluated.

1.9.4.1 ELISA

Enzyme-linked immunosorbent assay (ELISA, **Figure 10**) is an assay based on interactions between antigens and antibodies (51). In this thesis, ELISA is conducted to evaluate the amount of active TNF- α present in samples. 96-well plates coated with TNF- α antibody are exposed to samples from an inflammatory assay. Active TNF- α in the samples will thereby bind to the antibodies before the TNF- α antibody is added to make a so-called ELISA-sandwich. Afterwards, antibody-binding reagents are added, resulting in a colour change based on the concentration of TNF- α in the samples. Absorbance is then measured to evaluate the degree of colour change.

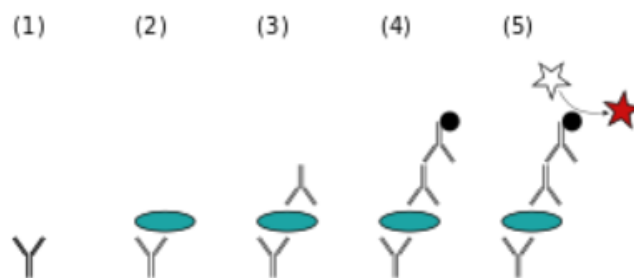


Figure 10: Illustration of the steps in ELISA; antibody (1), antibody coupled with antigen (2), ELISA-sandwich (3), antibody-binding reagents coupled with ELISA-sandwich (4) and antibody-binding reagents coupled with ELISA-sandwich resulting in colour change (5).

The measured absorbance in the wells is used to calculate the concentration of active TNF- α present in the samples, using a standard curve explaining the relationship between the variables. At Marbio, the concentration of TNF- α is then used to calculate a score which corresponds to an activity-level given in **Table 4**.

Table 4: How the scores from the immunoassay correspond to each category; active (A), questionable (Q) and Inactive (I).

	Anti-inflammatory	Immunostimulatory
Category	Score (%)	Score (%)
A	> 50	> 10
Q	40-50	5-10
I	< 40	< 5

2 Aim of the Thesis

The aim of the thesis was to use UHPLC-HRMS to compare the metabolic and lipidomic profiles of algal extracts (*Porosira glacialis*) prepared by two different extraction methods and to identify possible bioactive compounds in the same extracts. Multiple steps were needed to achieve this:

- Extraction of the diatom microalgae *Porosira glacialis* using two different extraction methods
- Acquiring UHPLC-HRMS data using two different analytical platforms
- Analyse the HRMS data and generate metabolic and lipidomic profiles of the different extracts
- Test extracts for bioactivity
- Dereplicate active extracts/fractions and isolate possible bioactive compounds

3 Materials and Methods

3.1 Extraction Method for Metabolomics

The extraction method prior to metabolomic analyses consisted of an aqueous SLE followed by an organic SLE. The equipment and chemicals used for the metabolomic extraction method are given in **Table 5**.

Table 5: Equipment and chemicals used for extraction, flash chromatography and LC-MS analyses.

Equipment and Chemicals	Specifications	Distributor
2-propanol		VWR Chemicals (Radnor USA)
Acetone		VWR Chemicals
Acetonitrile (MeCN)		VWR Chemicals
Centrifuge	Multifuge 3 S-R	Thermo Fisher Scientific (Waltham, USA)
Diaion® HP-20SS		Supelco® Analytical Products (Bellefonte, USA)
Dichloromethane (DCM)		VWR Chemicals
Dimethyl sulfoxide (DMSO)		Merck Life Science (Darmstadt, Germany)
Flash chromatographic instrument	Biotage SP4	Biotage (Uppsala, Sweden)
Freeze dryer	FreeZone®, Labconco	VWR Chemicals
Methanol (MeOH)		VWR Chemicals
Milli-Q water (MQ-water)		Merck Millipore (Burlington, USA)
Pipetboy		VWR Chemicals
Rotavapor	Laborota 4002 Control	Heidolph Instruments GmbH & Co. KG (Schwabach, Germany)

3.1.1 Aqueous Extraction

Microalgal biomass was weighed into a centrifugation bottle and extracted with Milli-Q (MQ) water (15 mL per g biomass) for 3 hours at 4 °C. The mixture was then centrifuged at 5 °C, 4600 rpm for 30 minutes and the supernatant was transferred to a Duran glass bottle for temporary storage, using a 25 mL pipetboy. The precipitate was reextracted with MQ-water for 30 minutes at 4 °C before centrifuged again at 5 °C, 4600 rpm for 30 minutes. The supernatant was transferred to the Duran glass bottle, while the precipitate remained in the centrifugation bottle. Both were stored at 4 °C overnight.

The next day the aqueous extract was distributed to 4 zip lock bags, while the precipitate was transferred to a Pyrex form and covered with aluminium foil. When rapidly freezing an aqueous sample, the volume of the sample will expand, resulting in minor explosions caused by trapped air, which could result in spillage of sample. Zip lock bags are well suited to reduce the risk of losing sample and make it easy to powder the extract after freeze drying by squeezing the bags.

It is also important to secure the possibility of gas exchange when freeze drying. Therefore, the zip lock bags were not completely locked, while some holes were poked in the aluminium foil. The zip lock bags and the Pyrex form were stored for 1.5 hours at -20 °C, followed by 2 hours in a -80 °C freezer, and then freeze dried for approximately 48 hours. After freeze drying, the aqueous extract was collected in a Duran glass bottle and stored at 4 °C until further use. The precipitate was stored at -20 °C until the organic extraction phase.

3.1.2 Organic Extraction

The freeze-dried microalgal precipitate was weighed and powdered as much as possible using a spatula to increase the surface area. The precipitate was then extracted with DCM:MeOH (1:1 v/v, 20 mL per g precipitate) at 4 °C for 20 hours. After extraction, the mixture was filtered with a Whatman filter paper using suction filtration. The supernatant was collected in a round flask, while the precipitate was reextracted with DCM:MeOH (1:1 v/v) at 4 °C for 1 hour. The mixture was filtered the same way as the first round, and the supernatant was collected while the precipitate was discarded. In the end, the supernatant was dried using a rotavapor, resulting in a completely dry organic extract. The organic extract was stored at 4 °C until further use.

3.2 Flash Chromatographic Method

3.2.1 Column and Extract Preparation

The columns prepared in this method are reverse phase columns consisting of a resin called Diaion® HP20-SS (75-150 µm). For each prepared column, 4 g of Diaion® HP-20SS was weighed and incubated with 75 mL MeOH in Erlenmeyer flasks for 20 minutes. After the incubation was complete, MeOH was removed by decantation from the Erlenmeyer flasks. A vacuum manifold was prepared for use by connecting a tap water hose to create vacuum, as well as attaching empty columns to the top of the manifold. A small amount of MQ-water was added to the empty columns before the columns were packed with column material. It was always ensured enough MQ-water (1 cm above column material) to prevent the columns from drying up when packing the columns. The prepared columns were stored at 4 °C until use.

The aqueous extract (3 g) was resuspended in 20 mL 90 % MeOH, while 3 g of the organic extract was resuspended in 25 mL acetone:DMSO (5:1). Both resuspension processes were carried out by rotation in a rotavapor with no vacuum at room temperature. When dissolution was achieved, 1.2 g of Diaion® HP-20SS was added to each of the extracts. The aqueous extract

was dried using a rotavapor. For the organic extract, acetone was evaporated using a rotavapor, before DMSO was evaporated by freeze drying overnight.

3.2.2 Chromatography

The dried sample-Diaion® HP-2SS mixture was loaded onto the pre-packed flash column by pouring into the headspace after equilibrating the column to the starting conditions of the flash gradient. The aqueous and organic extracts were loaded onto two separate columns in two separate chromatographic runs. The flash chromatographic instrument used was a Biotage SP4 system and a total of 27 filled test tubes were collected for the aqueous extract, while a total of 31 filled test tubes were collected for the organic extract. After completing flash chromatography, 3 to 6 test tubes were pooled and dried, yielding 8 fractions as illustrated in **Figure 11**. In the flash chromatographic method, a stepwise gradient was used for the mobile phase, where the strength of the mobile phase increased through the runtime. For test tubes 1 - 18 (yielding the finished fractions 1 - 6) a mixture of MeOH and MQ-water was used as mobile phase, while for test tubes 19 – 27 (yielding the finished fractions 7 and 8) a mixture of MeOH and acetone was used. At the end of the MeOH:MQ gradient, the UV detector of the flash system is set to prolong the final elution step. This caused the MeOH:MQ step to yield 22 filled test tubes in the organic extracts as opposed to the standard 19 test tubes illustrated in **Figure 11**. The extra 4 test tubes were pooled together with test tubes 16-18 to yield the finished fraction 6. The concentrations of the different solvents and an illustration of the flash chromatographic method is given in **Figure 11**.

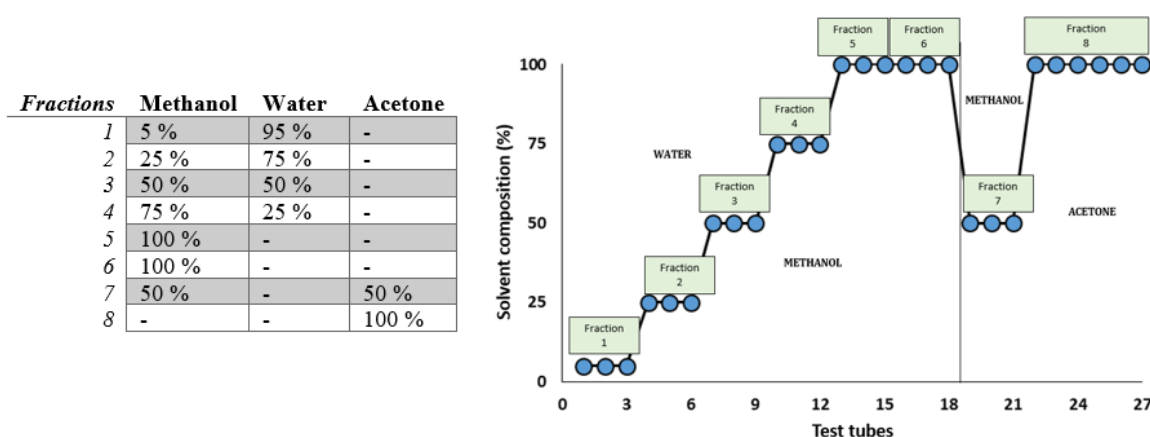


Figure 11: Solvent composition used as mobile phase and an illustration of the different fractions in the flash chromatographic method.

3.2.3 Drying the Fractions

The filled test tubes from the flash chromatography were transferred to 8 tared Polyvap-tubes, depending on which fraction the test tubes belonged to. The fractions were then dried in a Polyvap-instrument at 40 °C, 60 rpm under vacuum. When the fractions were dry, the Polyvap-tubes were weighed and the weight of the sample powder for each fraction was calculated. It was not possible to completely dry the organic fraction 1 using the Polyvap-instrument. Therefore, the remaining volume of the solvent in this fraction was removed by freeze drying overnight.

3.2.4 Dissolution of Fractions to Known Concentrations

Before mass spectrometric analyses and bioactivity testing, a minor preparation step was necessary, where the fractions were dissolved in DMSO to known stock concentrations. The amount of DMSO used for dissolution and the chosen concentration depended on the amount of recovered sample material for each fraction. Three different stock concentrations were used: 10 mg/mL, 40 mg/mL and 80 mg/mL. The calculated volumes of DMSO were pipetted and added to the polyvap-tubes. The polyvap-tubes containing sample material and DMSO were then placed on a shaker until complete dissolution. It was endeavoured to use at least a volume of 300 µL DMSO to ensure dissolution of as much as possible of the dried fractions.

3.3 Lipid Extraction Method for Lipidomics

3.3.1 Extraction

Freeze dried microalgal biomass (100 mg) was weighed in a glass tube, before being extracted with 2 mL DCM:MeOH (2:1 v/v). The mixture was gently shaken for a couple of minutes before 2 mL NaCl 5 % in MQ-water (w/v) was added. After some more gently shaking for a couple of minutes, the mixture was centrifuged for 5 minutes at 23 °C and 2000 G. When the centrifugation was complete, the aqueous phase was discarded using a pipette, while the organic phase was transferred to a tared round flask. The organic extract was then dried using rotary evaporation, and the yield was determined. The extract was stored at -20 °C until further use.

3.4 UHPLC-HRMS Methods

3.4.1 Preparation of Samples

The organic and the lipid extract were solved in isopropanol:MeOH (1:1) to a concentration of 1 mg/mL before metabolomic analyses, and 2.5 mg/mL before lipidomic analyses. The aqueous and organic fractions solved in DMSO were diluted with aqueous MeOH (50 %, v/v) to a concentration of 1.6 mg/mL prior to analyses.

3.4.2 Metabolomic Analysis (UHPLC-IMS-qToF)

3.4.2.1 UHPLC Method

A Waters Acquity I-class UHPLC was used to conduct the chromatographic separation of metabolites. The column used was a Waters Acquity BEH C₁₈ reverse phase column with a diameter of 2.1 mm, a length of 150 mm and a 1.8 µm particle size. A gradient elution program involving two different solvents was performed. Solvent A consisted of MQ-water, while solvent B consisted of acetonitrile (MeCN). Both solvents were modified with 0.1 % formic acid (CH₂O₂) to increase the degree of ionization of basic compounds. The starting composition of the mobile phase consisted of 90 % of solvent A and 10 % of solvent B, and there was a linear gradient until 12 minutes where the composition was 100 % of solvent B. From 12 to 13.50 minutes, the composition remained isocratic before the mobile phase changed back to starting conditions to equilibrate for the next analysis. The injection volume was 5 µL, the flow rate was 0.45 mL/minute, and the column temperature was 40 °C.

3.4.2.2 IMS-qToF Method

The metabolomic MS analyses were conducted using a Vion IMS-qTOF (Waters) with an incorporated ESI system. For the metabolomic comparison between the organic and the lipid extracts, the ESI was operated in positive mode, while for analyses of the fractions the ESI was operated in both positive and negative mode. In the MS² method the ions were set to collide with gaseous nitrogen in the collision chamber and the instrument was set to alternate between low collision energy (LCE, 5 eV) and high collision energy (HCE, 20-60 eV). LCE is used to retrieve low fragmentation data, while HCE is used to retrieve high fragmentation data. In total, the alternation setup gives a broad range of data beneficial for the identification of compounds. While the LCE has a static voltage, the HCE has a dynamic voltage with a gradual increase from 20 eV to 60 eV. The gradient ensures detection of ions fragmenting at all the intermedial voltages, instead of only detecting ions fragmenting at one selected static high voltage. The most vital parameters for the MS method are given in **Table 6**.

Table 6: Parameters associated with the IMS-qToF MS method.

IMS-qToF MS Parameters	Content/Value
Scan range (m/z)	150-2000
Ionization mode	Positive/Negative (+/-)
Cone voltage	30 V
Low collision energy (LCE)	5 eV
High collision energy (HCE)	20-60 eV
ESI source temperature	120 °C
Scan time	0.2 s
Collision gas	Nitrogen (N ₂)

3.4.2.3 Data Interpretation Method for Metabolomic Comparison

After all the metabolomic HRMS data were retrieved, it was imported to the software Progenesis QI. An alignment was performed where a list of markers was retrieved based on an algorithm ran by the software. The markers from the alignment were transferred to the statistical software EZInfo where general differences between the extracts were investigated. To dive deeper into the material a S-plot analysis comparing the organic and the lipid extract based on the variation and abundance of the markers was generated. Utilizing the S-plot, the markers with a relative variation > 0.05 were selected to closer investigate the markers contributing the most to the variation between the extracts. The selected markers concluded in a total of 64 potential compounds, 32 from the lipid extract and 32 from the organic extract. These selected compounds were then closely investigated utilizing Progenesis QI and UNIFI® software.

3.4.3 Lipidomic Analysis (UHPLC-Orbitrap MS)

3.4.3.1 UHPLC Method

A Thermo Scientific UHPLC system was used to conduct the chromatographic separation of the lipids. The column used was a Waters Acquity Premier C₁₈ reverse phase column with a diameter of 2.1 mm, a length of 100 mm and a 1.7 μ m particle size. A gradient elution program involving two different mobile phases was performed. Mobile phase A consisted of a mixture of MQ-water:MeCN (1:1 v/v), while mobile phase B consisted of 2-propanol:MeCN (1:1 v/v). Each mobile phase also contained 1 mM ammonium formate (NH₄FA) and 0.01 % formic acid (CH₂O₂). The gradient elution program consisted of a gradual increase in mobile phase strength (**Table 7 / Figure 12**). The injection volume was 2 μ L, the flow rate was 0.6 mL/minute, and the column temperature was 60 °C. The total analysis time for each injection was 30 minutes.

Table 7: The exact setup for the mobile phase gradient over time used in lipidomic analyses.

No	Time	Flow [ml/min]	%B	Curve
1	-2.500		Equilibration	
2	-2.500	0.600	30.0	5
3	0.000	0.600	30.0	5
4	New Row			
5	0.000		Run	
6	0.000	0.600	30.0	5
7	20.000	0.600	75.0	5
8	25.000	0.600	95.0	5
9	New Row			
10	30.000		Stop Run	



Figure 12: An illustration of the mobile phase gradient over time. Mobile phase A consisted of a mixture of MQ-water and acetonitrile (1:1), while mobile phase B consisted of 2-propanol:acetonitrile (1:1).

3.4.3.2 Orbitrap MS Method

The lipidomic MS analyses were conducted using a Thermo ID³ Tribrid Orbitrap MS (Thermo Scientific) with an ESI operating in positive mode. To acquire data for all lipids of interest, a data acquisition method set up in AcquireX was used. The method consisted of a full scan with a chosen m/z range between 250-1500. Three injections of the organic and the lipid extracts were analysed in full scan mode (6 in total). In addition, three injections of a blank sample (2-propanol:MeOH 1:1 v/v) were analysed to exclude possible contamination and five injections of the ID sample were analysed to retrieve fragmentation data. The full scan parameters are given in **Table 8**.

Table 8: Parameters used in the MS full scan orbitrap method.

Orbitrap MS Parameters	Content/Value
Scan range (m/z)	250-1500
Ionization mode	Positive (+)
Orbitrap resolution	120 000

MS² HCD-fragmentation was conducted on the ions present in the ID-sample which had an intensity over 1×10^5 acquired from the full scans. Depending on the acquired data from the HCD-fragmentation, the precursor ions would take one of two pathways (**Figure 13**). If the instrument detected a m/z value corresponding to a PC head group MS² CID-fragmentation was initiated on the precursor ion to acquire additional fragmentation of one of the FAs associated with the lipid (left pathway). On the other hand, when a m/z value corresponding to a neutral

loss from a TG ion was detected, a MS³ CID-fragmentation was initiated on the fragment to acquire additional fragmentation of two of the FAs in the TG (right pathway). To ensure fragmentation of multiple precursor ions, an exclusion list was continuously updated to exclude precursor ions where fragmentation data already were acquired. Utilizing this fragmentation setup in AcquireX secured valuable fragmentation data for full identification of lipids.

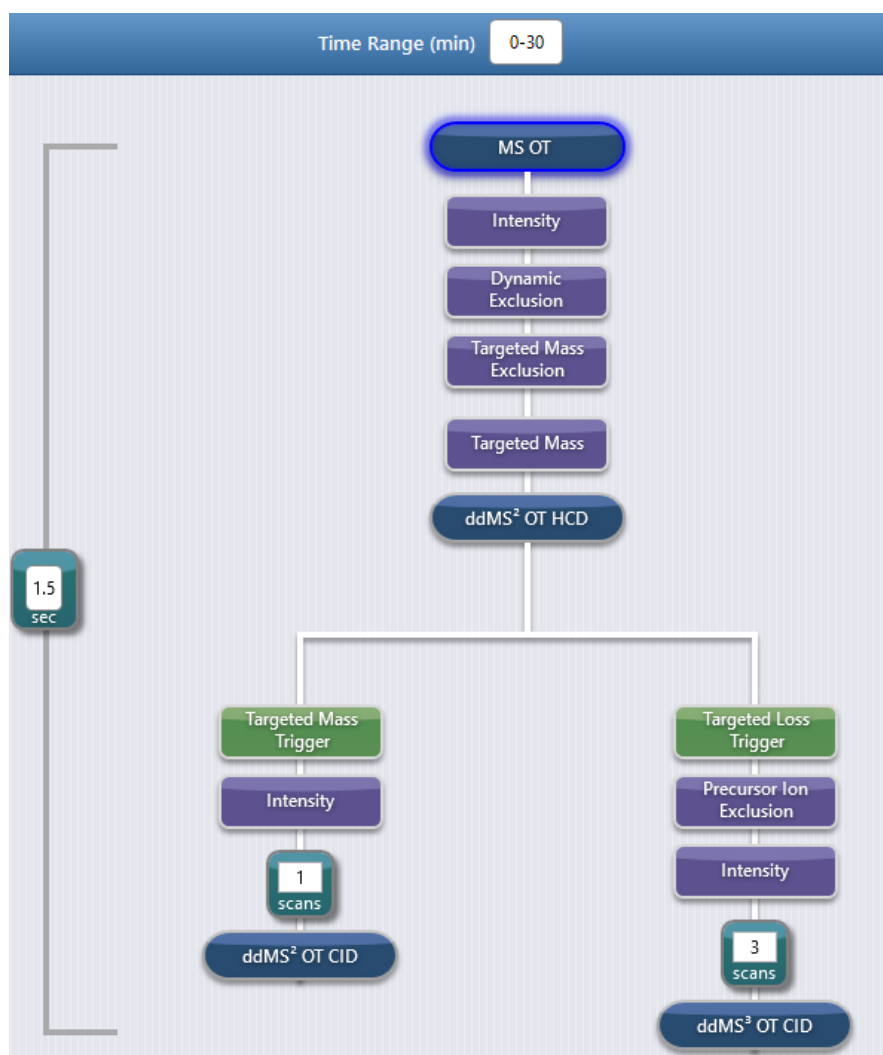


Figure 13: The mass spectrometric method performed on the orbitrap. The illustration shows how the MSⁿ method is setup to acquire information for lipid identification.

3.4.3.3 Data Interpretation Method for Lipidomic Comparison

After all the lipidomic HRMS data was retrieved, it was imported to LipidSearch where an alignment of the data was conducted. LipidSearch was further used to generate plots and to investigate fragmentation patterns of the retrieved data.

3.5 Bioassays

Table 9: Equipment and chemicals used in bioassays.

Equipment and Chemicals	Distributor
Anti-Human TNF alpha biotin	Thermo Fisher Scientific
Anti-Human TNF alpha purified	Thermo Fisher Scientific
CellTiter 96® AQOS one solution reagent	Promega, WI, USA
Aquamax4000 plate washer	Molecular Devices LLC (San Jose, USA)
Blood agar plates	SUMP Media Kitchen UNN (Tromsø, Norge)
Bovine serum albumin (BSA)	Merck Life Science
Brain Heart Infusion (BHI)	Sigma Aldrich (Saint-Louis, USA)
Bürker counting chamber	VWR Chemicals
Crystal violet solution 1 %	Merck Life Science
Deep well plate (DWP)	VWR Chemicals
Dimethyl sulfoxide (DMSO)	Merck Life Science
Dulbecco's modified eagle's medium (DMEM)	Merck Life Science
Electronic multi-channel pipettes	Thermo Fisher Scientific
Erlenmeyer flask	VWR Chemicals
Extravidine-alkaline phosphatase	Merck Life Science
Falcon tubes	VWR Chemicals
Fetal bovine serum (FBS)	VWR Chemicals
Fetal bovine serum (FBS), low endotoxin	Biochrom (Cambridge, United Kingdom)
Gentamycin	VWR Chemicals
Glucose	Sigma Aldrich
Glutamine stable 200 nM	VWR Chemicals
Glycine	Merck Life Science
Human TNF alpha recombinant protein	Thermo Fisher Scientific
Incubator 37 °C	Panasonic Healthcare (Chicago, USA)
Inoculation loop	VWR Chemicals
Lipopolysaccharide (LPS)	Sigma Aldrich
Microtiter plates	VWR Chemicals
Milli-Q water (MQ-water)	Merck Millipore
Mueller-Hinton (MH) broth	Difco (Corpus Christi, USA)
Nunc Maxisorp 96F well plate	VWR Chemicals
Phorbol myristate acetate (PMA)	Sigma Aldrich
Phosphatase substrate (pNPP)	Merck Life Science
Phosphate buffer saline (PBS)	Sigma Aldrich
Pipetboy	VWR Chemicals
Roswell Park Memorial Institute (RPMI) 1640, low endotoxin	Biochrom
Shaking incubator	Heidolph Instruments GmbH & Co. KG
Tecan Spark plate reader	Tecan Trading AG (Mannedorf, Switzerland)
Trisaminomethane (TRIS)	Merck Life Science
Trypan blue	VWR Chemicals
Trypsin	VWR Chemicals
Tryptic Soy Broth (TSB)	Merck Millipore
Victor Multilabel Counter	PerkinElmer (Waltman, USA)

Table 10: Pathogens and cell-lines used in bioassays.

Pathogens	Distributor, product number
<i>Enterococcus faecalis</i>	LGC Standards (Teddington, United Kingdom), ATCC 29212
<i>Escherichia coli</i>	LGC Standards, ATCC 25922
Human melanoma A2058	LGC standards, ATCC CRL-1147
Human monocyte THP-1	LGC Standards, ATCC TIB-202
<i>Pseudomonas aeruginosa</i>	LGC Standards, ATCC 27853
<i>Staphylococcus aureus</i>	LGC Standards ATCC 25923
<i>Staphylococcus epidermidis</i> (RP62A 42-77)	LGC Standards ATC 35984
<i>Staphylococcus haemolyticus</i> (clinical isolate 8-7A)	Host-microbe interaction research group UiT, (Tromsø, Norway)
<i>Streptococcus agalactiae</i>	LGC Standards, ATCC 12386

3.5.1 Bioassays Preparation

Before conducting an assay, a deep well plate (DWP) containing all the different fractions was prepared. This included eight organic fractions (org1 – 8) and eight aqueous fractions (aq1 – 8). MQ-water was used to dilute DMSO stock solutions of all the fractions to 1 mg/mL in the DWP.

When working with cells and bacteria, it is important to secure as sterile conditions as possible, to prevent contamination of the samples. Therefore, all precarious work was conducted in a class II sterile cabinet. A sterile workflow, such as using ethanol to sterilize all the equipment was also performed.

It is known from previously conducted lab work that human cells can tolerate a concentration of 0.25 % DMSO. Since the fractions are solved in DMSO, it is important to secure sufficient dilution to prevent an undesirable effect on the cells. For the aq5 - 8, it was only possible to lower the DMSO concentration to 1 % in the assays, because of the low amount of recovered sample. Therefore, a negative control containing 1 % DMSO had to be included in assays involving human cells to observe the influence of DMSO.

3.5.2 Inhibition of Biofilm Formation Assay

3.5.2.1 Preparation of Pathogens

The pathogens used in this assay were *Staphylococcus epidermidis* and *Staphylococcus haemolyticus*. *S. epidermidis* is a biofilm-producing specie, while *S. haemolyticus* does not produce biofilm. The pathogens were collected from a biofreezer (-80 °C) and streaked on blood agar plates as shown in **Figure 14**. The streaked blood agar plates were incubated at 37 °C overnight.

The next day, one colony of *S. epidermidis* and one colony of *S. haemolyticus* from blood agar plates were transferred to two separate falcon tubes containing 5 mL growth medium consisting of tryptic soy broth (TSB). The falcon tubes were then incubated at 37 °C, 100 rpm for approximately 20 hours.

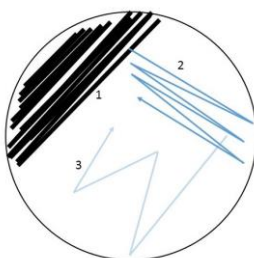


Figure 14: How pathogens were streaked on blood agar plates.

3.5.2.2 Conducting the Assay

Each 1 mg/mL fraction (20 µL) was transferred from the earlier prepared DWP to a microtiter plate and diluted with MQ-water to a concentration of 200 µg/mL. Each diluted fraction (50 µL) was further transferred in triplets to the wells in columns 1-6 in a new microtiter plate. For the remaining empty wells, 50 µL MQ-water was added.

When the fractions had been added to the microtiter plate, the next step was to add the pathogens. First, 10 mg/mL glucose in growth medium was prepared and autoclaved as diluent, before both the *S. haemolyticus* and the *S. epidermidis* overnight culture were diluted 1:10. Secondly, 50 µL of diluted *S. haemolyticus* overnight culture was transferred to column 11, while 50 µL diluted *S. epidermidis* overnight culture was transferred to column 1-10 of the microtiter plate using a multichannel pipette (**Table 11**). Lastly, 50 µL 10 mg/mL glucose in culture medium was added to column 12 as a blank. The microtiter plate containing bacteria, growth medium and 100 µg/mL of the fraction was then incubated at 37 °C overnight.

Table 11: An overview of the microtiter plate in the inhibition of biofilm assay. Column 1-6 are test columns where samples are added. 1-1 indicates the first fraction of the aqueous extract, while 2-1 indicates the first fraction of the organic extract. Column 7-10 are positive controls and column 11 is a negative control, while column 12 is a blank.

	1	2	3	4	5	6	7	8	9	10	11	12		
A	1-1	1-1	1-1	2-1	2-1	2-1	<i>S. epidermidis</i> (biofilm producer)				<i>S. haemolyticus</i> (not biofilm producer)		Medium blank	
B	1-2	1-2	1-2	2-2	2-2	2-2								
C	1-3	1-3	1-3	2-3	2-3	2-3								
D	1-4	1-4	1-4	2-4	2-4	2-4								
E	1-5	1-5	1-5	2-5	2-5	2-5								
F	1-6	1-6	1-6	2-6	2-6	2-6								
G	1-7	1-7	1-7	2-7	2-7	2-7								
H	1-8	1-8	1-8	2-8	2-8	2-8								

To retrieve the results of the assay, some small preparation steps had to be done. First, the absorbance of all the wells in the microtiter plate was measured on a Victor plate reader, to control for bacterial growth. Afterwards, the microtiter plate was turned upside down and tapped dry against cell paper. Every well was then rinsed carefully with tap water two times repeatedly, before tapped dry again. The biofilm was then fixated at 65 °C for 1 hour. After fixation, all wells were stained with 70 µL 0.1 % crystal violet solution for 5 minutes. The crystal violet solution was then removed, and the wells were rinsed two times with tap water before tapped dry. Aqueous ethanol 70 % (70 µL) was added to all wells and incubated on a shaker for 5 minutes. The absorbance for all wells was then measured using a Victor plate reader to evaluate biofilm formation.

3.5.3 Anti-bacterial Growth Assay

3.5.3.1 Preparation of Pathogens

In this assay, *Enterococcus faecalis*, *Escherichia coli*, *Pseudomonas aeruginosa*, *Staphylococcus aureus* and *Streptococcus agalactiae* were used as pathogens. The pathogens were streaked on separate blood agar plates as illustrated in **Figure 14**, and incubated at 37 °C overnight. The next day a scoop of each pathogen from blood agar plates was transferred to separate falcon tubes containing 8 mL growth medium. Mueller-Hinton (MH) broth was used as growth medium for *E. coli*, *P. aeruginosa* and *S. Staphylococcus*, while brain heart infusion (BHI) medium was used for *E. faecalis* and *S. agalactiae*. Each bacterial culture was then incubated at 37 °C for 20 hours.

3.5.3.2 Conducting the Assay

Each 1 mg/mL fraction (20 µL) was transferred from the earlier prepared DWP to a microtiter plate and diluted with MQ-water to a concentration of 200 µg/mL. The diluted fractions (50 µL) were then transferred in duplicates to column 2-11, while 50 µL MQ-water was added to column 1 and 12 (**Table 12**). Growth medium (50 µL) was then added to column 1, resulting in a blank control.

One microtiter plate for each pathogen was prepared. Each prepared overnight culture (2 mL) was transferred to Erlenmeyer flasks containing 25 mL growth media and incubated at 37 °C, 100 rpm for 1.5-2.5 hours. Afterwards, the bacterial suspensions were diluted 1:1000 with growth media, before 50 µL was added to column 2-12. The addition of bacterial suspension

dilutes the fraction concentration to 100 µg/mL. In the end, each prepared microtiter plate was incubated at 37 °C overnight.

In addition to the sample plates, a gentamycin positive control microtiter plate was prepared, where a dilution series from 0.02 µg/mL to 16 µg/mL of gentamycin was tested for each pathogen.

Table 12: An overview of the microtiter plates in the anti-bacterial growth assay. Column 2-11 are test columns, column 1 is a medium blank and column 12 is a negative control. 1-1 indicates the first fraction tested against the first bacterial strain, while 2-1 indicates the first fraction tested against the second bacterial strain. Separate microtiter plates were prepared for each extract.

	1	2	3	4	5	6	7	8	9	10	11	12
A	Medium blank	1-1	1-1	2-1	2-1	3-1	3-1	4-1	4-1	5-1	5-1	Growth control
B		1-2	1-2	2-2	2-2	3-2	3-2	4-2	4-2	5-2	5-2	
C		1-3	1-3	2-3	2-3	3-3	3-3	4-3	4-3	5-3	5-3	
D		1-4	1-4	2-4	2-4	3-4	3-4	4-4	4-4	5-4	5-4	
E		1-5	1-5	2-5	2-5	3-5	3-5	4-5	4-5	5-5	5-5	
F		1-6	1-6	2-6	2-6	3-6	3-6	4-6	4-6	5-6	5-6	
G		1-7	1-7	2-7	2-7	3-7	3-7	4-7	4-7	5-7	5-7	
H		1-8	1-8	2-8	2-8	3-8	3-8	4-8	4-8	5-8	5-8	

To retrieve the results for the assay, the absorbance was measured using a Victor plate reader. Visual inspection of the microtiter plates was also conducted in case of contamination or insufficient growth.

3.5.4 Viability Assay

3.5.4.1 Preparation of Cell Culture

Cell culture media and a 50 mL falcon tube containing MQ-water were prewarmed to 37 °C. The cell culture media consisted of Dulbecco's modified eagle's medium (DMEM), fetal bovine serum (FBS), Gentamycin and stable Glutamine. The cell line A2058 stored in an ampoule in a biofreezer (-80 °C) was collected and transferred to the prewarmed MQ-water. When the cells had been thawed, 1 mL was transferred to a 50 mL Falcon tube and 9 mL cell culture media was added. The cells in the falcon tube were centrifuged at 150 G for 5 minutes. After centrifugation the supernatant was removed and the cells were resuspended in 15 mL cell culture media, before being transferred to a cell culture flask. The cells were incubated at 37 °C with 5 % CO₂.

3.5.4.2 Maintaining the Cell Culture

The cells must always have space to grow, to prevent them from adjusting their metabolism. The cells were therefore monitored daily using microscopy. When there was no more space to grow, the cells were split to maintain their metabolic properties. Firstly, the cell culture media was carefully removed from the cell culture flask, without damaging the cell layer. Secondly, the cell layer was carefully washed with phosphate buffer saline (PBS) without detaching the cells from the flask before trypsin was added to initiate the detachment. Excessive trypsin was removed while ensuring that the whole cell layer was covered in trypsin. With the help of microscopy, it was ensured that all the cells had detached. The cells were then resuspended in 10 mL culture media, and 1 mL of cell suspension was transferred to a new culture media flask to maintain the cell culture. New culture media (9 mL) was added, before incubation at 37 °C with 5 % CO₂.

3.5.4.3 Conducting the Assay

The first step was to add the cells in a known concentration to a microtiter plate. Trypan blue (100 µL) and cell suspension (100 µL) were mixed. The mixture (10 µL) was added to a Bürker counting chamber and the cells were counted under a microscope for cell counting. The counted number of cells was used to calculate the volume of cell suspension needed to make a desirable concentration of cell suspension. The volume of cell suspension needed to produce the correct assay concentration of the cells will vary both between each passage of a cell culture and between different cell types. In this case, 240 µL cell suspension was diluted with 15 mL cell culture media. Using a multichannel pipette 100 µL of diluted cell suspension was added to each well and incubated overnight at 37 °C with 5 % CO₂.

The second step was to add the samples to the microtiter plate. The cells were observed under a microscope to control attachment to the bottom of the wells. Afterwards, the cell culture media in all the wells was removed carefully, to prevent detachment of the cells. Using a multichannel pipette, 95 µL culture media was added to column 1-10 and 90 µL was added to column 12. In addition, 100 µL cell culture media was added to column 11 as a negative control. The samples (5 µL) were added as triplets to column 2-9 as illustrated in **Table 13**, creating a final sample concentration of 50 µg/mL. 10 µL DMSO was added to column 12 as a 10 % DMSO positive control. DMSO 10 % (5 µL) was added to column 10 as an additional negative control making a DMSO concentration of 0.5 %. Some of the samples contained 0.5 % DMSO, and it was therefore necessary to control that this concentration of DMSO didn't influence the cells. After

all samples were added to the microtiter plate, it was incubated at 37 °C with 5 % CO₂ for 72 hours.

Table 13: An overview of the microtiter plate in a viability assay. Column 2-9 are test columns, while column 10-12 are control columns. The samples are added as triplets. 1-1 represents the first fraction in the aqueous extract, while 2-1 indicates the first fraction in the organic extract.

	1	2	3	4	5	6	7	8	9	10	11	12
A												
B		1-1	1-2	1-3	1-4	1-5	1-6	1-7	1-8	0.5 % DMSO (negative control)	Cell control (negative control)	10 % DMSO (positive control)
C		1-1	1-2	1-3	1-4	1-5	1-6	1-7	1-8			
D		1-1	1-2	1-3	1-4	1-5	1-6	1-7	1-8			
E		2-1	2-2	2-3	2-4	2-5	2-6	2-7	2-8			
F		2-1	2-2	2-3	2-4	2-5	2-6	2-7	2-8			
G		2-1	2-2	2-3	2-4	2-5	2-6	2-7	2-8			
H												

To retrieve the results, 1 mL of AQOS one solution (containing the MTS salt) was prepared in a reservoir. Using a multichannel pipette, 10 µL AQOS one solution was added to each well in the microtiter plate. The plate was then incubated for 1.5 hours, and a visual inspection was performed. The absorbance of each well was then measured using a Tecan spark plate reader.

3.5.5 Immunoassay

The cell line used in the assay was Thp-1 cells, which are very sensitive, and it was therefore important to use pure substances when conducting the assay. Endotoxins have earlier been measured to induce a slight inflammatory response in Thp-1 cells, which makes it necessary to use substances containing endotoxins under the detection limit set to < 0.01 EU/mL (Endotoxin units / mL).

3.5.5.1 Preparation of Assay

Cell culture medium consisting of Roswell Park Memorial Institute (RPMI) 1640 medium with added 10 % FBS was prewarmed to 37 °C. Thp-1 cells were visually inspected under a microscope before centrifuged in a 50 mL Falcon tube at 150 G for 5 minutes. The old cell culture medium was removed, and the cells were resuspended in 25 mL of the new prewarmed medium. The cell suspension (50 µL) was transferred to a Cryotube with 450 µL trypan blue and mixed. The mixture (10 µL) was then transferred to a Bürker counting chamber, and the number of living cells was counted under a microscope using a protocol for cell counting. The counted number of cells was then used to make a cell suspension with a 10⁶ cells/mL density.

Cell suspension (10 per microtiter plate) was prepared, and 0.5 μL 50 ng/mL phorbol myristate acetate (PMA) was added to the suspension. PMA is used to differentiate Thp-1 cells into macrophages, which are cells that give inflammatory response when triggered. The cell suspension (100 μL) was added to each well in a microtiter plate and the cells were then incubated at 37 $^{\circ}\text{C}$, 5 % CO_2 for 48 hours. After incubation, the differentiation of the cells was controlled under a microscope before the cells were washed with endotoxin-tested PBS. In the end, 100 μL of new culture media without PMA was added to each well, followed by a 24-hour incubation at 37 $^{\circ}\text{C}$ with 5 % CO_2 .

3.5.5.2 Adding Samples

Before the fractions could be added, the old cell culture medium had to be removed. The fractions and new prewarmed culture medium were then added to the wells according to **Table 14**, and incubated for 1 hour at 37 $^{\circ}\text{C}$, 5 % CO_2 . For the anti-inflammatory assay lipopolysaccharide (LPS) was added to all columns except cell control columns. For the immunostimulatory assay, LPS was only added to the LPS control wells. LPS solution is known to stimulate inflammatory response (52), which is desired in the anti-inflammatory assay and not in the immunostimulatory assay. The test concentration was 50 $\mu\text{g}/\text{mL}$ and the LPS concentration was 1 ng/mL in wells with a total volume of 100 μL . In the end, the microtiter plates were incubated at 37 $^{\circ}\text{C}$, 5 % CO_2 for 6 hours, before being transferred to a -80 $^{\circ}\text{C}$ biofreezer and stored until the start of the ELISA.

Table 14: An overview of the microtiter plate in an immunoassay. Column 2-9 are test columns, while column 10-12 are control columns. The samples are added as triplets. 1-1 indicates the first fraction in the aqueous extract, while 2-1 indicates the first fraction in the organic extract.

	1	2	3	4	5	6	7	8	9	10	11	12
A										<i>LPS control</i>	<i>Cell control</i>	
B		1-1	1-2	1-3	1-4	1-5	1-6	1-7	1-8			
C		1-1	1-2	1-3	1-4	1-5	1-6	1-7	1-8			
D		1-1	1-2	1-3	1-4	1-5	1-6	1-7	1-8			
E		2-1	2-2	2-3	2-4	2-5	2-6	2-7	2-8			
F		2-1	2-2	2-3	2-4	2-5	2-6	2-7	2-8			
G		2-1	2-2	2-3	2-4	2-5	2-6	2-7	2-8			
H												

3.5.5.3 Conducting ELISA

Two Nunc Maxisorp 96F-well plates (96F-WPs) were coated with TNF- α by adding 100 μ L 2 μ g/mL anti-human TNF- α to the wells, followed by incubation at 4 °C overnight. The next day, the fraction microtiter plates were taken out of the -80 °C biofreezer and left at 23 °C to thaw. The TNF- α coated 96F-WPs were washed using an Aquamax4000 plate washer. Afterwards, 200 μ L of a blocking buffer consisting of trisaminomethane and bovine serum albumin (10 mM TRIS with 2 % BSA) was added and incubated on a shaker for 1 hour to prevent TNF- α and TNF-antibody binding to the bottom of the wells in later steps. The 96F-WPs were then once again washed using Aquamax4000.

The fractions from the tawed microtiter plate with LPS were added to one 96F-WP, while the fractions from the tawed microtiter plates without LPS were added to the other 96F-WP. The LPS-controls (5 μ L) and the cell controls (50 μ L) were also added to the plates, in addition to a dilution series of TNF- α (see **Table 15**). An assay buffer consisting of 10 mM TRIS buffer with 1 % BSA was used as dilution medium in the wells, and all wells contained a total volume of 100 μ L. The fraction with added LPS was diluted 1:20, while fractions without LPS were diluted 1:2. After the addition of the fractions, the microtiter plates were incubated at 23 °C for 2 hours, before being washed in the Aquamax4000.

Table 15: An overview of the microtiter plate when conducting ELISA. Column 1-8 are test columns, column 9-10 are control columns and column 11-12 are used for the TNF- α dilution series.

	1	2	3	4	5	6	7	8	9	10	11	12
A	1-1	1-1	2-1	2-1	3-1	3-1	4-1	4-1	LPS control 1	Cell control 1	2000 pg/mL	
B	1-2	1-2	2-2	2-2	3-2	3-2	4-2	4-2			1000 pg/mL	
C	1-3	1-3	2-3	2-3	3-3	3-3	4-3	4-3			500 pg/mL	
D	1-4	1-4	2-4	2-4	3-4	3-4	4-4	4-4			250 pg/mL	
E	1-5	1-5	2-5	2-5	3-5	3-5	4-5	4-5	LPS control 2	Cell control 2	62.5 pg/mL	
F	1-6	1-6	2-6	2-6	3-6	3-6	4-6	4-6			31.3 pg/mL	
G	1-7	1-7	2-7	2-7	3-7	3-7	4-7	4-7			15.6 pg/mL	
H	1-8	1-8	2-8	2-8	3-8	3-8	4-8	4-8			Blank 0 pg/mL	

After the microtiter plates were washed, 100 μ L of 3 μ g/mL anti-human TNF- α biotin in assay buffer was added to all wells, followed by another washing step in the Aquamax4000. The microtiter plates were then incubated at 23 °C on a shaker for 1 hour, before 100 μ L of EtrAvidin-alkaline phosphatase diluted 1:2000 in assay buffer was added to all wells. The microtiter plates were then incubated on a shaker at 23 °C for 30 minutes. A soak wash program was then run on the microtiter plates using the Aquamax4000. Soak wash is a more thorough

washing step with a 4-minute washing time. After the soak wash, 100 μL of 1 mg/mL phosphatase substrate (pNPP) substrate in glycine buffer was added, followed by incubation at 23 $^{\circ}\text{C}$ for at least 30 minutes. In the end, the absorbance at 405 nm was measured in a Tecan Spark plate reader.

3.6 Dereplication Method for Metabolomic Analyses

Dereplication was done using UNIFI[®]. To identify some of the 64 compounds provided by Progenesis IQ, the m/z -value and R_t were used to locate the same compounds in UNIFI[®]. When a compound was located, the isotope pattern was investigated to decide what atoms to include in the search in databases for known compounds. If the pattern did not match the isotope patterns for chloride and bromide, these atoms were excluded from the search. The adduct chosen for the search was either protonated or deprotonated depending on which ionization mode used in the analysis. The most vital search parameters are listed in **Table 16**.

Table 16: The most vital search parameters for dereplication in UNIFI[®]

Search parameter	Value
Selected Adducts	-H / +H
Selected elements	C, H, N, O, P, S, (F, Cl, Br)
m/z tolerance	2 mDa
Minimum i-FIT confidence	10 %
Minimum double bond equivalents (DBE)	-1.5
Maximum DBE	50
ChemSpider libraries	All

When investigating the bioactivity observed in the tested fractions UNIFI[®] was used for dereplication. The strategy was to compare the chromatograms of active fractions to chromatograms of non-active fractions. Visible peaks in the active fractions not observed in non-active fractions were closely investigated. Comparison mode in UNIFI[®] was used to visualize differences between extracts, as well as generate a list of possible differences utilizing the software algorithm. The m/z -value and R_t of peaks in active fractions were used to specifically search for the compounds in non-active fractions. The bioactivity in aq5 and org7 were dereplicated, where the top bioactivity candidate from aq5 was selected for isolation. To be a good candidate for isolation, the peak had to be narrow and well separated from other peaks.

3.7 Isolation and Bioactivity Testing of Top Candidate

3.7.1 Isolation Preparation of the Aqueous Extract

The freeze-dried aqueous extract (2.1047 g) was dissolved as much as possible in 100 mL of 90 % MeOH (v/v) in an Erlenmeyer flask. Using a pipetboy, the mixture was transferred to 4 separate falcon tubes and centrifuged at 4000 rpm for 5 minutes. The supernatant was then transferred to a round flask and the sample was evaporated using rotary evaporation to almost dryness. This process was repeated for the remaining unsolved aqueous extract. After centrifugation, the second supernatant was combined with the first supernatant in the round flask and the total sample was dried to almost dryness. The sample was transferred to a new falcon tube using a glass pipette. MeOH (5 mL) was used to secure transfer of as much sample as possible to the falcon tube from the round flask. The sample was centrifuged at 4000 rpm for 5 minutes, and the supernatant was stored in a falcon tube at 4 °C until isolation on preparative HPLC.

3.7.2 Isolation Method

The isolation was conducted using a preparative-HPLC-MS system consisting of a 600 HPLC Pump, a 2996 Photodiode Array UV detector, a 3100 Mass detector, and a 2767 sample manager (Waters, MA, USA). The column used was an XSELECT™ CSH™ Prep Fluorophenyl column (**Figure 15**) with a diameter of 10 mm, a length of 250 mm and a 5 µm particle size (Waters).

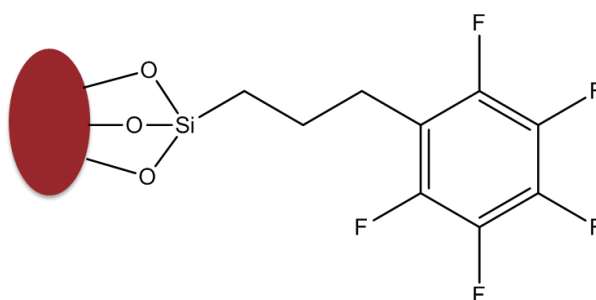


Figure 15: The structure composition of a fluorophenyl column.

A gradient elution program involving two mobile phases was used. Mobile phase A was MQ-water with 0.1 % formic acid, while mobile phase B was MeCN with 0.1 % formic acid delivered as a gradient over 15 minutes, starting with 10 % B and ending with 100 % B, followed by 100 % B over 5 minutes before returning to start conditions, all at a 6 mL/minute flow rate. The instrument was set to collect eluate when a m/z -value at 338.5 was detected for isolation of the compound of interest. The injection volume was 200 µL for each run. The

isolation method was performed multiple times in an attempt to recover enough sample for NMR analysis and bioactivity testing. After isolation, the isolate was dried in a tared round bottle using a rotary evaporator.

3.7.3 Bioactivity Testing of the Isolate

The isolate was dissolved in 20 μL DMSO and transferred to a cryotube. The viability assay was prepared, and five different concentrations (3.13, 6.25, 12.5, 25 and 50 $\mu\text{g}/\text{mL}$) were tested in triplicates against the human melanoma A2058 cancer cell line by the head engineer at Marbio. In short, the cell culture was prepared as described in section 3.4.4.1. and the assay was conducted as described in section 3.5.4.3., with some minor modifications. In brief, 10 μL containing the isolate at 10x assay concentration was transferred to each assay well. The assay well contained 90 μL cell medium with adherent cells attached to the bottom, thus diluting the sample to the desired assay concentration. An overview of the microtiter plate for the bioactivity testing of the isolate is given in **Table 17**.

Table 17: An overview of the microtiter plate set up for testing the anti-cancer activity against melanoma A2058 cancer cells for the isolated compound. Five different concentrations were tested in triplicates (50, 25, 12.5, 6.25 and 3.125 $\mu\text{g}/\text{mL}$) in column 8-10. Column 11 is a negative control, while column 12 is a positive control.

	1	2	3	4	5	6	7	8	9	10	11	12
A												
B		No added samples (blanks)						50	50	50	Cell control (negative control)	10 % DMSO (positive control)
C								25	25	25		
D								12.5	12.5	12.5		
E								6.25	6.25	6.25		
F								3.125	3.125	3.125		
G								0	0	0		
H												

4 Results and Discussion

4.1 Recovery of Extracts and Fractions

Two different extraction methods were used, resulting in a lipid extract, an organic and an aqueous extract. The organic and the lipid extracts were directly compared to each other before the aqueous and the organic extracts were fractionated prior to bioactivity testing and dereplication.

4.1.1 Recovery of Extracts

The recovery was 9.4 % (one parallel) for the lipid extract, 10.6 % (average of two parallels) for the organic extract and 45.1 % (one parallel) for the aqueous extract. When comparing the recovery between organic and the lipid extraction methods, a higher recovery was observed in the organic extraction method. Since a more polar extraction medium was used in the organic extraction compared to the lipid extraction, it is plausible that there is a greater contribution of more polar compounds in the organic extraction compared to the contribution of more lipophilic compounds in the lipid extraction. To investigate if the difference in recovery is reproducible, multiple extractions must be carried out and compared. The recovery of the aqueous extract can be considered high, where visual inspections suggested a high abundance of salts and fibres.

4.1.2 Recovery of Fractions

The recovery of fractions obtained from the organic and the aqueous extract is summarized in **Table 18**. In general, the recovery was higher for the organic fractions compared to the aqueous fraction, except aq1. Visual inspection of aq1 revealed that this fraction contained a lot of salt, which made complete dissolution of this fraction difficult and therefore an uncertain calculation of the concentration. It also seemed like the column was overloaded during flash fractionation of the aqueous extract, which resulted in elution of excessive components in aq1. During dissolution of org6 - 8, it was assumed that the fractions reached saturation before fully dissolved in DMSO. The colours of these fractions were dark, almost black, which suggested a high concentration of compounds.

Table 18: An overview of the different stock concentrations, the amount of recovered sample material and the volume of solvent DMSO for each fraction.

Fraction	Stock Concentration (mg/mL)	Sample material (mg)	Volume DMSO (µL)
Aq1	80	2523.1**	5046
Aq2	80	82.9	1036.5
Aq3	40	44.8	1120
Aq4	40	18.7	467.5
Aq5	10	7.7	770
Aq6	10	3.2	320
Aq7	10	3.0	300
Aq8	10	2.9	290
Org1	80	162.9	2036
Org2	40	77.3	1933
Org3	40	34.0	850
Org4	40	31.2	780
Org5	80	252.9	3161
Org6	80*	652.1	8151
Org7	80*	580.1	7251
Org8	80*	337.7	4221
<p><i>*Not completely dissolved due to saturation.</i> <i>**Contained a lot of salt, which makes calculations uncertain.</i></p>			

4.2 Comparing the Extraction Methods

For a more in-depth comparison of the extraction methods, metabolomic and lipidomic analyses were conducted to compare the contents of the extracts. It was only considered valuable to compare the lipid extract to the organic extract, and thereby exclude the aqueous extract. This is because the aqueous extract is inherently different to the others, which makes this kind of comparison excessive, especially in the lipidomic comparison.

4.2.1 Metabolomic Comparison

A visual chromatographic comparison between the organic and the lipid extracts analysed in positive mode is shown in **Figure 16**. In general, the peak distribution looks similar, but some peaks had higher signal intensity in one or the other extract. Importantly, the signal intensity is not directly related to compound concentration. Signal intensity depends on the degree of ionization, which varies between compounds. This means that a compound with a low degree of ionization could be more abundant than what the signal intensity portrays. In addition, matrix differences can be influential for the degree of ionization, resulting in differences in observed signal intensities between extracts. Differences in signal intensity between the extracts can be influenced by matrix differences, as well as random sampling handling errors prior to injection.

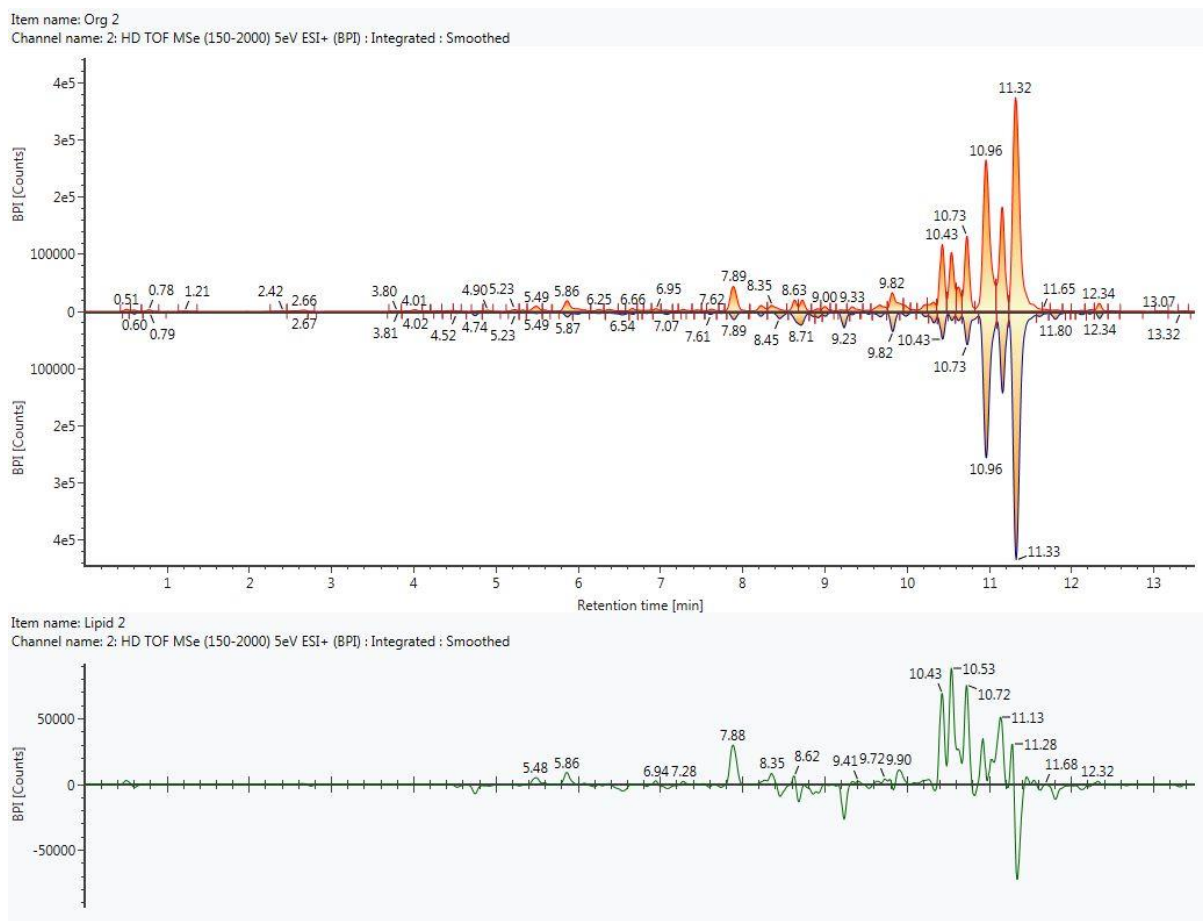


Figure 16: The organic and the lipid positive ionization integrated base peak intensity (BPI) chromatogram from injection 2 compared in UNIFI. The BPI chromatogram with the green line shows the difference in response between the extracts).

A comparison between the organic and the lipid extracts in a principal component analysis (PCA) showed a relative variation between the extracts (**Figure 17**). These type of analyses does not show how big the variation is, but that the extracts in general are not completely alike. In addition to the relative variation between the extracts, it was also observed a relative variation between the sequential injections. The first injections varied compared to the second and third injections, indicating a possible parametric drift in instrumentation during the analysis. Excluding the first injections did not seem to alter the results in any way, and therefore all injections were used to compare the extracts. The relative variation between the extracts was greater than the relative variation between the injections, meaning that the choice of extraction method was more vital for the result than the differences in injection. Alignment of the data retrieved a total of 3654 markers. An ANOVA-test showed that the observed signal intensities of 51 % (n=1877) of the markers were considered significantly different ($p < 0.05$) between the extracts.

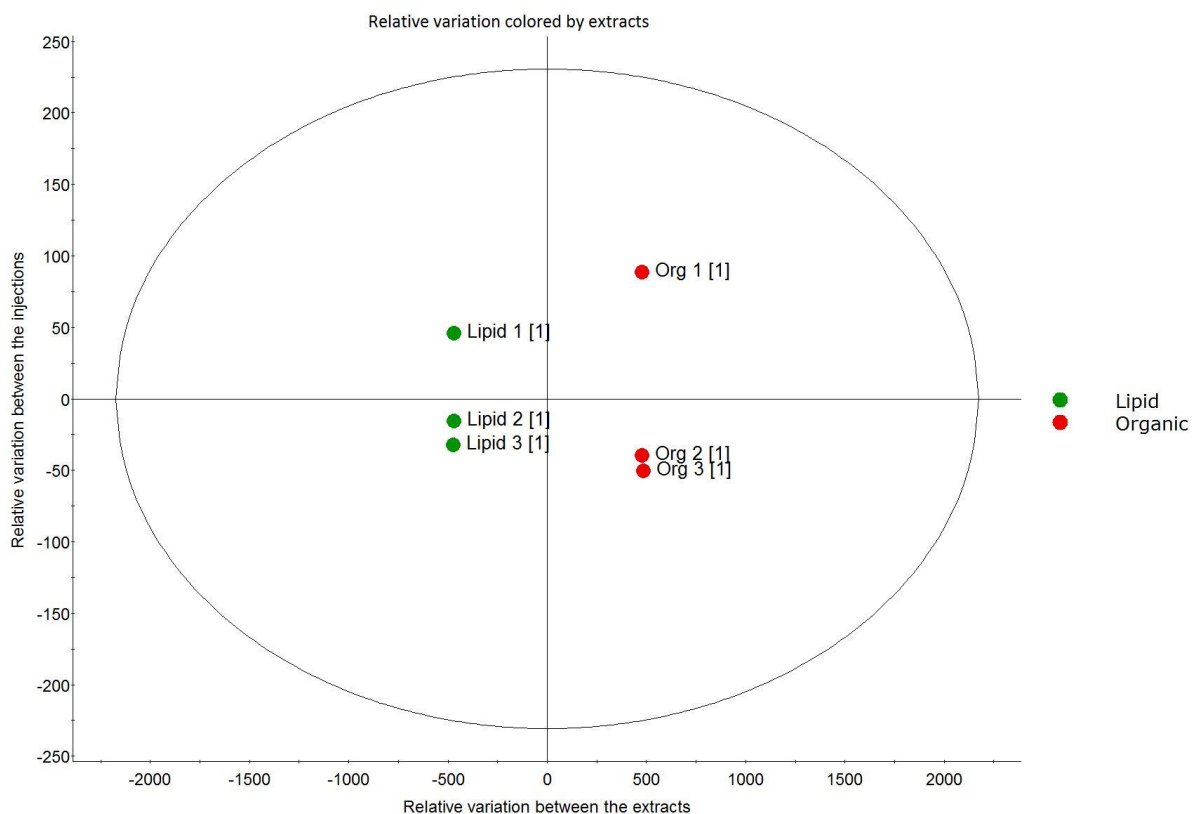


Figure 17: PCA-plot showing the relative variation between the organic and the lipid extracts with three sequential injections. The x-axis represents the relative variation between the extracts, while the y-axis represents the relative variation between the injections of the extracts.

An S-plot analysis was conducted to more closely investigate the markers contributing the most to the variation between the extracts (**Figure 18**). In the S-plot analysis, the variation between the two extracts is plotted against the reliability of the results. The x-axis shows the variance, while the y-axis shows the reliability of the variance. This means that the most reliable variations between the extracts are found in the bottom left and the top right corner of the S-plot. The S-plot shows 64 compounds marked in red contributing with a variation > 0.05 but is primarily dominated by markers with no or little variation between the extracts.

Investigation of the 64 compounds contributing the most to the variation between the extracts, showed that there was one compound ($m/z = 355.1886$, $z = 2$, $R_t = 8.35$ minutes) only observed in the organic extract compared to the lipid extract. Dereplication of this compound suggested the elemental composition $C_{39}H_{52}N_2O_{10}$ (i-FIT = 77.13 %) and two possible identifications with one fragment match ($m/z = 465.2289$). The two almost identical possible identifications consisted of a steroid skeleton with a substituted group (**Figure 19**). It is hard to say that these compounds will receive two charges when ionized, which weakens the confidence of the identifications. Other suggested compounds for this peak did not have any fragment matches,

nor an intuitive possibility for double ionization. The maximum signal intensity of this compound was low (1549) compared to other compounds, and it is therefore not possible to conclude if the result is directly connected to the differences in the extraction method or not. There will always be a possibility of contamination during preparation of extracts.

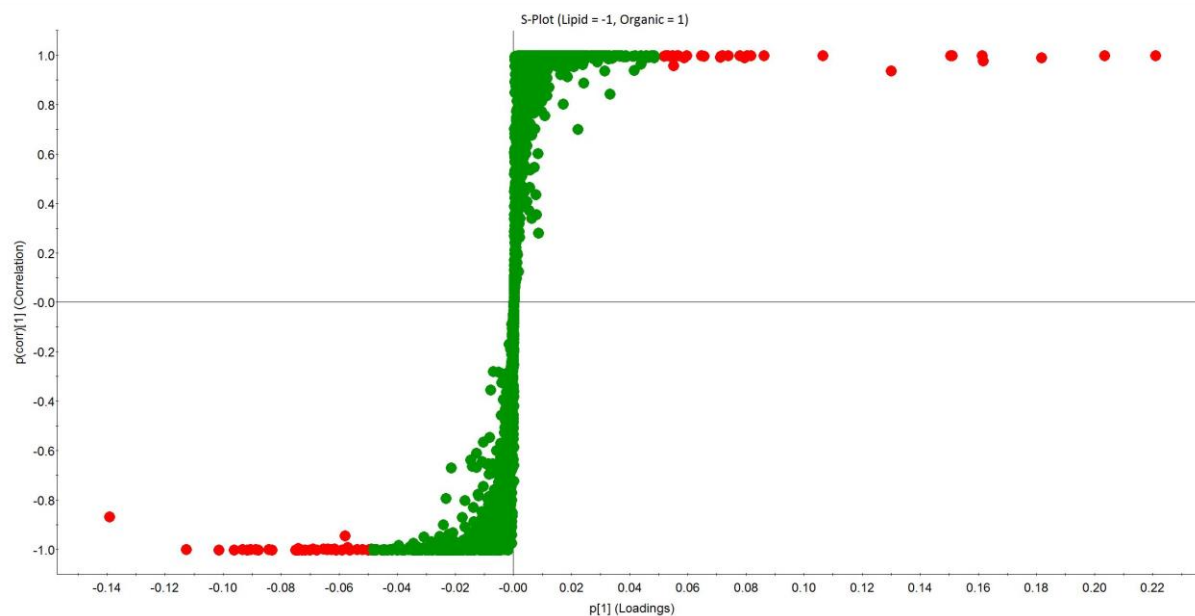


Figure 18: S-plot comparing the lipid to the organic extract. The points marked in red were selected for comparing the organic and the lipid extracts (created in EZInfo).

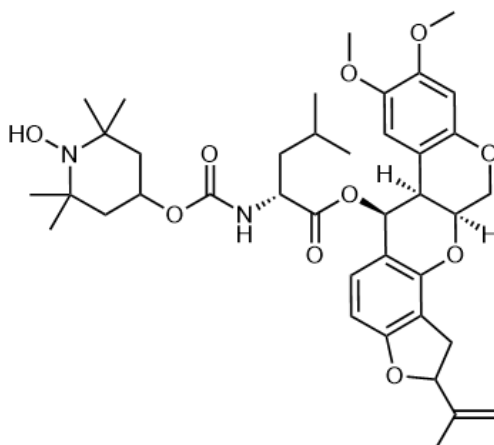


Figure 19: A possible identification of the compound ($C_{39}H_{52}N_2O_{10}$, i -FIT = 71.13 %) only observed in the organic extract with $m/z = 355.1886$, $z = 2$ (Created in ChemDraw).

An interesting pattern was observed when investigating the max fold change ratio between the extracts for the 64 compounds. Compounds from the lipid extract had in general higher ratios than compounds from the organic extract. This indicates that there are some compounds which are more likely observed when doing the lipid extraction compared to the organic extraction.

Looking at the compounds with more than a 10 times max fold change ratio between the extracts, there were 8 compounds (28 %) in the organic extract and 21 compounds (72 %) in the lipid extract. In the chromatograms (**Figure 16**) the peak at $R_t = 9.23$ minutes had a visually more intense signal in the lipid extract than the organic extract, which led to a max fold change ratio at 17.1, implying a 17 times higher signal intensity in the lipid extract compared to the organic extract. Dereplication of this peak suggested the elemental composition $C_{17}H_{35}NO$, i-FIT = 100 %, which fits multiple structure compositions, but most probably a long-chained molecule like for example N-octylnonanamide (**Figure 20**). A fragment with $m/z = 158.1534$ was observed, which concludes a plausible fragmentation pattern for the proposed structure since cleavages next to amide groups are likely.

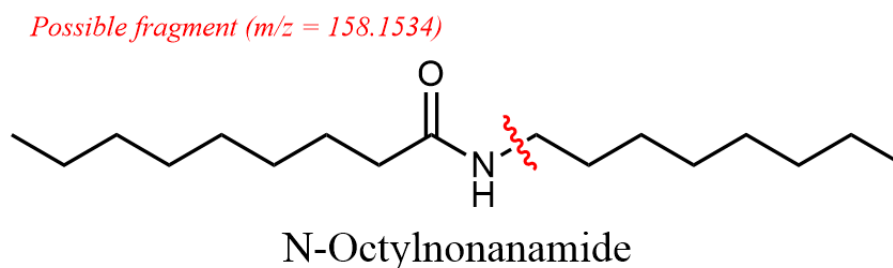


Figure 20: Illustration of a plausible fragmentation of N-Octylnonanamide (Created in ChemDraw).

Investigation of the 10 compounds with the highest observed signal intensity from the 64 selected, suggested a difference in concentration of these compounds between the extracts. Almost every compound (90 %) had a higher intensity in the organic extract compared to the lipid extract (**Figure 21**), which suggests a higher recovery of these compounds in the organic extract. Since only one parallel of each extraction method was compared to each other, there is no way of knowing if the difference in signal intensity has been influenced by random dilution errors. It is also possible that the degree of ionization is greater in the organic extract compared to the lipid extracts. Investigation of observed adducts from the 64 selected compounds between the extracts showed an even distribution of $[M+H]^+$, $[M+Na]^+$ and $[M+K]^+$. Ammonium-adducts $[M+NH_4]^+$ were only observed in the lipid extract, which could suggest a lower degree of ionization in the organic extract. If this is the case, the concentration difference between the extracts is possibly greater than what the signal intensities imply. To research differences in recovery, a quantitative analysis of these compounds with multiple parallels must be conducted.

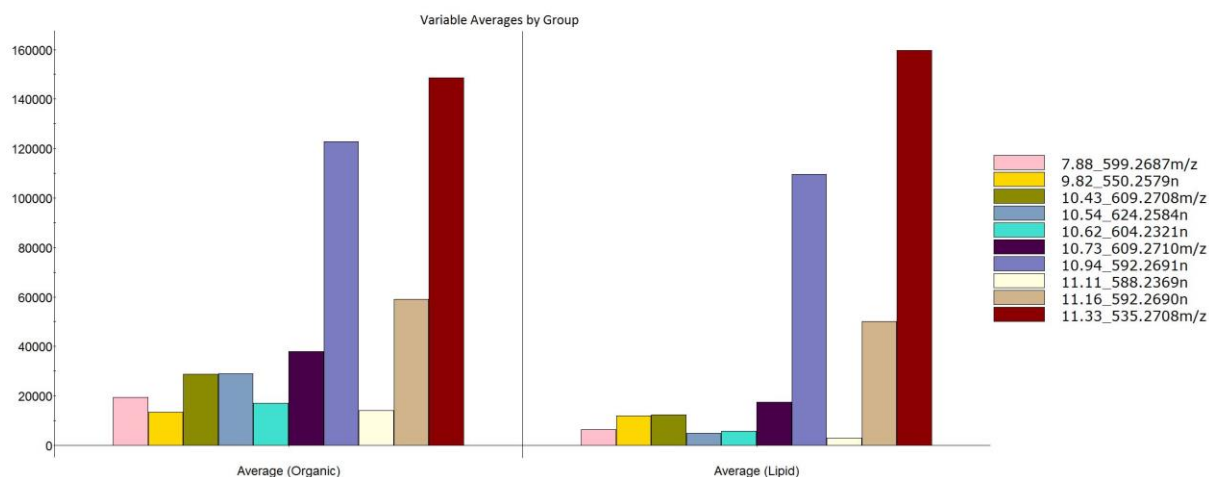


Figure 21: A bar chart of the 10 compounds with the highest observed signal intensity from the 64 selected showing the average signal intensity of the compounds for each extract. The legend presents the retention time and either the observed m/z or the neutral mass of the compounds, depending on if the software could identify the neutral mass or not.

The only compound with a higher signal intensity in the lipid extract of the 10 compounds with the highest signal intensity was identified as pyropheophorbide a (i-FIT = 70.46, 25 fragment matches, 43 % predicted intensity, **Figure 22**), which is a chlorophyll related compound often observed in algae (53). It is important to note that this compound was the only one of the 64 selected compounds where the difference between the extracts was not significant ($p = 0.122$). This compound contributed to the variation between the extracts because of its high signal intensity and not because of the reliability of the result. Pyropheophorbide a ($m/z = 535.2708$) is observed as the highest peak in the chromatograms (see **Figure 16**) with $R_t = 11.33$ minutes.

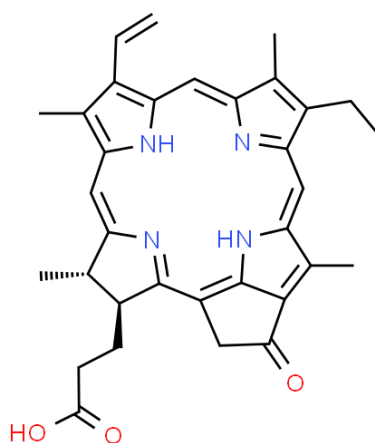


Figure 22: A possible identification for the peak with the highest signal intensity ($R_t = 11.33$ minutes) in the analysis, pyropheophorbide a (structure retrieved from ChemSpider).

A reasonable prediction before assessing the results was that the lipid extraction would result in identification of more lipophilic compounds, while the organic extraction would result in

identification of more hydrophilic compounds. This prediction was simply based on the ratio of the extraction medium used. The ratio between MeOH and DCM was 1:2 in the lipid extraction, while it was 1:1 in the organic extraction. The investigation of the 64 selected compounds partially supported this hypothesis. The most lipophilic compounds ($R_t = 11.24 - 13.31$ minutes) had a higher signal intensity in the lipid extract than in the organic extract, but there was not a clear trend for the most hydrophilic ($R_t = 4.74 - 9.22$ minutes). For the $R_t = 9.41 - 11.20$ minutes, there was an overweight of compounds with higher signal intensity in the organic extract. This was the R_t window where the most intense compounds eluted, which again could suggest a concentration difference between the extracts for the most intense peaks in the analysis. Lipidomic analyses of the same extracts with a different gradient showed that there are a lot of lipids which does not elute during the running time of the metabolomic analysis. While pyrophephorbide a is one of the last peaks eluting in the metabolomic analysis ($R_t = 11.33$ minutes), it elutes in the first minutes in the lipidomic analyses ($R_t = 4.02$ minutes, **Figure 25**). This shows that the metabolomic analyses only present a rather small selection of all the compounds present in the extracts.

The last variable necessary to discuss is the p-value for the 64 selected compounds. Investigation shows that the most significant compounds were more frequently observed in the lipid extract, while the lesser significant compounds were more frequently observed in the organic extract. This is an interesting observation, but it is important to notice that 63 of the 64 compounds were significantly different ($p < 0.05$) between the extracts.

To summarize the results, the positive mode comparison does not prove that one or the other extraction method is better for metabolomic analysis. Out of the 64 compounds, the distribution was 50:50 between the extracts suggesting that the variance from each extract cancelled each other out. Closer investigation showed that most of the organic extract compounds were included because of higher signal intensities, while lipid extract compounds were included because of rarity. This could suggest that the lipid extraction is better for qualitative metabolomic analysis of *P. glacialis*, while the organic extraction is better if recovery of the most intense peaks is of interest. To confirm or deny these suggestions, multiple analyses must be conducted. In this thesis, only one parallel of each extraction and each dilution prior to the analysis was performed. Adding more parallels to the method could reduce the risk of random errors influencing the results.

4.2.2 Lipidomic Comparison

Lipidomic analyses of 2.5 mg/mL of the organic and the lipid extracts showed high detection of TG and some detection of DG, but low detection for other lipid classes (**Figure 23/Figure 24**). One of the blanks was excluded from the results because it was considered an outlier. Despite the exclusion, some TGs were observed in the blanks, which is most likely explained by contamination of the samples, as TGs occur naturally in the human skin. Overall, the lipidomic profile differed from earlier lipidomic analyses on biomass from the same microalgal specie. In previous work conducted by Kristine Haugland, high amounts of PC, PE and PG were detected in lipid extracts from the same microalgal specie. Haugland used a lipid concentration of 1 mg/mL and a different batch of microalgal biomass (23). For the microalgal biomass used in this thesis, just a few lipids for PC, PG and PEt were detected despite using a higher concentration than Haugland. Multiple concentrations and multiple batches of the microalgal biomass were analysed during this thesis, in addition to a lot of troubleshooting around the extraction and the analytical method. In the end, it seemed like the lipidomic profile was not reproducible for the same concentrations across different batches.

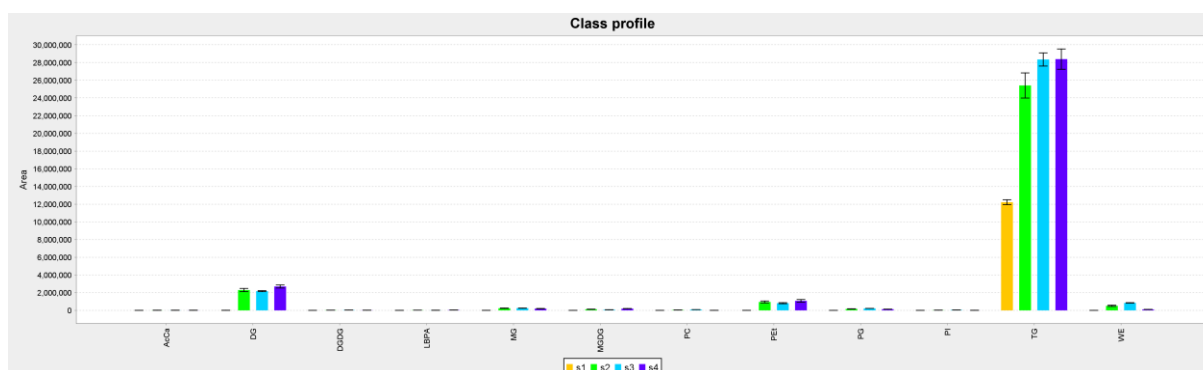


Figure 23: Lipidomic profile of 2.5 mg/mL microalgal biomass extracts from *Porosira glacialis*. The figure shows detection of lipid classes in a blank sample (S1), a mixed sample (S2), the organic extract (S3) and the lipid extract (S4).

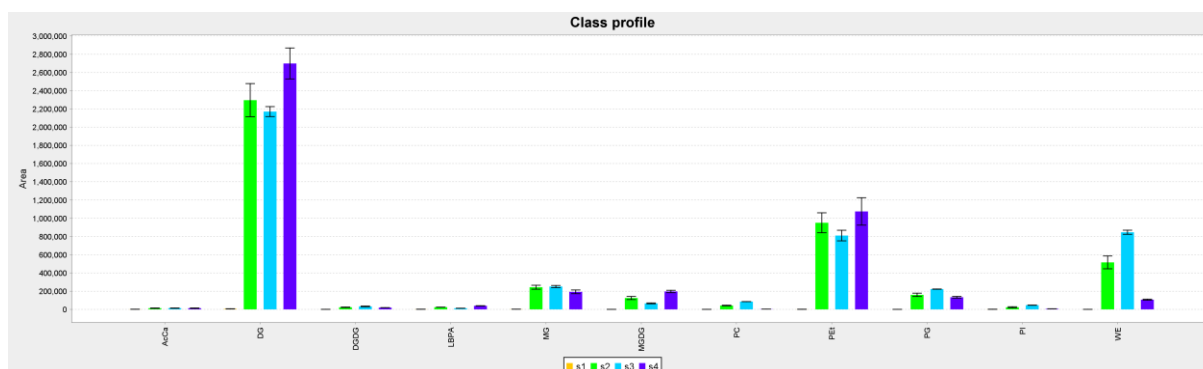


Figure 24: Lipidomic profile of 2.5 mg/mL microalgal biomass extracts from *Porosira glacialis* when the lipid class TG is excluded. The figure shows detection of lipid classes in a blank sample (S1), a mixed sample (S2), the organic extract (S3) and the lipid extract (S4).

There could be multiple explanations for lipid variation across batches. Previous research has shown that the lipidomic composition of algal biomass is highly dependent on growth conditions like light, temperature, and pH (21, 54, 55). In addition, it is shown that the FA composition varies between different growth stages of marine diatom algae (56). Variation in these factors between batches could therefore influence the lipidomic profile observed for the microalgal biomass. For *P. glacialis*, the different batches are harvested in different growth stages, and it is also known that the growth conditions are adjusted according to the algal growth stage. There is therefore a possibility that the batch analysed in this thesis was harvested under conditions giving a low lipid yield in the biomass.

Assuming the lipidomic profile observed in the algal extracts in this thesis is accurate, it seems like there has been an increase in TGs at the expense of a decrease in PLs. This has been observed before in the diatom *Phaeodactylum tricornutum* where a deficiency in phosphorus (P) altered the metabolic pathways in the algae, resulting in gene expression favouring TG synthesis over synthesis of PLs (57). A similar observation has been described for the diatom *Thalassiosira pseudonana*, where deficiency of P resulted in accumulation of other non-phosphorus lipids (58). Even though the P levels are monitored during cultivation of *P. glacialis* there could have been unpredictable circumstances resulting in harvesting of algal biomass exposed to low levels of P. Another possibility for the lack of observed PLs could be contamination of bacteria or fungi producing phospholipases. Phospholipases are enzymes hydrolysing PLs by cleavage of the ester bond between the glycerol backbone and the phosphate group. In the cultivation facility of *P. glacialis* used in this thesis, there have been observed contaminations of microorganisms in the past.

When comparing the organic extract to the lipid extract there was in general not a clear difference in lipidomic profile between the extracts observed in LipidSearch (**Figure 23**). When comparing the chromatograms of the extracts, a slight difference in compound signal intensities was observed (**Figure 25**). The more polar peaks had a higher intensity in the organic extract, while the more lipophilic peaks had a higher intensity in the lipid extracts. The explanation for this is most likely the difference in extraction medium used between the extraction methods. For the lipid extraction method, a higher ratio of DCM was used resulting in a more lipophilic extraction medium, and thereby a higher content of lipophilic compounds observed. The observation therefore suggests that the ratio of DCM and MeOH in the extraction methods affects the compounds extracted. What is interesting to notice, is that the peak at $R_t = 4.02$ minutes was identified as Phyropheophorbide a, which was one of the last eluting peaks in the

metabolomic analysis ($R_t = 11.33$ minutes, **Figure 16**). This shows that the lipidomic analysis covers a much wider range of compounds than the metabolomic analysis. The downside is that all the peaks separated in metabolomic analyses elute in the first minute of lipidomic analyses, making it hard to differentiate between these compounds. In the lipidomic analyses, free FAs are normally observed before $R_t = 5$ minutes, PLs are normally observed between $R_t = 5$ minutes and $R_t = 16$ minutes, while TGs are normally observed in the end of the analysis after $R_t = 15$ minutes. In the chromatogram in **Figure 25**, multiple of the TGs identified are barely visible for $R_t = 24 - 26$ minutes.

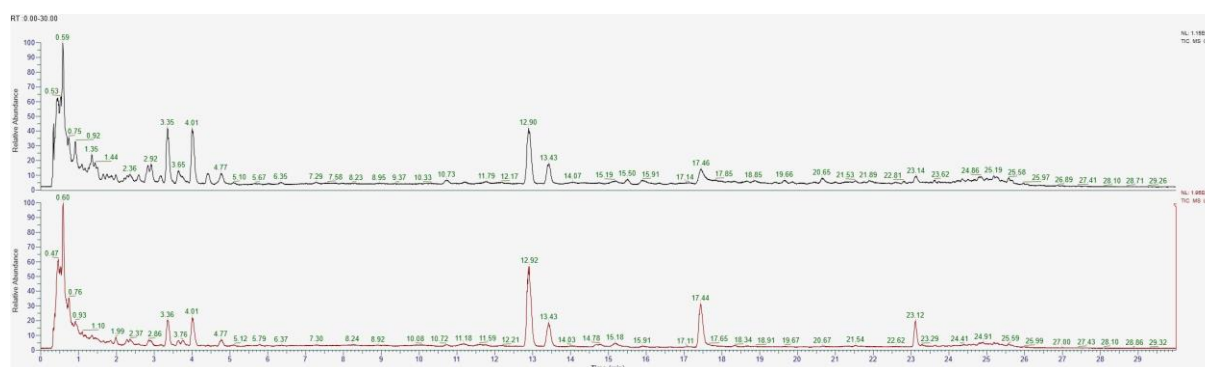


Figure 25: TIC of 2.5 mg/mL of the lipid (red) and the organic (black) extracts.

LipidSearch has a grading system for identification of lipids ranging from A to D, where A is considered optimal identification. When excluding identifications with grades C and D, only the lipid classes TG and DG were observed for the extracts (**Figure 26**). This shows that the confidence in identifications of lipid classes observed in the extracts was in general low.

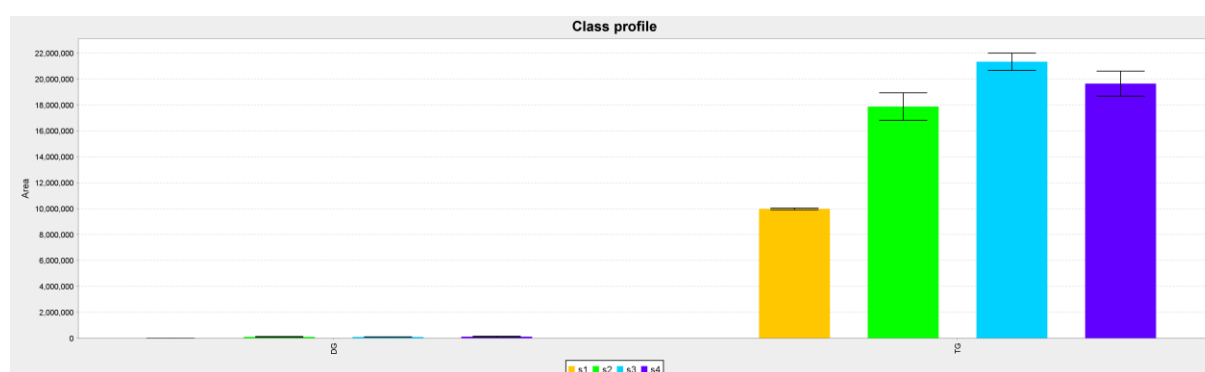


Figure 26: Lipidomic profile of 2.5 mg/mL microalgal biomass extracts from *Porosira glacialis* with identification grade A or B. The figure shows detection of lipid classes in a blank sample (S1), a mixed sample (S2), the organic extract (S3) and the lipid extract (S4).

To give an example of an identified lipid in LipidSearch, a TG ($R_t = 24.20$ minutes) with grade A identification was selected. Both a NH_4^+ - ($m/z = 868.7389$) and a Na^+ -adduct ($m/z = 873.6943$) were observed for this TG, concluding a calculated neutral molecular mass of

850.7050 Da. For the NH_4^+ -adduct, LipidSearch detected substituent-specific fragments and substituent-derived fragments for all three FAs. For the Na^+ -adduct, only substituent-derived fragments for all three FAs were detected. This resulted in a top grading for the identification (**Appendix 4**), where the identified FAs were 16:0 (16 carbons and 0 double bonds), 16:1 and 20:5, concluding a TG elemental composition of $\text{C}_{55}\text{H}_{94}\text{O}_6$ (**Figure 27**).

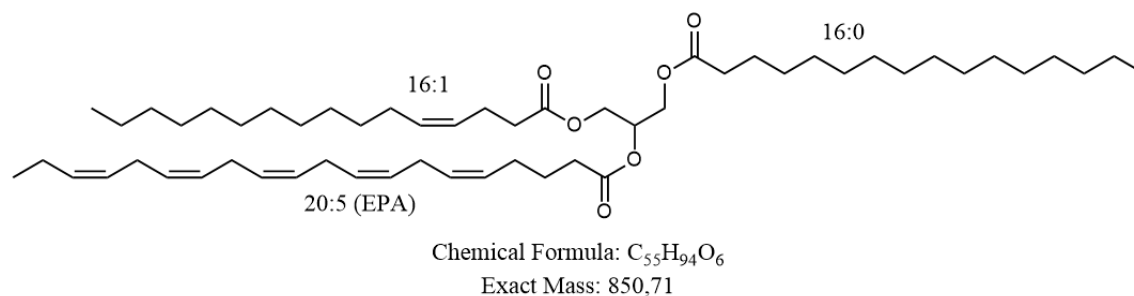


Figure 27: A possible structure composition of the identified triglyceride ($R_t = 24.20$ minutes) with the fatty acids 16:0, 16:1 and 20:5.

When comparing the area of the identified TG across samples (**Figure 28**), the area was evidently greater in the organic extract (s3) compared to the lipid extract (s4). This seemed to be a trend for most of the TGs consisting of at least one 20:5 FA, which is the essential FA named eicosapentaenoic acid (EPA). Since EPA is not naturally occurring in the human skin, there is a lower risk that the semi-quantification of TGs comprising at least one EPA has been influenced by human contamination. These semi-quantifications can therefore be considered more trustworthy than semi-quantifications of TGs with possible human origin. When only looking at the TGs with one or multiple EPAs, it is observed a better recovery in the organic extraction compared to the lipid extraction. Assuming that these are the only reliable semi-quantifications, one could argue that there is a difference between the organic and the lipid extracts, but because of low signal intensities and problems with reproducing results across the lipidomic analyses as described earlier, further testing is necessary to assess the hypothesis.

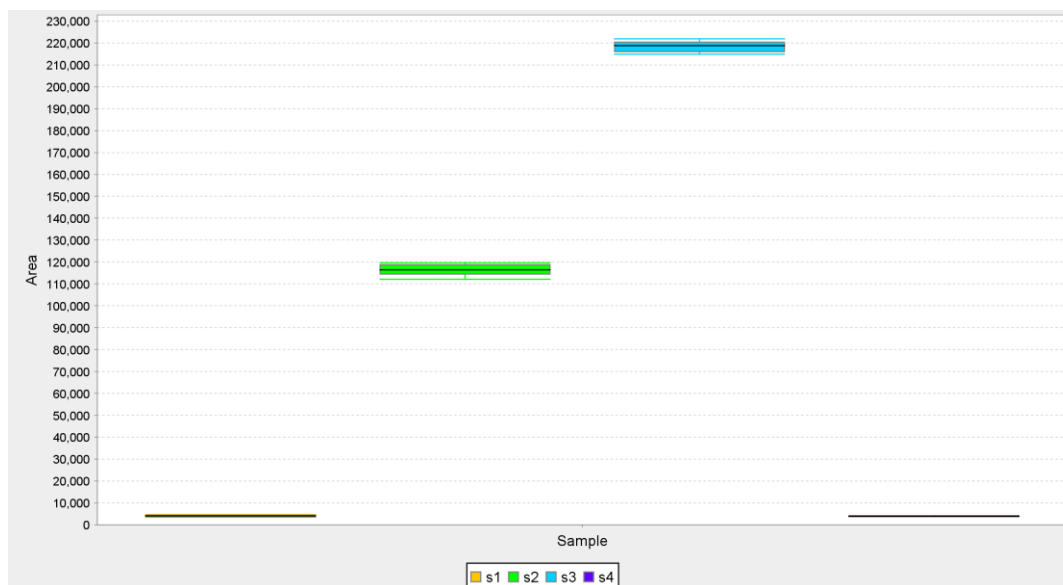


Figure 28: A semi-quantification plot of the abundance of the TG with elemental composition $C_{55}H_{94}O_6$ in the blank sample (s1), the mixed sample (s2), the organic extract (s3) and the lipid extract (s4). The concentration of the organic and the lipid extracts were 2.5 mg/mL.

4.2.3 Summary of the Extraction Method Comparison

To summarize the comparison between the organic and the lipid extraction method, it is not possible to choose one or the other for both metabolomic and lipidomic analyses based on the results in this thesis. There are still some trends to notice for further investigation. When looking at the metabolomic and the lipidomic comparison put together, results are supporting the hypothesis that the organic extraction method with the more polar extraction medium extracts more of the polar compounds, while the lipid extraction with the more lipophilic extraction medium extracts more of the lipophilic compounds. For the metabolomic analysis, this trend is just partially observable, but looking at the lipidomic analysis presenting a wider view of the extract's components, the trend is clearer. In general, it seems like there is not a significant difference between the results of the extraction methods. There is therefore an argument that it doesn't matter which extraction method is chosen. If this is the case, it is worth mentioning that the lipid extraction can be done in a couple of hours, while the organic extraction is done over two days. Therefore, the lipid extraction could be favourable from a time efficiency perspective.

4.3 Bioassay Results

In the metabolomic extraction method, both an aqueous and an organic extract was obtained. These extracts were fractionated into eight aqueous and eight organic fractions and then prepared for bioactivity testing. The fractions were tested for activities against formation of

biofilm, bacterial growth, and viability of a cancer cell line. In addition, the fractions were tested for inflammatory and anti-inflammatory response.

4.3.1 Biofilm Formation

None of the fractions tested were considered active against formation of biofilm (**Table 19**). Aq5 reached the lowest score with 68.9 %, which could suggest some reduction in biofilm formation, despite being categorized as inactive. This fraction could possibly be categorized as active if the fraction concentration was increased and retested. There were no significant differences in bacterial growth in the fractions, but for aq5 the measured absorbance for bacterial growth was reduced compared to the other fractions. This could mean that the small reduction in biofilm formation could be explained by a small reduction in bacterial growth, rather than actual inhibition of the biofilm formation. The results therefore suggest that aq5 possibly contains a compound or multiple compounds active against formation of biofilm or the bacteria used in the bioassay, at concentrations higher than 100 µg/mL. Higher concentrations of the fractions could be tested for activity against biofilm formation to confirm or deny this hypothesis.

Table 19: Results of the inhibition of biofilm assay showing no active fractions.

Fraction	Aq1	Aq2	Aq3	Aq4	Aq5	Aq6	Aq7	Aq8	Org1	Org2	Org3	Org4	Org5	Org6	Org7	Org8
Score	94	103	100	103	69	101	99	117	107	101	94	84	91	87	102	128
Category	I	I	I	I	I	I	I	I	I	I	I	I	I	I	I	I

4.3.2 Anti-bacterial Growth Assay

Aq5 showed activity against *S. agalactiae* in the anti-bacterial growth assay with an absorbance of 0.036 indicating very low growth of bacteria (**Table 20**). Org5 had questionable activity against the same bacterial strain. An interesting observation was that aq5 had reduced growth for all Gram-positive bacterial strains (*E. faecialis*, *S. aureus* and *S. agalactiae*) even though the fraction was only considered active against *S. agalactiae*. The difference between Gram-positive and Gram-negative bacteria is the composition of the cell wall, where the cell wall of Gram-negative bacteria is generally said to be more robust (59). These results create a hypothesis, that the mechanism of the bioactive compound could be related to rupture of the cell membrane. It is also possible that the bioactive compound is only able to diffuse over Gram-positive membranes and the mechanism of action takes place inside the cells.

Table 20: Results of the antibacterial growth assay showing scores for each bacterial strain. Score values marked in red are considered active (absorbance < 0.05), while score values marked in orange have questionable activity (absorbance = 0.05 - 0.09).

Fraction	The score for each bacterial strain				
	<i>E. faecialis</i>	<i>E. coli</i>	<i>P. aeruginosa</i>	<i>S. aureus</i>	<i>S. agalactiae</i>
Aq1	0.218	0.5015	0.637	0.4125	0.25
Aq2	0.249	0.561	0.4365	0.382	0.1935
Aq3	0.26	0.6385	0.4805	0.2915	0.217
Aq4	0.2875	0.5775	0.4475	0.2725	0.2175
Aq5	0.1065	0.4055	0.528	0.158	0.036
Aq6	0.226	0.475	0.458	0.4165	0.2535
Aq7	0.203	0.559	0.4255	0.3635	0.277
Aq8	0.2845	0.5255	0.477	0.3875	0.2455
Org1	0.2355	0.5655	0.4805	0.3775	0.164
Org2	0.222	0.5635	0.4595	0.4135	0.1825
Org3	0.234	0.5685	0.493	0.302	0.2115
Org4	0.2065	0.4965	0.486	0.315	0.133
Org5	0.1475	0.387	0.4575	0.1145	0.0605
Org6	0.1575	0.514	0.4565	0.1425	0.1295
Org7	0.184	0.5605	0.458	0.276	0.233
Org8	0.166	0.5175	0.466	0.2915	0.139

4.3.3 Viability

Results from the viability assay showed reduced growth of the human melanoma cancer cell line A2058 for aq5 – aq7. Aq5 was considered active with a score of 22 % (A), aq6 had questionable anti-proliferative effect, while aq7 was considered not active despite a reduction in cell growth (see **Table 21**). The results suggest that there are one or more active compounds in aq5. Since the reduction in cell growth follows a gradient from aq5 to aq7, the bioassay may visualize a concentration-dependent activity. In this case, the bioactive compound will be observed in all these fractions, but with a higher concentration in aq5 than in aq6 and aq7.

Table 21: Results of the viability assay showing activity against human melanoma cancer cell line A2058 for aqueous fraction 5 (aq5) marked in red and questionable activity for aqueous fraction 6 (aq6) marked in orange.

Fraction	Aq1	Aq2	Aq3	Aq4	Aq5	Aq6	Aq7	Aq8	Org1	Org2	Org3	Org4	Org5	Org6	Org7	Org8
Score	138	119	117	109	22	56	62	105	157	123	111	103	98	122	119	103
Category	I	I	I	I	A	Q	I	I	I	I	I	I	I	I	I	I

The viability assay was the only assay where visual observation could be conducted to predict the results. In **Figure 29** reduced cell growth in B6 - D6, B7 - C7 and B8 - C8 can be observed by the lack of dark colour in the wells.

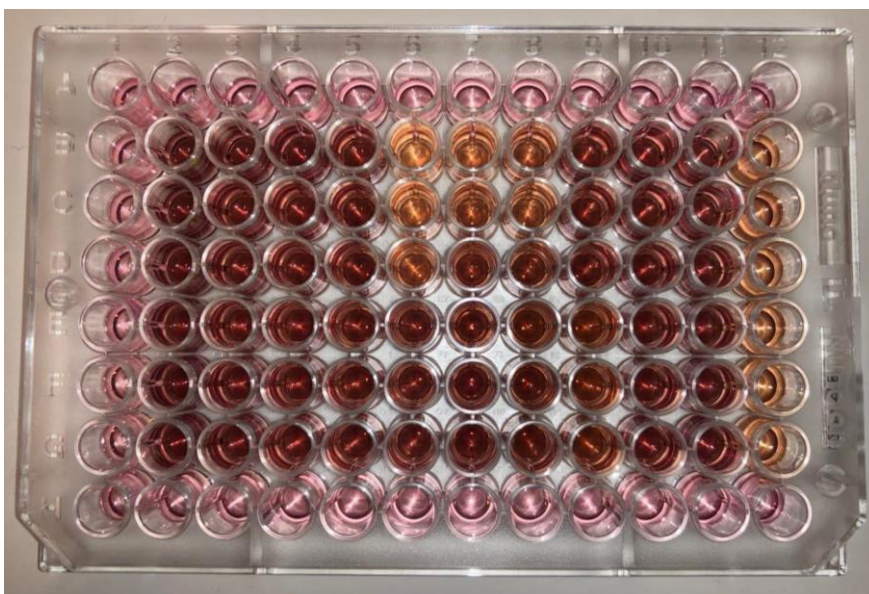


Figure 29: Visual result of viability assay. Column 2-9 are test columns, columns 10 and 11 are negative controls, and column 12 is a positive control. Dark colour indicates cell growth.

4.3.4 Immunoassay (ELISA)

Results from the immunoassay showed anti-inflammatory activity for aq5 - aq7 and org7, while org8 had questionable activity (**Table 22**). The anti-inflammatory activity is only valid if a secretion of TNF- α by living cells has taken place, followed by an inhibition of the cytokine. Since aq5 - aq7 showed reduced cell growth in the viability assay, the immune cells presumably died before a significant amount of TNF- α was secreted. It is therefore reasonable to believe that the activity for aq5 - aq7 is not valid.

Since org7 showed anti-inflammatory activity, followed by questionable activity in org8, there are probably one or multiple possible bioactive compounds in these fractions. These fractions are highly lipophilic, and it is therefore a high chance that the observed anti-inflammatory effect is linked to one or multiple lipids. Lipids are known to often induce some kind of bioactive response (60), and anti-inflammatory lipids have earlier been identified in marine extracts (61), which supports this hypothesis.

There were no fractions showing immunostimulatory activity. Aq6 and aq8, in addition to org7 showed questionable activity, which could be worth investigating further. Since immunoassays are very sensitive, multiple executions of the assay must be conducted to present conclusive results. The results of this one execution of the assay are best used as a screening tool for further investigation.

Table 22: Results of immunoassay showing activity (A) in red and questionable activity (Q) in orange. The scoring system is different for immunostimulatory activity compared to anti-inflammatory activity.

Fraction	Anti-inflammatory		Immunostimulatory	
	Score	Category	Score	Category
Aq1	22	I	-1	I
Aq2	0	I	0	I
Aq3	14	I	-1	I
Aq4	15	I	-1	I
Aq5	100	A	3	I
Aq6	90	A	9	Q
Aq7	102	A	3	I
Aq8	15	I	7	Q
Org1	31	I	-1	I
Org2	7	I	2	I
Org3	15	I	4	I
Org4	19	I	2	I
Org5	23	I	2	I
Org6	25	I	3	I
Org7	54	A	6	Q
Org8	47	Q	2	I

4.3.5 Summary of Bioassay Results

The most interesting fraction based on the bioassay results is aq5. This fraction was active against the bacterial strain *S. agalactiae* and the melanoma cancer cell line A2058. In addition, it was marked as anti-inflammatory in the immunoassay, which is likely explained by apoptosis rather than actual anti-inflammatory response. These results make it feasible to assume that Aq5 contains one or multiple compounds with bioactive abilities or a mixture of compounds which together creates bioactive responses. One could assume that there is an unselective mechanism responsible for both the anti-bacterial growth and the anti-cancer effect, but it is also possible that these effects have separate mechanisms.

Org7 showed an anti-inflammatory response in the immunoassay and therefore qualifies as an interesting fraction to further investigate. Since this fraction is highly lipophilic, it is reasonable to assume that the bioactivity is connected to one or multiple lipids. Since immunoassays classify as sensitive assays, little is needed to shift the results. To address if the bioactivity observed in org7 is reliable, more immunostimulatory testing must be done.

4.4 Dereplication of Bioactivity

To further investigate the bioactivity in aq5 and org7, dereplication was done for these fractions. The active fraction aq5 was compared to the inactive aq4, while org7 was compared to org6 to nominate candidates for isolation. The dereplication was done for both positive and negative mode.

4.4.1 Bioactivity in Aqueous Fraction 5

Comparison between aq4 and aq5 in positive mode showed one distinct difference between the fractions at $R_t = 12.70$ minutes with an observed $m/z = 338.3416$ (**Figure 30**). The observed intensity of this peak in aq5 (intensity in aq5 = 75348) was 6.2 times higher than in aq4 (intensity in aq4 = 12136). Dereplication of this compound strongly suggests the elemental composition $C_{22}H_{43}NO$ (i-FIT = 100 %), with 1 fragment match ($m/z = 321.3147$) suggesting a loss of an amine group.

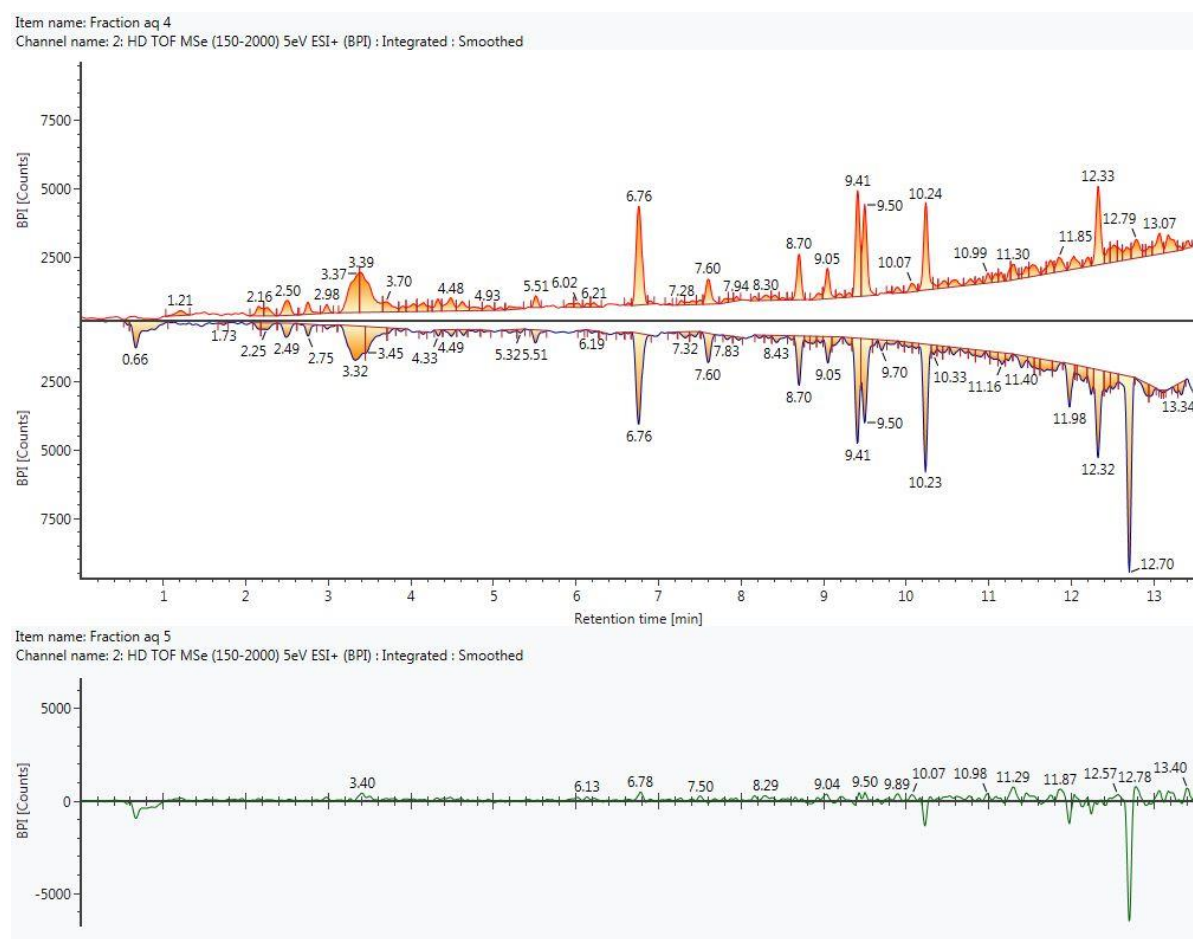


Figure 30: The positive mode ionization BPI integrated chromatograms for aq4 and aq5 compared in Unifi, showing a distinct difference for $R_t = 12.70$ minutes.

When searching for known compounds, matching the retrieved data for the peak with $R_t = 12.70$ minutes, the most cited compound is erucamide with one fragment match (**Figure 31**). The fragment observed ($m/z = 321.3146$) indicates cleavage of the amine group, which is a probable observation for the substance. Research has shown that erucamide is a potent acetylcholinesterase inhibitor with potential in use against Alzheimer's disease, depression, and anxiety. In addition, an article concluded that erucamide was toxic to human liver HepG-2 cancer cells when testing the bioactivity of aqueous extracts from a sea squirt (62). This suggests that there is a possibility that erucamide is the active agent against melanoma A2058 cancer cells and the bacterial strain *S. agalactiae*.

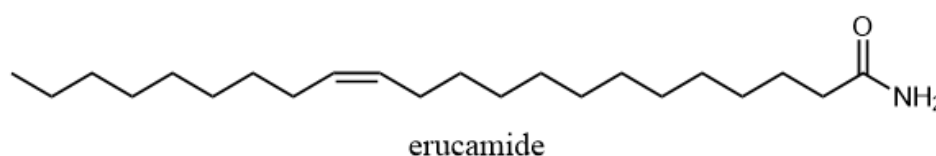


Figure 31: The molecular structure of erucamide ($C_{22}H_{43}NO$, ChemDraw).

When searching for erucamide in other fractions, the intensity was in general low compared to the intensity in aq5. An exception was aq1, where the intensity was higher than in aq5 (intensity in aq1 = 113 557). In the bioassays, aq1 was always inactive, which could suggest that erucamide is not the bioactive agent in aq5. Since the composition of aq1 and aq5 is very different, many factors could play a role for the activity. Aq1 could be seen as an outlying fraction, because of high salt concentrations, where the calculated concentration of the fraction was not reliable. In addition, high abundance of salt can in theory cause inactivation of bioactive compounds, as well as pH differences could play a role. It is therefore still possible that erucamide is the active agent, despite being observed with high intensity in inactive aq1.

Comparison between aq4 and aq5 in negative mode showed multiple peaks with differences in intensity between the fractions (**Figure 32**). Two of the peaks were identified as EPA ($R_t = 10.94$ minutes) and docosahexaenoic acid (DHA, $R_t = 11.27$ minutes). These are well known as Omega-3 FAs with multiple proven health benefits (63). There is a possibility that these FAs are responsible or part-responsible for some of the bioactivities observed, but because of their prominence, they were not nominated for isolation. EPA and DHA had high intensities in most of the lipophilic fractions, so if they were the active compounds against melanoma A2058 cancer cells and the bacterial strain *S. agalactiae*, then the activity was inconsistent between fractions. The observed m/z -value for the remaining peaks ($R_t = 11.96, 12.23, 12.47$ and 12.75

minutes) were between 700 and 820. Searches in databases suggested multiple possible compounds of these peaks, where most of them were big lipophilic molecules with different ring structures. All these peaks could have a connection to the observed bioactivity in aq5, and an attempt of isolation of these peaks could therefore be interesting.

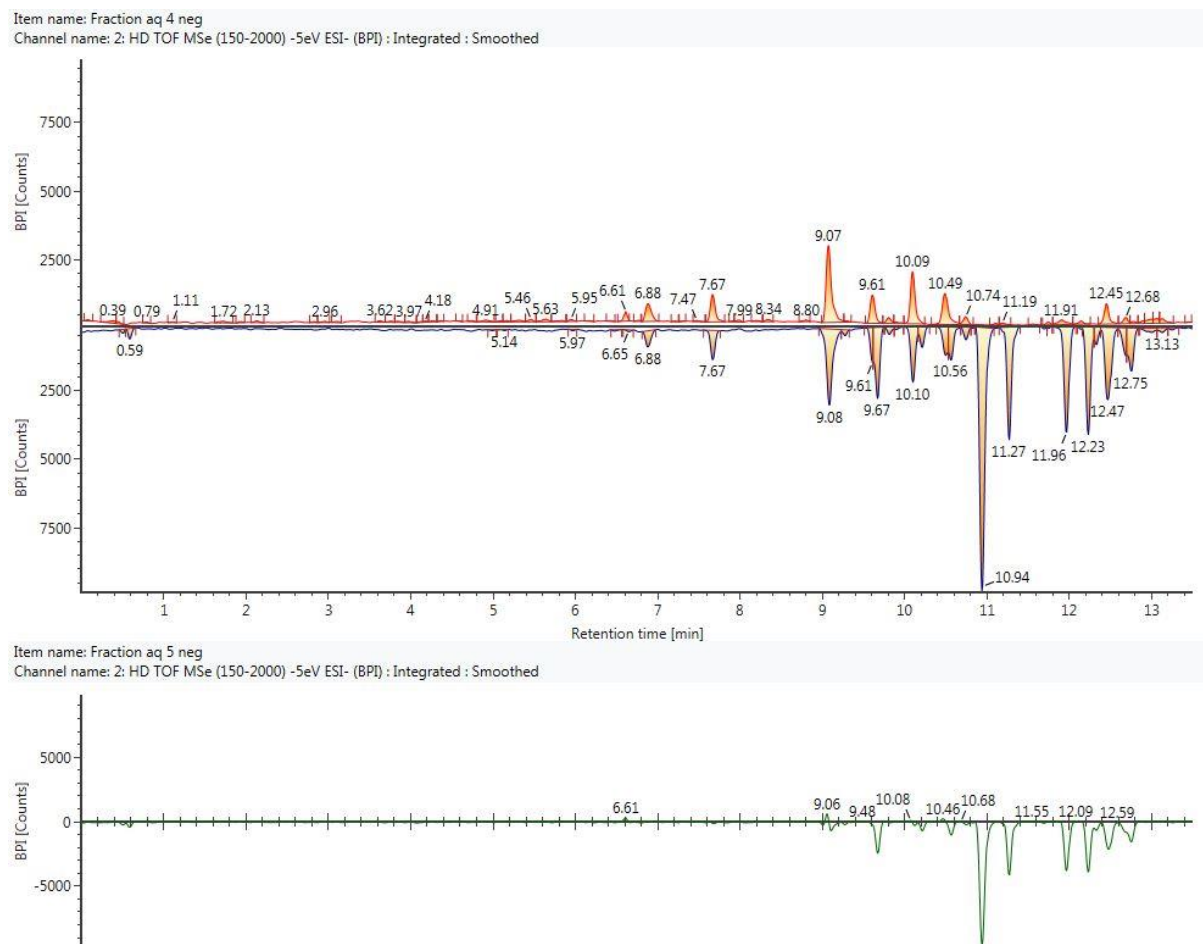


Figure 32: The negative mode ionization BPI integrated chromatograms for aq4 and aq5 compared in Unifi.

4.4.2 Bioactivity in Organic Fraction 7

Anti-inflammatory activity was observed in org7, and the fraction was therefore compared to the non-active org6. There were no distinct peaks in org7 compared to org6 in negative modus. In positive mode, a peak with the proposed identification of scortechinone K (Rt = 11.09 minutes, $m/z = 609.2696$, i-FIT = 48.7 %, 16 fragment matches, **Figure 33**) was observed with high intensity in both org6 and org7. The signal intensity was higher in the active fraction, which could suggest that this compound has anti-inflammatory activity at higher concentrations. This compound was also observed with high intensity in org5 and org8. Org8 had questionable anti-inflammatory activity, while org5 was inactive.

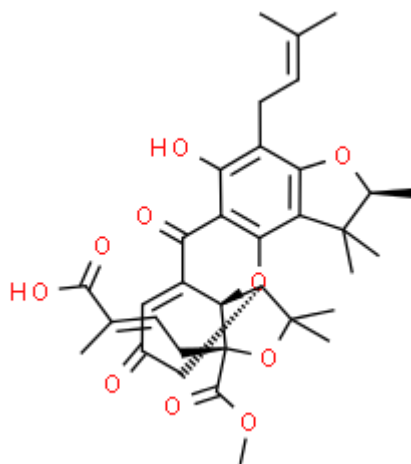


Figure 33: The structure composition of scortechinone K, $C_{34}H_{40}O_{10}$ (retrieved from ChemSpider).

There were no other distinct peaks in org7 compared to org6. Since these are lipophilic fractions, there are highly lipophilic compounds that do not eluate in time for the metabolomic analysis. It is therefore possible that the anti-inflammatory activity comes from lipophilic compounds only visible in lipidomic analyses. Since immunoassays are sensitive, it requires multiple runs to be confident of the observed activity. Even though the fractions are less complex than the extracts themselves, the complexity is still evident. There are therefore many factors that could influence the result in such sensitive assays.

4.5 Isolation and Bioactivity Testing of Isolate

It was decided to do isolation of a compound from the active aq5 because the activity in this fraction was the most evident. The selected compound for isolation was the compound earlier mentioned as erucamide, with an observed m/z -value of 338.3416. This was a narrow peak in the chromatogram with a high intensity suggesting a high probability of successful isolation. One of the BPI chromatograms from the isolation on the preparative-HPLC is given in **Figure 34**, where the pink area indicates the R_t window where sample was collected. The chromatogram shows successful isolation, with a high intensity narrow peak and no overlapping in the positive mode chromatogram.

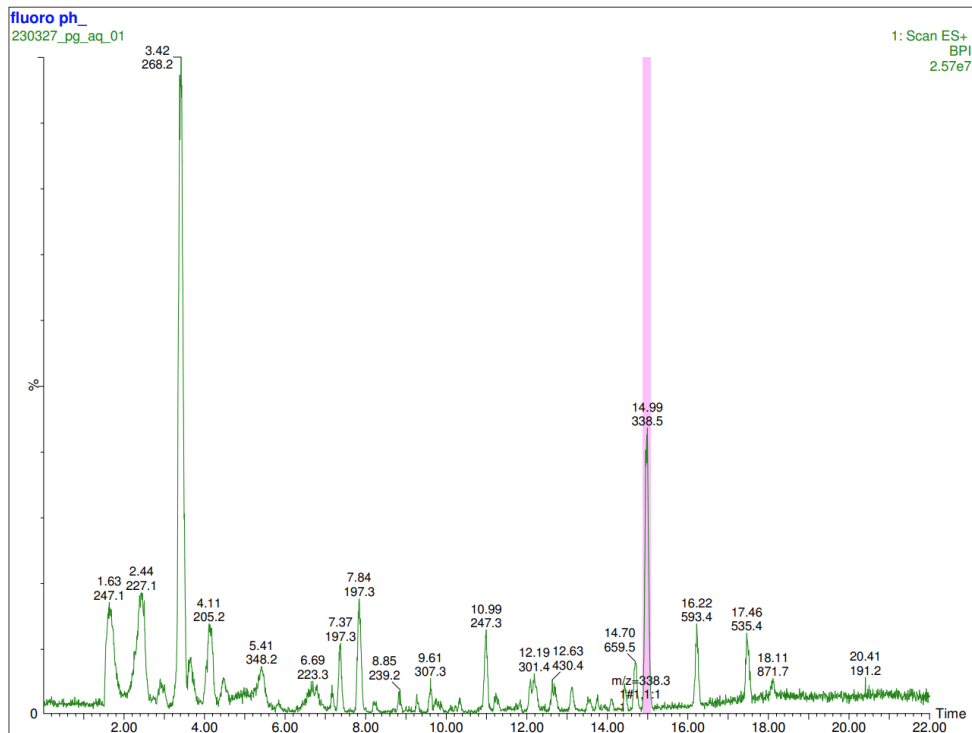


Figure 34: BPI chromatogram from preparative-HPLC, showing isolation of the peak with $R_t = 14.99$ minutes and $m/z = 338.5$. The purple line indicates the collected area.

The belonging mass spectrum for the isolated peak suggests high purity of the compound of interest (**Figure 35**). The strongest signals are the MI at $m/z = 338.49$ and what is most likely a dimer at $m/z = 675.77$.

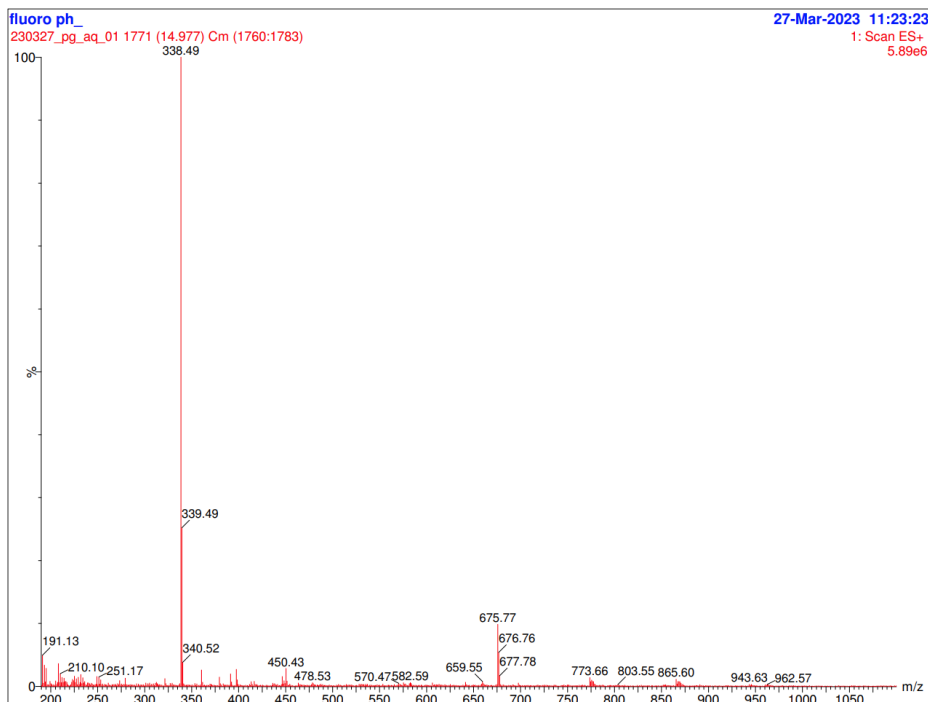


Figure 35: The mass spectrum for the isolated compound at $R_t = 14.99$ minutes with $m/z = 338.49$.

The yield of the isolate was 0.2 mg (0.095 ‰), which was enough for running a bioassay on anti-cancer activity against melanoma cancer- cell line A2058. From the five different concentrations tested (3.13, 6.25, 12.5, 25 and 50 µg/mL) none were active (scores > 80 ‰). It is therefore likely that the observed activity in aq5 derives from a different compound. To identify the compound responsible for the activity, more investigation and possibly more bioactivity testing must be done.

The proposed identification of the isolated compound was erucamide, using the HRMS data obtained in this thesis. Running an NMR-analysis could contribute to structural clarification of the compound, and thereby a more confident identification. In this case, there was not enough yield of the isolate to run an NMR-analysis. With a longer time perspective and by using a greater amount of the aqueous extract, a greater yield is achievable, which will open up this possibility.

4.6 Limitations

In the metabolomic and lipidomic comparison between the organic and the lipid extracts, only one parallel of each extract was analysed. Without multiple parallels, the results presented can't be defined as significant and is therefore only a basis for further research. In addition, the extracts were only compared in positive ionization mode, which lead to an exclusion of compounds only ionizable in negative modus.

In the lipidomic analysis, not many lipids were detected, and the results were not consistent with earlier findings. It is therefore hard to say if an error had occurred during the cultivation, the extractions, or the analysis, or that the inconsistency was due to low repeatability across batches.

The bioactivity testing of the fractions was conducted once for every bioassay. Every fraction was tested with 2-3 parallels, but it is still possible that random errors could have influenced the results. The bioassay results are still valuable as pinpointers for bioactivity to look after in microalgal biomass from the specie *P. glacialis*.

Only one batch of microalgal biomass from *P. glacialis* was used for the results in this thesis. The metabolic and the lipidomic profile can therefore not be considered consistent across batches. There is also no guarantee that the observed bioactivity is consistent with other batches of *P. glacialis* microalgal biomass.

4.7 Conclusion and Future Perspectives

The UHPLC-HRMS comparison between the two different extraction methods showed that the extracts had similar metabolic and lipidomic profiles. There were some trends observed, such as higher lipophilic yield using the lipidomic extraction method, and higher polar yield using the organic extraction method. Since the lipidomic analysis wasn't consistent with previous findings, there is uncertainty around the accuracy of the results. At the same time, the comparison involved only one parallel of each extract, which lower the significance level of the results. Overall, there is an argument that it doesn't matter which extraction method is used prior to metabolomic and lipidomic analyses. To consider this hypothesis, multiple parallels of each extraction method on different batches of microalgal biomass from *P. glacialis* must be analysed and compared.

Bioactivity testing of fractions obtained from microalgal biomass from *P. glacialis* revealed multiple bioactivities to pursue. An aqueous fraction had anti-cancer activity against human melanoma A2058 cancer cells and growth inhibition activity against the bacterial strain *S. agalactiae*. Dereplication of this fraction revealed a couple of compounds which could be responsible for the bioactivity. The compound with the proposed identification of erucamide was isolated and tested for bioactivity against melanoma cancer cell A2058. The results of isolate testing suggested that erucamide was not the compound responsible for the anti-cancer activity. In one of the organic fractions, anti-inflammatory activity was observed, possibly caused by a highly lipophilic compound which couldn't be identified. Despite observing various bioactivities in bioassays, no bioactive compounds were identified in the work of this thesis. With more bioactivity testing and investigation of the microalgal biomass in the future, there is still a potential for discovering bioactive compounds.

Works Cited

1. 2030 climate target plan Official EU Website: European Commission; [cited 2023 9. may]. Available from: https://climate.ec.europa.eu/eu-action/european-green-deal/2030-climate-target-plan_en.
2. Miljømålene i EUs taksonomi nho.no: Næringslivets Hovedorganisasjon; [cited 2023 9. may]. Available from: <https://www.nho.no/tema/energi-miljo-og-klima/artikler/miljomalene-i-eus-taksonomi/>.
3. Hva spiser oppdrettslaks? matportalen.no: Havforskningsinstituttet; 2007 [updated 2015, 10. june; cited 2023 9. may]. Available from: https://www.matportalen.no/temaoversikt/hva_spiser_oppdrettslaks.
4. Poduri R. Drug discovery and development: from targets and molecules to medicines. Gateway East, Singapore: Springer; 2021.
5. Paterson R, Lima N. Bioprospecting: success, potential and constraints. Cham: Springer International Publishing AG; 2016. 1-303 p.
6. Newman DJ, Cragg GM. Natural products as sources of new drugs over the nearly four decades from 01/1981 to 09/2019. *Journal of Natural Products*. 2020;83(3):770-803.
7. Ramoutsaki IA, Askitopoulou H, Konsolaki E. Pain relief and sedation in Roman Byzantine texts: *Mandragoras officinarum*, *Hyoscyamos niger* and *Atropa belladonna*. *International Congress Series*. 2002;1242:43-50.
8. Norwegian Prescription Database (NorPD) Norwegian Institute of Public Health; 2022 [cited 2023 9. may]. Available from: www.reseptregisteret.no.
9. Miner J, Hoffhines A. The discovery of aspirin's antithrombotic effects. *Texas Heart Institute Journal*. 2007;34(2):179-86.
10. Norges kyst og havområder Regjeringen.no: Klima- og miljødepartementet; [updated 2021, 11. october; cited 2022 9. may]. Available from: <https://www.regjeringen.no/no/tema/klima-og-miljo/naturmangfold/innsiktsartikler-naturmangfold/hag-og-kyst---behov-for-a-sikre-arts-mangfold/id2076396/>.
11. Svenson J. MabCent: Arctic marine bioprospecting in Norway. *Phytochemistry Reviews*. 2013;12(3):567-78.
12. Dalheim L. *Porosira glacialis* as a possible source of lipids for human consumption and aquaculture feed: UiT - the Arctic University of Norway; 2021.
13. Larkum AWD, Grossman AR, Raven JA. Photosynthesis in algae: biochemical and physiological mechanisms. Cham: Springer International Publishing: Imprint: Springer; 2020.
14. Kim S-K. Handbook of marine microalgae: biotechnology advances. Amsterdam, Netherlands: Academic Press; 2015.
15. Jain S. Fundamentals of invertebrate palaeontology: microfossils. New Delhi: Springer (India) Private Limited; 2020. 1-323 p.
16. Tréguer PJ, De La Rocha CL. The world ocean silica cycle. *Annual Review of Marine Science*. 2013;5(1):477-501.
17. Seckbach J, Annenkov VV, Gordon R. Diatom morphogenesis. Hoboken, NJ: John Wiley & Sons, Inc.; 2022.
18. Orefice I, Musella M, Smerilli A, Sansone C, Chandrasekaran R, Corato F, et al. Role of nutrient concentrations and water movement on diatom's productivity in culture. *Scientific Reports*. 2019;9(1):1479-.
19. Throndsen J, Tangen K, Hasle GR. Norsk kystplanktonflora. Oslo: Almatel forl.; 2003.
20. Pike J, Crosta X, Maddison EJ, Stickley CE, Denis D, Barbara L, et al. Observations on the relationship between the Antarctic coastal diatoms *Thalassiosira antarctica* Comber and *Porosira glacialis* (Grunow) Jørgensen and sea ice concentrations during the late Quaternary. *Marine Micropaleontology*. 2009;73(1):14-25.
21. Svenning JB, Dalheim L, Eilertsen HC, Vasskog T. Temperature dependent growth rate, lipid content and fatty acid composition of the marine cold-water diatom *Porosira glacialis*. *Algal research* (Amsterdam). 2019;37:11-6.

22. Artamonova EY, Vasskog T, Eilertsen HC. Lipid content and fatty acid composition of *Porosira glacialis* and *Attheya longicornis* in response to carbon dioxide (CO₂) aeration. *PLoS One*. 2017;12(5):e0177703-e.
23. Haugland K. Identification and semi-quantitative analysis of lipids in the diatom *Porosira glacialis*: UiT - the Arctic University of Norway; 2022.
24. Arivaradarajan P, Misra G. Omics approaches, technologies and applications: integrative approaches for understanding omics data. Singapore: Imprint: Springer; 2018.
25. Sussulini A. Metabolomics: from fundamentals to clinical applications. Cham: Springer International Publishing; Imprint: Springer; 2017.
26. Sirtori CR, Fumagalli R. LDL-cholesterol lowering or HDL-cholesterol raising for cardiovascular prevention. A lesson from cholesterol turnover studies and others. *Atherosclerosis*. 2006;186(1):1-11.
27. Martins J, Steyn N, Rossouw HM, Pillay TS. Best practice for LDL-cholesterol: when and how to calculate. *Journal of Clinical Pathology*. 2023;76(3):145-52.
28. Pedersen-Bjergaard S, Gammelgaard B, Halvorsen TG. Introduction to pharmaceutical analytical chemistry. Hoboken, NJ: Wiley; 2019.
29. Vuckovic D. Current trends and challenges in sample preparation for global metabolomics using liquid chromatography–mass spectrometry. *Analytical and Bioanalytical Chemistry*. 2012;403(6):1523-48.
30. Basics in centrifugation: Eppendorf Handling Solutions; [cited 2022 31. october]. Available from: <https://handling-solutions.eppendorf.com/sample-handling/centrifugation/safe-use-of-centrifuges/basics-in-centrifugation/>.
31. Breil C, Abert Vian M, Zemb T, Kunz W, Chemat F. "Bligh and Dyer" and folch methods for solid-liquid-liquid extraction of lipids from microorganisms. Comprehension of solvation mechanisms and towards substitution with alternative solvents. *International Journal of Molecular Sciences*. 2017;18(4):708-.
32. Siranjevi RPMM. Isolation and characterization of new secondary metabolites form the Arctic marine bryozoans *Securiflustra securifrons* and *Dendrobeania murrayana*. Tromsø: UiT - the Arctic University of Norway, Faculty of Biosciences, Fisheries and Economics, The Norwegian College of Fishery Science; 2019.
33. Hansen KØ. Isolation and characterisation of bioactive secondary metabolites from arctic, marine organisms: UiT - the Arctic University of Norway; 2014.
34. Kaklamanos G, Aprea E, Theodoridis G. Mass spectrometry: principles and instrumentation. Second ed. Waltham:2020.
35. Ekman R. Mass spectrometry : instrumentation, interpretation, and applications. Hoboken, N.J.: John Wiley & Sons; 2009.
36. Hoffmann Ed, Stroobant V. Mass spectrometry : principles and applications. Chichester, West Sussex, England; Hoboken, N.J.: J. Wiley; 2007.
37. Wilburn DB, Richards AL, Swaney DL, Searle BC. CIDer: a statistical framework for interpreting differences in CID and HCD fragmentation. *Journal of Proteome Research*. 2021;20(4):1951-65.
38. Liu Y, Uboh CE, Soma LR, Li X, Guan F, You Y, et al. Efficient use of retention time for the analysis of 302 drugs in equine plasma by liquid chromatography-MS/MS with scheduled multiple reaction monitoring and instant library searching for doping control. *Analytical Chemistry*. 2011;83(17):6834-41.
39. Miller TH, Musenga A, Cowan DA, Barron LP. Prediction of chromatographic retention time in high-resolution anti-doping screening data using artificial neural networks. *Analytical Chemistry*. 2013;85(21):10330-7.
40. Crews P, Rodríguez J, Jaspars M. Organic structure analysis. Second ed. New York: Oxford University Press; 2010.
41. Han X. Lipidomics: comprehensive mass spectrometry of lipids. Hoboken, New Jersey: John Wiley & Sons, Incorporated; 2016.
42. Moe MK, Anderssen T, Strøm MB, Jensen E. Vicinal hydroxylation of unsaturated fatty acids for structural characterization of intact neutral phospholipids by negative electrospray ionization

tandem quadrupole mass spectrometry. Rapid Communications in Mass Spectrometry. 2004;18(18):2121-30.

43. UNIFI Scientific Information System; a single platform for chromatography, mass spectrometry, data management, and laboratory workflow: Waters; [cited 2023 3. march]. Available from: https://www.waters.com/waters/en_US/UNIFI-Scientific-Information-System/nav.htm?locale=en_US&cid=134801648.
44. Answer your biological question with Progenesis QI: Nonlinear Dynamics and Waters; [cited 2023 3. march]. Available from: <https://www.nonlinear.com/progenesis/qi/>.
45. AcquireX intelligent data acquisition workflow: Thermo Scientific; [cited 2023 3. march]. Available from: <https://www.thermofisher.com/no/en/home/industrial/mass-spectrometry/liquid-chromatography-mass-spectrometry-lc-ms/lc-ms-software/lc-ms-data-acquisition-software/acquirex-intelligent-data-acquisition-workflow.html>.
46. O'Toole GA. Microtiter dish biofilm formation assay. Journal of Visualized Experiments. 2011(47).
47. Adan A, Kiraz Y, Baran Y. Cell proliferation and cytotoxicity assays. Current Pharmaceutical Biotechnology. 2016;17(14):1213-21.
48. McCauley J, Zivanovic A, Skropeta D. Bioassays for anticancer activities. Methods in Molecular Biology. 2013;1055:191-205.
49. Laxminarayan R, Duse A, Wattal C, Zaidi AK, Wertheim HF, Sumpradit N, et al. Antibiotic resistance-the need for global solutions. The Lancet Infectious Diseases. 2013;13(12):1057-98.
50. Wheeler MJ. Immunoassay techniques. Methods in Molecular Biology. 2006;324:1-23.
51. Jaria G, Calisto V, Otero M, Esteves VI. Monitoring pharmaceuticals in the aquatic environment using enzyme-linked immunosorbent assay (ELISA)—a practical overview. Analytical and Bioanalytical Chemistry. 2020;412(17):3983-4008.
52. Tucureanu MM, Rebleanu D, Constantinescu CA, Deleanu M, Voicu G, Butoi E, et al. Lipopolysaccharide-induced inflammation in monocytes/macrophages is blocked by liposomal delivery of G(i)-protein inhibitor. International Journal of Nanomedicine. 2018;13:63-76.
53. Suzuki Y, Doi M, Shioi Y. Two enzymatic reaction pathways in the formation of pyropheophorbide a. Photosynthesis Research. 2002;74(2):225-33.
54. Spilling K, Brynjólfssdóttir Á, Enss D, Rischer H, Svavarsson HG. The effect of high pH on structural lipids in diatoms. Journal of Applied Phycology. 2013;25(5):1435-9.
55. Suparmaniam U, Lam MK, Lim JW, Yusup S, Tan IS, Lau SY, et al. Influence of environmental stress on microalgae growth and lipid profile: a systematic review. Phytochemistry Reviews. 2022.
56. Liang Y, Mai K. Effect of growth phase on the fatty acid compositions of four species of marine diatoms. Journal of Ocean University of China. 2005;4(2):157-62.
57. Alipanah L, Winge P, Rohloff J, Najafi J, Brembu T, Bones AM. Molecular adaptations to phosphorus deprivation and comparison with nitrogen deprivation responses in the diatom *Phaeodactylum tricorutum*. PLOS ONE. 2018;13(2):e0193335.
58. Martin P, Van Mooy BAS, Heithoff A, Dyhrman ST. Phosphorus supply drives rapid turnover of membrane phospholipids in the diatom *Thalassiosira pseudonana*. The ISME Journal. 2011;5(6):1057-60.
59. Gupta R, Gupta N. Fundamentals of bacterial physiology and metabolism. Singapore: Springer; 2021.
60. Stillwell W. Chapter 20 - Bioactive Lipids. In: Stillwell W, editor. An Introduction to Biological Membranes. Second ed: Elsevier; 2016. p. 453-78.
61. Jaworowska A, Murtaza A. Seaweed derived lipids are a potential anti-inflammatory agent: a review. International Journal of Environmental Research and Public Health. 2022;20(1).
62. Zhu Y, Han S, Li J, Gao H, Dong B. Aqueous extract of sea squirt (*Halocynthia roretzi*) with potent activity against human cancer cells acts synergistically with doxorubicin. Marine Drugs. 2022;20(5).
63. Swanson D, Block R, Mousa SA. Omega-3 fatty acids EPA and DHA: health benefits throughout life. Advances in Nutrition. 2012;3(1):1-7.

Appendix

Appendix 1: Parameters used in the MSⁿ method on the orbitrap.

PARAMETERS	MS ² OT HCD	MS ² OT CID	MS ³ OT CID
MS ⁿ level		2	3
Scan Priority		1	1
Isolation mode	Quadrupole	Quadrupole	
Isolation window (<i>m/z</i>)	1.5	2	1.5 (MS), 2 (MS ²)
Isolation offset	Off	Off	Off
Activation Type	HCD	CID	CID
Collision Energy Mode	Stepped	Fixed	Fixed
CID Collision Energy		32	35
CID Activation Time		10	10
HCD Collision Energy	Normalized		
HCD Collision Energies	20, 30, 35		
Activation Q		0.25	0.25
Multistage Activation		False	False
Detector Type	Orbitrap	Orbitrap	Orbitrap
Orbitrap resolution	15000	15000	15000
Scan Range Mode	Define First Mass	Auto	Auto
First Mass (<i>m/z</i>)	140		
AGC Target	Standard	Standard	Standard
Maximum Injection	Custom	Custom	Custom
Maximum Injection	50	50	65
Microscans	1	1	1
Data Type	Profile	Profile	Profile
Use EASY-IC™	True	False	False
Number of Dependent		1	3

Appendix 2: An overview of neutral loss of fatty acids and ammonia triggering MS³ OT CID in lipidomic analyses.

Neutral Loss of FA + NH ₃ (m/z)	Fatty Acid (FA)	Neutral Loss of FA + NH ₃ (m/z)	Fatty Acid (FA)
217.2042	12:0	323.2824	20:3
245.2355	14:0	321.2668	20:4
243.2198	14:1	319.2511	20:5
273.2668	16:0	343.3450	21:0
271.2511	16:1	357.3607	22:0
269.2355	16:2	355.3450	22:1
287.2824	17:0	353.3294	22:2
301.2981	18:0	351.3137	22:3
299.2824	18:1	349.2981	22:4
297.2668	18:2	347.2824	22:5
295.2511	18:3	345.2668	22:6
315.3137	19:0	371.3763	23:0
329.3294	20:0	385.3920	24:0
327.3137	20:1	383.3763	24:1
325.2981	20:2	413.4233	26:0

Appendix 3: An overview of the lipid classes identified in LipidSearch

Select	Class	Ion	Molec	Total Ion	Total Molec
<input checked="" type="checkbox"/>	DG	38	38	39	39
<input checked="" type="checkbox"/>	LBPA	2	2	2	2
<input checked="" type="checkbox"/>	WE	10	10	10	10
<input checked="" type="checkbox"/>	PC	1	1	1	1
<input checked="" type="checkbox"/>	TG	311	259	322	270
<input checked="" type="checkbox"/>	PG	6	6	6	6
<input checked="" type="checkbox"/>	DGDG	2	2	2	2
<input checked="" type="checkbox"/>	MGDG	4	4	4	4
<input checked="" type="checkbox"/>	PI	1	1	2	2
<input checked="" type="checkbox"/>	MG	7	7	7	7
<input checked="" type="checkbox"/>	PEt	8	8	17	17
<input checked="" type="checkbox"/>	AcCa	1	1	1	1

Appendix 4: An explanation of the grading system for identifications in LipidSearch.

1.2.1 Grade

Grade is calculated as follows using the product ion Category specified in the Database.

- [Category]

Category	Description
C0	Head group specific ions
C01	Head group-derived or substituent-derived ions specific to lipid class
C1	Substituent-specific ions
C2	Ions that do not identify structure

- [Condition]

Condition	Description
H1	C0 and C01 (or more than one C0) (or C01 for all substituents) are assigned
H2	C0 or C1 are assigned
S1	C01 or C1 are assigned for all substituents
S2	C01 or C1 are assigned for some substituents

- [Grade Assignment]

Grade	Description
A	(H1 and S1)
B	(H2 and S1) or (H1 and S2)
C	H2 or S1
D	Other

